POLITECNICO DI TORINO

Master's Degree Course
In Mechanical Engineering

Master's Degree Thesis
Design, Analysis and Investigation of
an Independent Suspension for Passenger cars

Supervisors
Prof. Mauro Velardocchia
Dr. Prof Basilio Lenzo

Candidate
Carlo N.Belluomo
Mat.No 227711

A.A.2017/2018

ABSTRACT

The suspension systems play a fundamental role in the dynamics of the vehicles. Several successful layouts, like The Macpherson strut and the Double Wishbone, were designed during the first part of the 20th century and nowadays they are still used in all the road and race cars. In the 1960's the Multi-link layout was designed and nowadays is used in specific application because of its complexity. During the last years, vehicles reached high performance and the suspension systems needed extreme level of accuracy. The development of the computer aided engineering made possible to analyse many configurations of suspension geometry allowing to satisfy demanding applications. For this thesis, Adams\Car was used to perform Multibody analysis.

Using SolidWorks,2-D drawings of the suspension layout are realized to identify the main parameters that define the suspension kinematics.

The work started defining specific setting targets to be achieved. The first part of the thesis involves the design of the all suspension components of the Macpherson strut. The main part of the thesis investigates the geometry of the suspension layout through a sensitivity analysis of the main hardpoints, determining the relations between the hardpoints position and the behaviour of the vehicle. The same work is made for the Multi-link layout and a comparison between the two system is offered, highlighting the better performance of the Multi-link.

At the end of the thesis, a full-vehicle assembly provided with the MacPherson strut is used to investigate the influences of the hardpoints on the body roll for different configurations.

ACKNOWLEDGEMENT

I want to take advantage of this opportunity to thank Professor Velardocchia for allowing me to make this wonderful teaching and personal experience, for giving me valuable advice even at a distance.

My gratitude goes to Professor Basilio Lenzo for welcoming me to Sheffield Hallam University and constantly following me relentlessly and patiently. The love for teaching and the effort to follow the students have been a motivation for me to improve my skills.

I want to thank the amazing people known in Sheffield who helped to make the experience much more beautiful: Federica, Sina, Javid and my roommates Julie, Chloé and Mairead.

I thank my friends Giulio, Andrea.C, Andrea.G, Francesco, Enzo,Simone,Riccardo and Stefano who have been close to me during these years in Turin and have made these last years really fun.

Finally, the biggest thanks goes to my family for supporting me all my life and allowing me to have some important experiences.

Table of Contents

1.LITTERATURE REVIEW

1.1Introduction and Role of suspension system in vehicle

The suspension system plays a fundamental role in the vehicle performance, for both road cars and racing cars. The suspension is the link between the entire vehicle and the road, so the suspension acts like a filter between the unevenness of the road and the passengers. Regardless the size and the power of the engine, the performance of the vehicle is strictly dependent on the ability of the suspension to transmit the torque produced by the engine to the ground through the contact forces. Riding, handling and comfort are achieved through a complex and accurate design. The main aim of the suspension system is to copy the road surfaces limiting the tire fluctuation providing a vertical compliance; allow safe manoeuvres ensuring the controlled position of the wheel; ensure that the vehicle responds favourably to the external road forces; isolate the passengers from the road unevenness. The design of a suspension system is unique for each type of car and differs for the several uses the car should deal with. While race cars suspension system demands the highest performance regardless any care about durability and comfort, the design of a suspension system for road cars must consider the reduction of the wheels wear so as so the reduction of the vibrations and the optimization of the comfort for the passengers while offering good handling. Through the study of the suspension design comes out that *the design of the suspension is a compromise between several performances and requirements; the design that makes perfect each suspension parameters simultaneously doesn't exist, yet.*

1.2 Degree of freedom of a Mechanism

A single body moving in the three-dimensional space without any kinematical constraints has the degree of freedom F=6.This is the minimal number of generalized coordinates required to identify the position of the body respect to some reference body. The kinematical constraints limit the motion of the body, the degree of freedom of the joint is $1 \leq f \leq 5$. The total constraints of the joint are $6 - f$. A mechanism concerns rigid bodies linked together through different kind of linkages or kinematic pairs that reduce the motion between the bodies. Talking about mechanisms, is it usual to refer to the total degree of freedom as *mobility. The* kinematics pairs are called lower pairs if the connection has F=1 or higher pairs for F>1. Two bodies cannot be connected by more than one joint. Considering the subject of the study, suspensions, the main aim is design a system which total mobility is equal to one. The goal of the suspension system is to guide the motion of each wheel along a vertical path limiting the variation of other parameters like Camber angle and Scrub radius.

Name of pair	Geometric form	Degrees of freedom
Revolute R	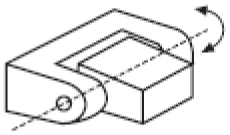	1
Prism P	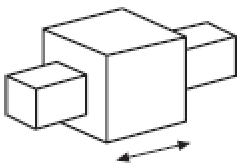	1
Cylinder C	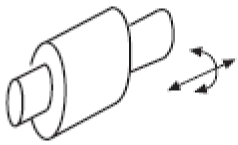	2
Sphere S	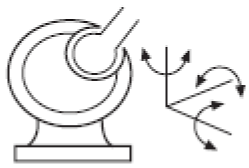	3

Figure 1.1 Kinematic pairs [4]

The total mobility for a complex mechanism can be computed from the following formula:

$$F = 6(l + k - g) - r + \sum_{i=1}^{g} f_i$$

In which l is the number of the arms of the kinematics chain, k is the number of the knuckles, r is the number of the rotations of the arms about their own axis that are not interesting in the total computation, g is the number of the joints and f_i is the degree of freedom of each joint. Considering figure 1.2, the previous formula can be used to compute the mobility of the Macpherson suspension and verify that $M = 1$.

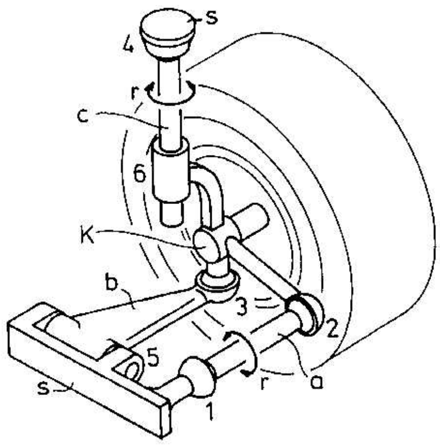

Figure 1.2 Macpherson layout [8]

1.3 Geometric parameters

The peculiarity of the suspension design is the big number of parameters that affect the suspension kinematics and dynamics that need to be considered. Many of these parameters can have the same or opposite influence on the global suspension behaviour. They are introduced and explained following.

1.3.1 Kingpin axis

The line passing through the upper ball joint and the lower ball joint of the knuckle is the steering axis or also called Kingpin axis. It can be geometrically definable, for some layouts like the Macpherson strut or the Double Wishbone, or ‘virtual’ like for the Multi-link system. In front view the angle between the kingpin axis and the vertical at the wheel is the kingpin angle (figure 1.3). Is it defined positive when the kingpin axis is inclined towards the centre of the vehicle. In side view, the inclination of the kingpin axis is called Caster angle (figure 1.4). Is it defined positive when the kingpin axis is inclined backward. In front view, the offset of the kingpin axis respect to the wheel centre is called Scrub radius. In side view, the offset of the kingpin axis respect to the wheel center is called Caster trail. Both this two angle and offset influence deeply the behaviour of the suspension.

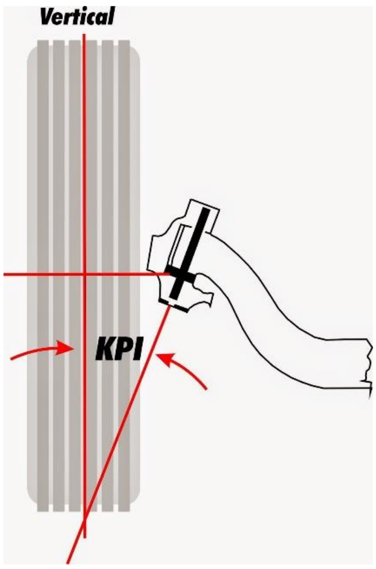

Figure 1.3 Kingpin inclination angle

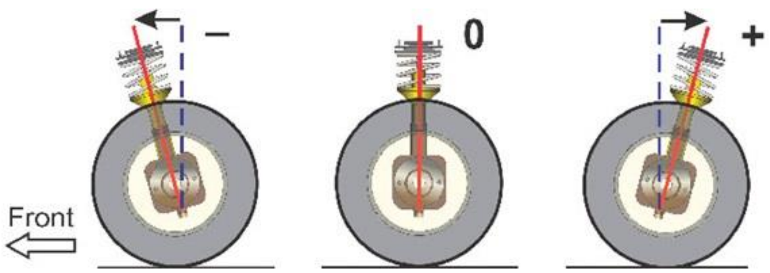

Figure 1.4 Caster angle

1.3.2 Instant Center

The instant center is the pivot point of the linkage about which all the suspension swings about. The instant center is found through the intersection of the axis passing through the linkages, figure 1.5. The word ‘instant’ refers to the fact that as the position of the linkages changes during the wheel bump the position of the center changes too. The concept of the instant center is valid for the two dimensions. In the front plane, the linkages swing about the front instant center while in the side view about the side view instant center or also called ‘pitch center’.

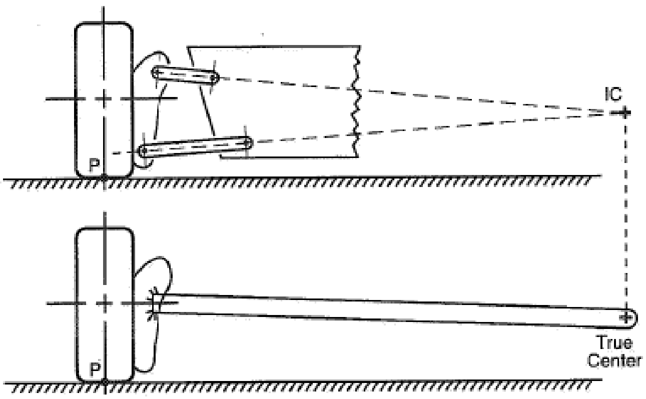

Figure 1.5 Instant center and front swing arm [3]

Considering the three dimensions, connecting the two points in front and side view the instant axis is obtained about which the suspension rotates, figure 1.6. Consider the projection of the instant axis on the front or the side view is useful to study many important suspension parameters.

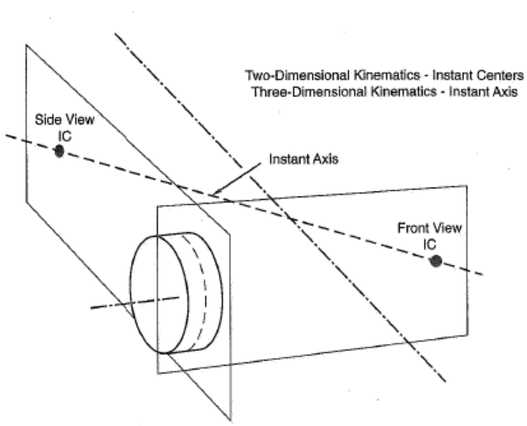

Figure 1.6 Instant axis [3]

- Front view

The front instant center is necessary to study the Roll center, the camber gain and the radius.

1.3.3 Roll center

The roll center is the pivot point about which the chassis swings. The Kennedy's theorem states that three instant centers lie in the same line. The intersection between the line that connects the wheel contact point with the instant center and the plane passing through the middle of the vehicle gives the roll center position. The roll center is also said to be the point at which a lateral force applied doesn't produce any body roll. The roll center height is fundamental for the stability of the vehicle. The line connecting the front roll center to the rear roll center is the 'roll axis' as visible in figure 1.7. When the vehicle is driven in a curve, to compensate the lateral force of the tire, the body is subjected to a lateral acceleration with opposite sign that makes the body roll outwards. The body roll affects the comfort of the passenger. The rolling torque is due to the lateral acceleration for 'H', the distance between the center of gravity and the roll axis at that point. The higher the roll axis the lower the roll. Therefore, is fundamental design the roll center height at front and rear properly to obtain a good stability during cornering. It is also important to make the roll center height at the front and at the rear vary in a small range during wheel bump or body roll.

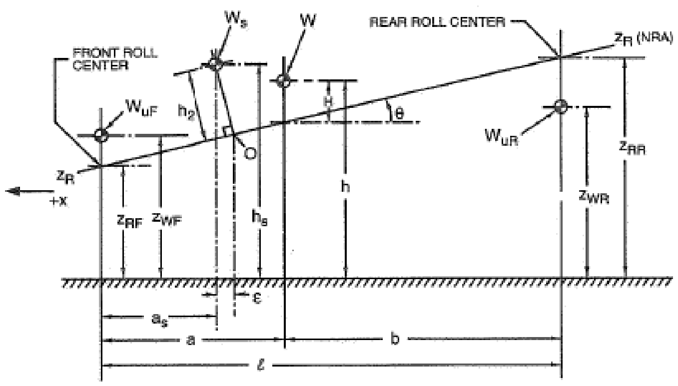

Figure 1.7 Roll center axis [3]

1.3.4 Camber gain

The wheel camber angle is the angle, measured in degrees, between the centre line of the wheel and the perpendicular to the ground, looking from the front. Camber is defined positive when the wheel tilts outwards while is defined positive when the wheels tilts inwards. It is desirable to have camber equal to zero. When the wheel is perfectly vertical can produce more forces on the ground. During cornering, the body rolls and pushes the wheels outwards, positive camber, reducing the lateral forces produced on the ground. Usually, car wheels are set with a small negative camber to balance the variation of camber during the curve.

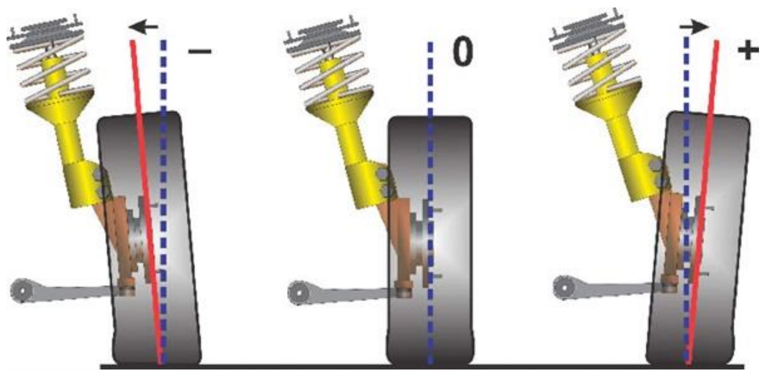

Figure 1.8 Camber variation

The camber gain is influenced only by the length of the front view swing arm. As visible in figure 1.9, the shortest the swing arm the larger the camber gain. A proper suspension design must consider this parameter, the layout that are shown in the next chapters will make clear that is not always possible to obtain a large camber gain with all type of suspension.

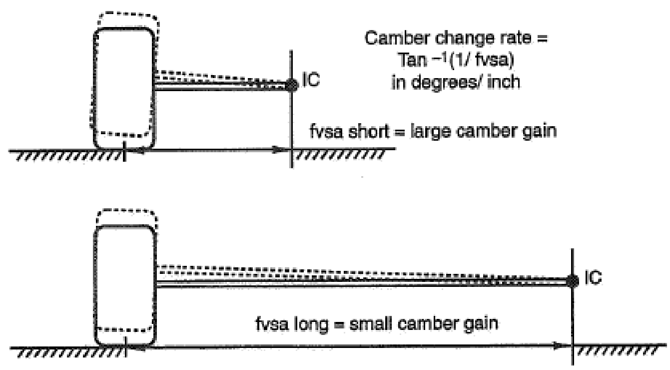

Figure 1.9 Camber gain and length of the swing arm [3]

1.3.5 Scrub radius

The scrub radius is the distance in front view between the kingpin axis and the center of the contact patch of the wheel, where both would theoretically touch the road. Scrub radius is defined negative when the contact point of the kingpin axis with the ground is outer at the wheel center. Contrarily, is defined positive.
Scrub radius increases the tire wear and produces vibrations. Depending on the design, sometimes, scrub radius is voluntarily design because it can lead to 'toe-in' behaviour during braking, increasing stability.

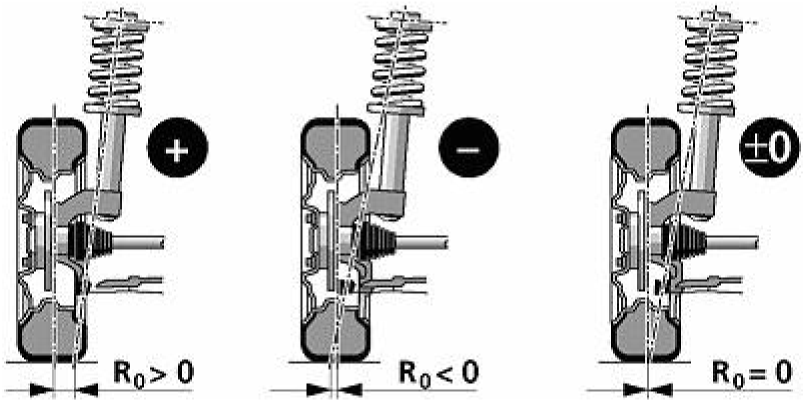

Figure 1.10 Scrub radius

1.3.6 Jacking

If the instant center is above the ground, the lateral forces exerted by the wheel produce a torque about the instant center making the vehicle raising (figure 1.11). Contrarily, if the instant center is below the ground the vehicle is pushed down. Body roll and Jacking are two opposite effects' order to have a small body roll, the roll center height, hence the instant center, must be as higher as possible, while to limit the Jacking the instant center should be as close as possible to the ground.

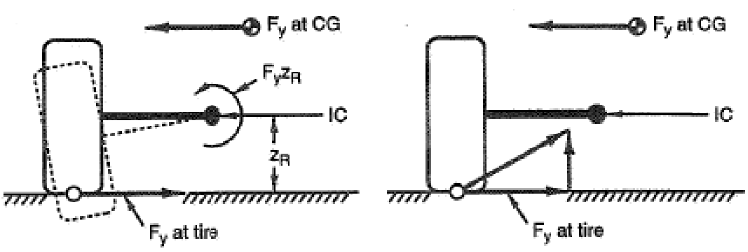

Figure 1.11 Jacking effect [3]

- Side view

The instant center in the side view, also called, ‘pitch center’ is useful to study the anti-properties of the vehicle like anti-dive or anti-lift.

1.3.7 Anti-properties

The "anti" effect in suspensions is a term that describes the longitudinal to vertical force coupling between the sprung and unsprung masses.The percentage of anti-property describes the distribution of forces between the elastic components, the springs, and the rigid components, the arms. Increasing the value of the anti - properties during braking or acceleration the vehicle bouncing is reduced, because the forces pass through the arms. The anti-properties don’t change the total load transfer, which is only dependent on the wheel base, the height of the center of gravity and the acceleration. In the following table, the anti-properties are explained.

Table 1.1

‘Anti’	Suspension	Effect	Condition
Anti-dive	Front	Reduce the lowering of the front	Braking
Anti-lift	Front	Reduce the raising of the front	Acceleration
Anti-squat	Rear	Reduce the lowering of the rear	Acceleration
Anti-lift	Rear	Reduce the raising of the rear	Braking

- Braking

  During braking the vehicle is subjected to a braking acceleration that make the vehicle pitch. The longitudinal load transfer depends only on the wheelbase, the height of the center of gravity and the braking acceleration, figure 1.12. The distribution of the braking force between front and rear axle is:

$$R = \frac{F_{xp}}{Fxa} \tag{1}$$

The longitudinal equilibrium of the forces:

$$m * a_x = F_{xa} + F_{xp} \tag{2}$$

Substituting (1) in (2):

$$m * a_x = F_{xa} + F_{xa} * R \tag{3}$$

So, the longitudinal forces can be expressed as:

$$F_{xa} = \frac{m * a_x}{(1+R)} \tag{4}$$

$$F_{xp} = \frac{m * a_x}{(1+R)} * R \tag{5}$$

The inertia force produces a front load transfer as visible in figure 1.12:

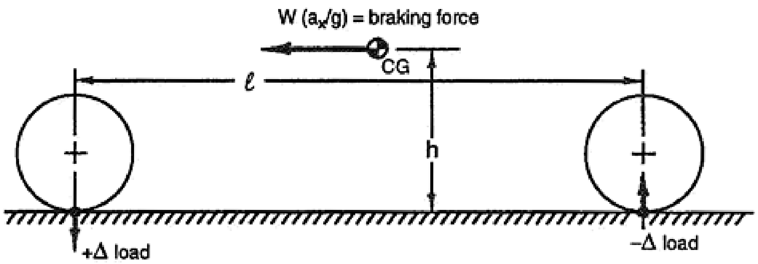

Figure 1.12 Load transfer during braking [3]

$$\Delta F_z = \frac{m * a_x * h_g}{l} \tag{6}$$

The longitudinal load transfer makes the vehicle pitch, compressing the front springs and extending the rear springs.

Braking: equilibrium of each suspension

The longitudinal forces counteract the effect of the longitudinal load transfer. Considering the rotation of each wheel about its own instant rotation center, the braking force makes the front springs extend while at the rear makes the springs compress. There are two opposite moments acting on the wheels:

$$M_a = F_{xa} * q_a - \Delta F_z * e_a \tag{7}$$

$$M_p = F_{xp} * q_p - \Delta F_z * e_p \tag{8}$$

M_a is called Anti-dive while M_p is called Anti-lift. The suspension can be designed to obtain the highest effects from the Anti-property.

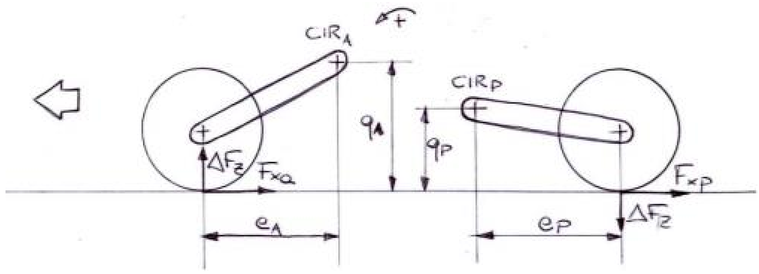

Figure 1.13 Equilibrium to rotation for each wheel

Substituting (4) and (6) in (7) the equation can be written as following:

$$M_a = \frac{m * a_x}{(1+R)} * q_a - \frac{m * a_x * h_g}{l} * e_a = m * a_x \left(\frac{1}{(1+R)} * q_a - \frac{h_g}{l} * e_a\right) \tag{9}$$

For the rear wheel, the same equation can be written substituting (5) and (6) in (8):

$$M_a = \frac{m * a_x}{(1+R)} * R * q_p - \frac{m * a_x * h_g}{l} * e_p = m * a_x \left(\frac{R}{(1+R)} * q_p - \frac{h_g}{l} * e_p\right) \tag{10}$$

Considering figure 2.11 the resultant of the forces acting on front wheel is inclined of angle equal to:

$$\alpha_{antidive} = \arctan\left(\frac{q_a}{e_a}\right) \tag{11}$$

For $q_a = 0$ or $e_a = \infty$ the antidive effect is null

The extreme condition is the one of 100% antideath inclination of the resultant of the forces for obtaining this condition derives from the following condition:

$$M_a = 0 = \left(\frac{1}{(1+R)} * q_a - \frac{h_g}{l} * e_a\right) = 0 \tag{12}$$

$$\frac{q_a}{e_a} = \frac{h_g}{l} * (1 + R) \tag{13}$$

$$\alpha_{100\%antidive} = arctan\left(\frac{h_g}{l} * (1 + R)\right) \tag{14}$$

The formula (14) expresses the necessary angle to have the 100% antidive, as can be seen, this formula considers only geometric parameters of the vehicle, not mentioning the suspension architecture, differently from equation (11).

The actual Antidive at the front is defined as:

$$Antidive\% = \frac{\alpha_{antidive}}{\alpha_{100\%antidive}} \tag{15}$$

Vehicle, generally, are designed with a percentage of Antidive below 40%. The extreme condition of 100% Antidive would lead the vehicle not to pitch but the suspension arms would be subjected to high stress. Moreover, a certain amount of pitch is necessary to transmit to the driver handling feelings. In the condition of not pitch, the driver can't understand the limit of the tire during cornering.
Through similar demonstration, is it possible to obtain the percentage of Antilift.Is it important to state that is impossible to have any antilift effect if there is no drive axle at the front as well as there is no antilift at the rear wheel if the traction is at the front.

1.3.8 Toe Angle

The toe angle can be defined like the angle between the longitudinal plane passing through the center of the wheel and the middle plane passing through the wheel. The toe can be defined also as the difference between the track width measured at the leading edge and measured at the trailing edge of the tire. It is expressed in degrees or radians. The toe affects the tire wear and the handling. During braking is desirable obtain a toe-in behaviour because increases the stability of the vehicle, while during cornering a certain amount of toe-out increases the handling. The value of the toe-in that is possible to gain during the maneuver depends on the architecture of the suspension and its compliance as is shown in the next chapters.

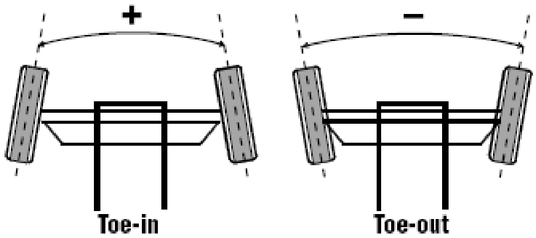

Figure 1.14 Sign convention

1.4 Types of suspension system

The choice of the type of suspension to design and use on a vehicle is the consequence of many requests and necessities. Manufacturing cost, complexity of the design, performances and packaging are the key points that dictate the final choice. Is it possible to consider two big groups of suspension: dependent and independent.

- The dependent suspension, like the *Beam axle* in figure, is characterized by a rigid connection between the wheels of the same axle. When one of the wheels faces a bump, the motion of the other wheel is affected in the same way. The Camber angle, the angle between the plane passing through the middle of the wheel and the vertical plane passing though the contact point, remains constant due the rigid connection between the two wheels reducing the tyre wear. The design is quite easy and are often used at the rear axle for commercial vehicles or off-road vehicles. The suspension is simple to design and to be manufactured. The disadvantages are the heavy weight and the space required.

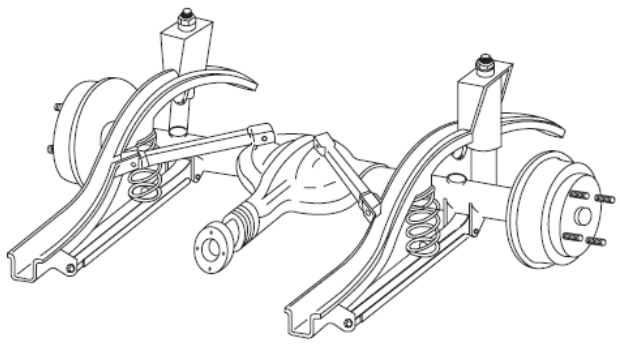

Figure 1.15 Trailing arm- rigid axle suspension [4]

- The independent suspension is nowadays the most used suspension system for vehicle because they provide good riding. The main characteristic is that the wheels of the same axle are not linked but each suspension is attached to the subframe. The main advantages are the wider design freedom and reduced packaging. The principal layouts used are the *Macpherson strut*, the *Double Wishbone* and the *Multi-link*.

1.4.1 Macpherson strut

The Macpherson strut is composed mainly of one lower arm, the knuckle, the spring and damper. The spring and the damper are mounted coaxially and perform both the elastic and structural role. The main advantages of this layout are that is easy to design, doesn't require wide horizontal space so it is suitable for passenger's car and is quite cheap. The main disadvantages involve the reduce gamber gain during body roll and the lack of noise reduction due to the small compliance of the lower control arm. Moreover, this layout requires wide spring travel.

Figure 1.16 Macpherson strut

1.4.2 Double Wishbone

The Double Wishbone layout is composed of two triangles, one lower control arm and one upper control arm. Differently from the Macpherson, the spring and the damper don't cover any structural role. This type of layout has been the most used suspension system for race cars. The two-arm structure makes the structure capable to resist high stress. This layout is characterized by a wide design freedom. One of the main advantages is the large camber gain. There are two version of Double Wishbone, parallel and same length arms or not parallel and different length. The latter is called SLA, short -long-arm like the one shown in figure 1.17.

Figure 1.17 Double Wishbone

1.4.3 Multi-link

The multi-link suspension can be thought like the evolution of the Double Wishbone. Is it also called five links suspension because each link can be independent from the other one. This layout gives designers completely freedom. The important innovation respect to the double wishbone is that the upper and lower ball joints close to knuckle are split into two ball joints each. This implies that the kingpin axis is not more physical but is said to be virtual. This permits the designer to have a small scrub radius to limits the noise and tire wear and match the desired roll center height for example. In figure 1.18 is shown one example of Multi-link suspension. In this case the two-upper links are merged in one control arm, similarly to the double wishbone design. The main disadvantage of the Multi-link layout is the complexity of the design that is expensive and time consuming.

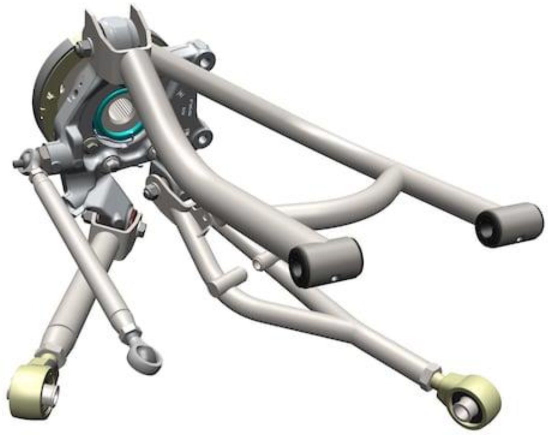

Figure 1.18 Multi-link

2. DESIGN OF THE SUSPENSION LAYOUT

2.1 Geometry Parameters

The input of the design are the main parameters of a commercial vehicle listed in Table 2.1. It is supposed to consider the height of roll axis, in correspondence of the center of gravity, equal to the 30% of the CG height, hence 210 mm. In addition, it is supposed to have a ratio between the roll center at the front axle and at the rear axle equal to 40 %, the computed values are shown in table 2.2.

Table 2.1

Parameters	Value	Unit of measure
Tires	235/55/ R19	mm
Wheelbase	2600	mm
Track	1616	mm
CG height	700	mm
a	1300	mm
b	1360	mm
Weight	2355	kg

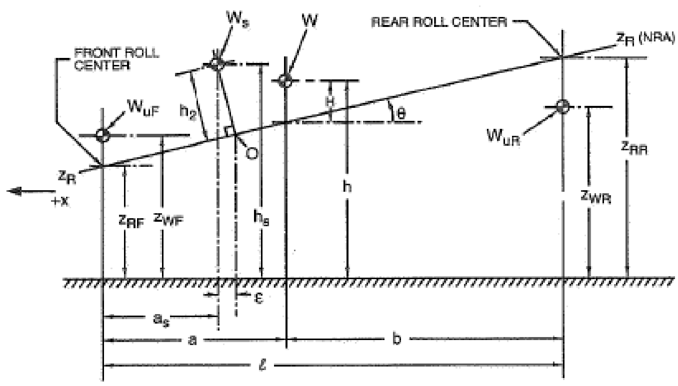

Figure 2.1 Roll axis [3]

Table 2.2

Parameters	Value	Unit of measure
Front Roll center height	120	mm
Rear Roll center height	300	mm

The topic of this thesis is to design two layouts of front suspension system: the Macpherson strut and the Multi-link, lead an optimization study and a final comparison. The rear roll center height is set but the rear suspension is not meant to be design. The design process starts with the aim to match the desired roll center height. The Macpherson layout can be studied preliminarily in 2-D easily. It is intuitive to understand the kinematics of the suspension approaching a geometric study drawing the components of the system. SolidWorks has been used to study the geometry of the layout and to analyse the variation of the main suspension parameters. The choice of the first setting of the hardpoints position started from the position of the point B. It was chosen to set it close to the brake disc and at the wheel center, considering the clearance for the drive shaft. The lower control arm length was supposed to be 350 mm while the strut, concerning the damper and the spring, equal to 600 mm. Each component lies in a proper plane which inclination is adjustable as shown in figure 2.3.

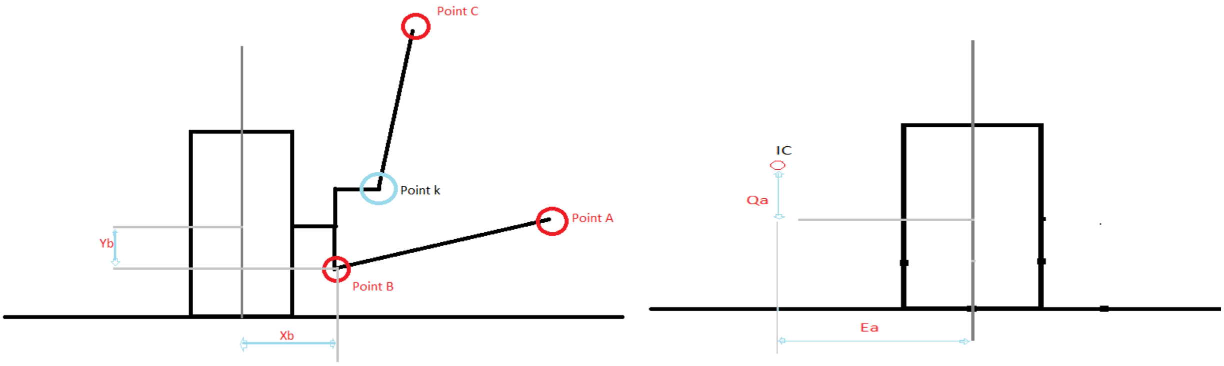

Figure 2.2 Wheel sketch in front view on the left and wheel in side view on the right

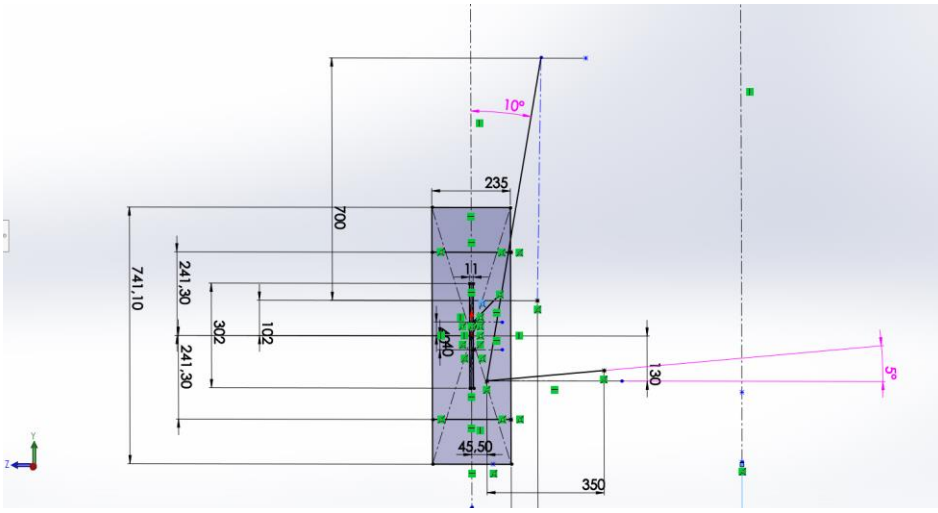

Figure 2.3 Wheel sketch in SolidWorks

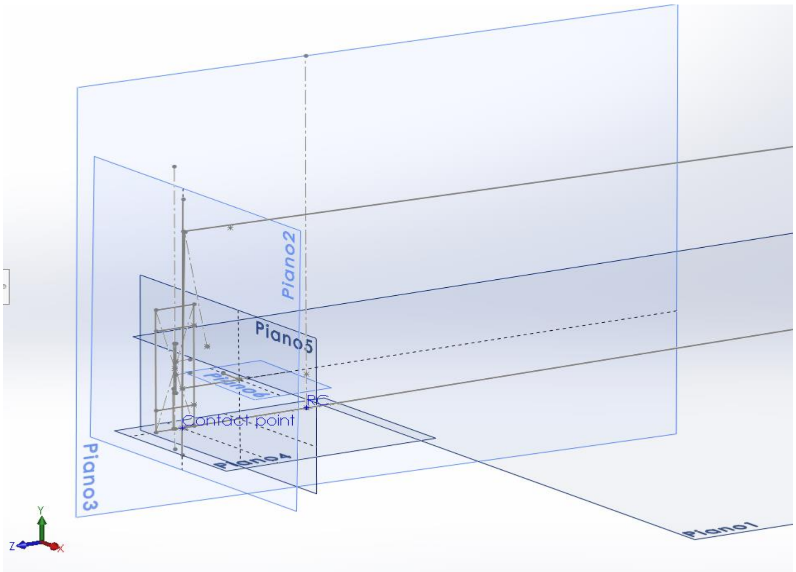

Figure 2.4 Geometric construction in Solidworks

Thanks to model created, it was possible to set some parameters as variables and see how they affect the other parameters. The following parameters will be varied:

- Kingpin angle
- Caster angle
- Lower arm inclination in front view
- Lower arm inclination in side view

The parameters to be analysed are:

- Roll centre height
- Scrub radius
- Caster trail
- Height of the pitch centre 'Qa' (Figure 2.2)
- Distance of the pitch centre from the centre of the wheel 'Ea' (Figure 2.2)

The 2-D was created to reproduce the Kingpin inclination angle, the caster angle and the inclination of the lower control arm in both front and side view. As explained in the previous chapter, the instant center ,in the front view, is found through the intersection of the plane passing through the lower control arm and the plane orthogonal to the strut. Similarly, in side view, the pitch center is found.

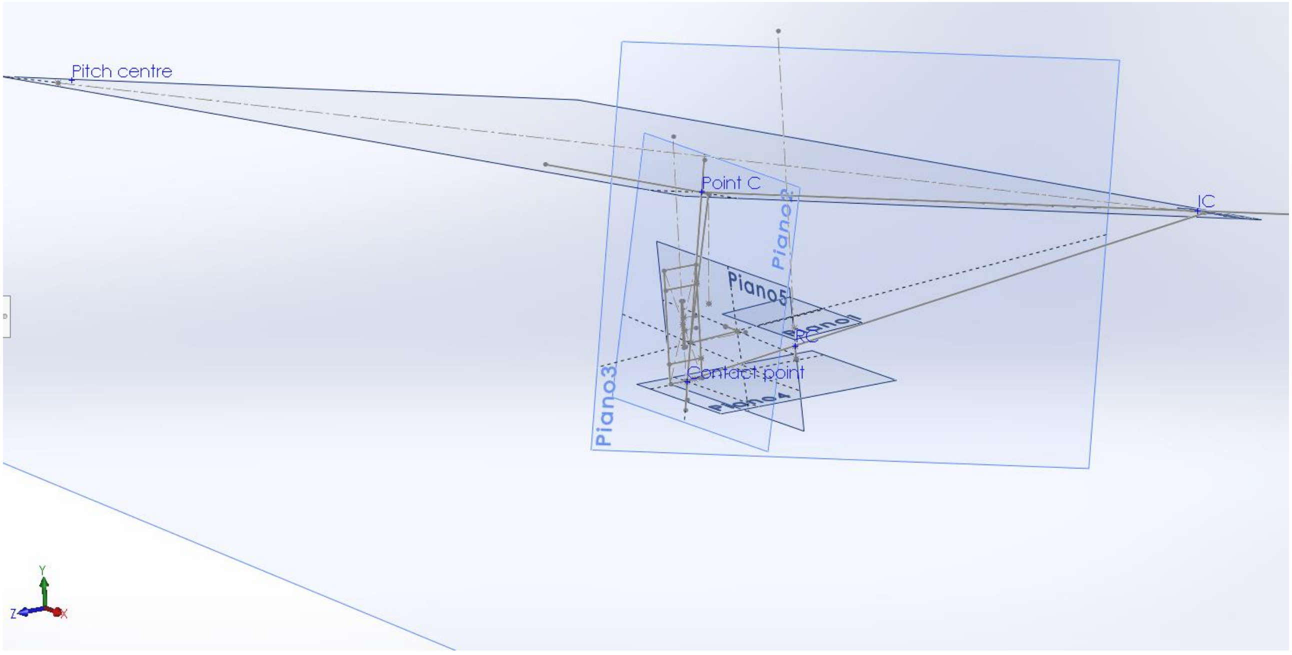

Figure 2.5 Instant axis in Solidworks

Is it possible to distinguish the influences of the planes inclination changes as following:

Front view

- Instant center height
- Roll center height
- Scrub radius

Side view

- Pitch center and anti-properties
- Caster trail

Through the graphic simulation , each parameter has been changed selectively, to study the influences on the global system. At the end a set of successful hardpoints setting is obtained.

Kingpin Angle

Table 2.3

Kingpin angle	Caster angle	Lower arm angle	Side view lower arm angle	Roll center height [mm]	Scrub radius [mm]	Caster trail [mm]	Qa [mm]	Ea [mm]	Antidive [mm]	%Antidive [mm]
10	1	0	0	4.21	-3.08	4.26	240.5	54726.5	0.25	0.9
12	1	0	0	13.75	-5.6	4.29	240.5	54726.5	0.25	0.9
14	1	0	0	23.27	-14.47	4.32	240.5	54726.5	0.25	0.9
16	1	0	0	32.73	-23.47	4.36	240.5	54726.5	0.25	0.9

Lower control arm inclination in front view

Table 2.4

Kingpin angle	Caster angle	Lower arm angle	Side view lower arm angle	Roll center height [mm]	Scrub radius [mm]	Caster trail [mm]	Qa [mm]	Ea [mm]	Antidive [mm]	%Antidive [mm]
10	0	1	0	4.21	-3.08	4.26	240.55	54726.53	0.25	0.9
10	1	1	0	21.88	-3.08	4.26	240.55	54726.53	0.25	0.9
10	2	1	0	39.5	-3.08	4.26	240.55	54726.53	0.25	0.9
10	3	1	0	57.16	-3.08	4.26	240.55	54726.53	0.25	0.9
10	4	1	0	74.79	-3.08	4.26	240.55	54726.53	0.25	0.9
10	5	1	0	92.44	-3.08	4.26	240.55	54726.53	0.25	0.9

Kingpin angle and lower arm angle

Table 2.5

Kingpin angle	Caster angle	Lower arm angle	Side view lower arm angle	Roll center height [mm]	Scrub radius [mm]	Caster trail [mm]	Qa [mm]	Ea [mm]	Antidive [mm]	%Antidive [mm]
10	1	5	0	92.4	-3.08	4.26	240.5	54726.5	0.25	0.90
12	1	5	0	101.7	-5.63	4.29	240.5	54726.5	0.25	0.90
14	1	5	0	110.9	-14.4	4.37	240.5	54726.5	0.25	0.90
16	1	5	0	119.9	-23.4	4.36	240.5	54726.5	0.25	0.90

Side view lower arm inclination

Table 2.6

Kingpin angle	Caster angle	Lower arm angle	Side view lower arm angle	Roll center height [mm]	Scrub radius [mm]	Caster trail [mm]	Qa [mm]	Ea [mm]	Antidive [mm]	%Antidive [mm]
14	1	5	1	112.2	-14.47	4.32	718.33	26516	1.55	5.59
14	1	5	2	113.5	-14.47	4.32	871.76	17457	2.85	10.3
14	1	5	3	114.9	-14.47	4.32	947.46	12987	4.17	15.03
14	1	5	4	116.23	-14.47	4.32	992.59	10323	5.49	19.79
14	1	5	5	117.6	-14.47	4.32	1022.5	8553	6.81	24.56
14.5	1	5	5	120	-16.71	4.33	1021.2	8531	6.82	24.59

Caster angle

Table 2.7

Kingpin angle	Caster angle	Lower arm angle	Side view lower arm angle	Roll center height [mm]	Scrub radius [mm]	Caster trail [mm]	Qa [mm]	Ea [mm]	Antidive [mm]	%Antidive [mm]
14.5	1	5	5	120	-16.7	4.33	1021.2	8531	6.82	24.5
14.5	2	5	5	120.5	-16.7	8.67	917	7371	7	25.5
14.5	3	5	5	121.1	-16.7	13	838.15	6493	7.3	26.5
14.5	4	5	5	121.6	-16.7	17.3	776	5807	7.6	27.4
14.5	5	5	5	122	-16.7	21.73	726.9	5256.2	7.87	28.37

Best hardpoints setting

The angle setting, listed in the previous table permits to match perfectly the desired Roll center height of 120 mm but considering a small value of caster angle. Caster angle has strong influences on the kinematics of the suspension because it improves the Camber gain and the Caster trail. More over the Caster angle improves the antidive property too. The value of 30% is used like threshold value. The following set of hardpoints is considered the best, considering all the suspension geometry parameters.

Table 2.8

Kingpin angle [Degree]	Caster angle [Degree]	Front view lower arm angle	Side view lower arm angle	Roll center height [mm]	Scrub radius [mm]	Caster trail [mm]	Qa [mm]	Ea [mm]	Antidive [mm]	%Antidive [mm]
14.5	5	5	5	120	-16.7	21.73	726.9	5256.2	7.87	28.37

2.2 Steering Mechanism

A car is usually steered by the driver imposing a torque on the steering wheel. This action is wanted and especially controlled by the driver. The design of the steering system needs to consider the accuracy of the vehicle to turn and the influence of the steering system in the kinematics of the suspension. The design of the steering system is based on the Ackermann geometry. This principle, stated by Rudolf Ackerman in the early years of the 19th century, links the turning angle of the inner wheel with the turning angle of the outer wheel during cornering. The base of the Ackermann principle is aimed to have all the four wheels turning around a common point during the maneuver. The goal of this effort is to not have any wheel slip angle between the front wheels reducing the tire wear. The condition of no slip angle during cornering is possible only at low speed, when the lateral forces are small, quite vanishing. This condition is called kinematic steering and concerns the pure rolling of the wheels. Consider a four wheels vehicle with front wheel steering like figure 2.6. To allow the wheel to have a pure rolling, the all the axis of the wheel need to intercept in point O. In so doing, the wheels run concentric trajectory. The following geometric relations can be obtained:

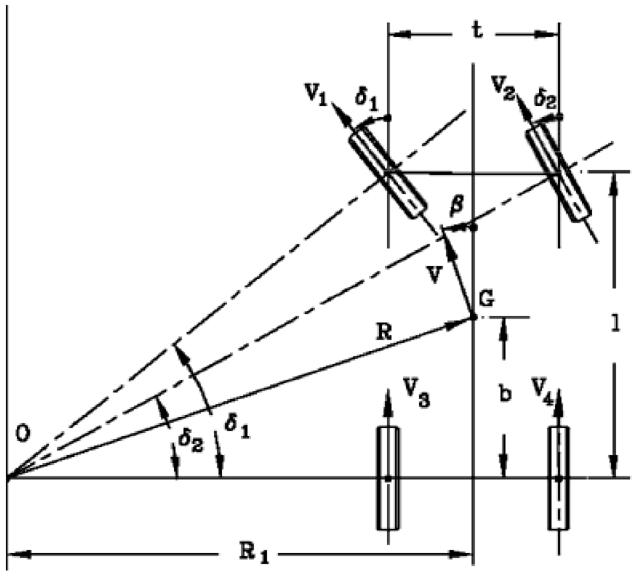

Figure 2.6 Kinematic steering [11]

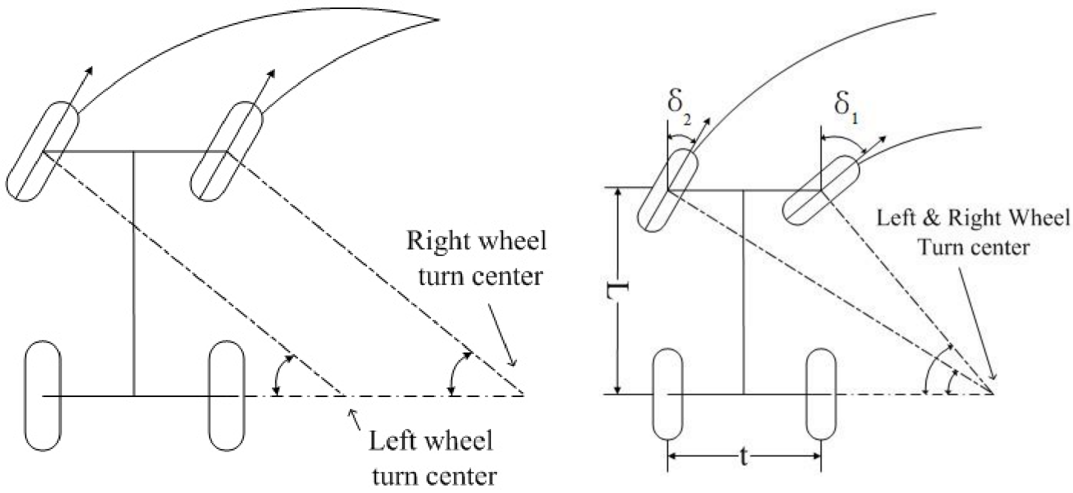

Figure 2.7 Different turning circles for parallel wheel (left) and Ackermann geometry (right)

$$\tan(\delta_1) = \frac{l}{R_1 - \frac{t}{2}}, \quad \tan(\delta_2) = \frac{l}{R_1 - \frac{t}{2}} \tag{3.1}$$

The *t* value in the previous equation is the track of the vehicle. This value should be the distance between the interception point of the kingpin axis with the ground of each wheel. The track doesn't consider the scrub radius and the caster trail. Equating the two relations (3.1), the turning radius vanishes and following relation is obtained:

$$\cot(\delta_1) - \cot(\delta_2) = \frac{t}{l} \tag{3.2}$$

The design that permits the wheels to follow the previous relation is said to be Ackermann geometry. The Ackermann geometry is an ideal condition that never is reached, due to the difficulty of design such a proper system. The condition of Ackermann is referred to an ideal condition of no wheel side slip that during high speed cornering never occurs. For this reason, the design of the steering system is aimed to reduce the steering error, that is the real value of steer angle compared to the one computed from equation 3.2.The steering error is linked to the angle γ ,defined in figure2.8.Jeantaud defined that ,if the steering arms intercept in the middle of the rear axle, the angle can be computed through the easy geometric relation:

$$\gamma = arctan\left(\frac{l_1}{2l}\right) \tag{3.3}$$

The Jeantaud relation can be used like a reference value, because the steering error is large. Moreover, the previous analysis of the steering error for the rack and pinion system follows other way. The longitudinal position of the outer tie-rod was set at 150 mm from the wheel center. Considered the actual scrub radius and caster trail for the designed suspension, the geometric construction proposed by Jeantaud has been drawn. The position of the outer tie-rod along the y-axis has been found. In the chapter of the simulation on Adams\Car will be discussed the results of this geometric choice.

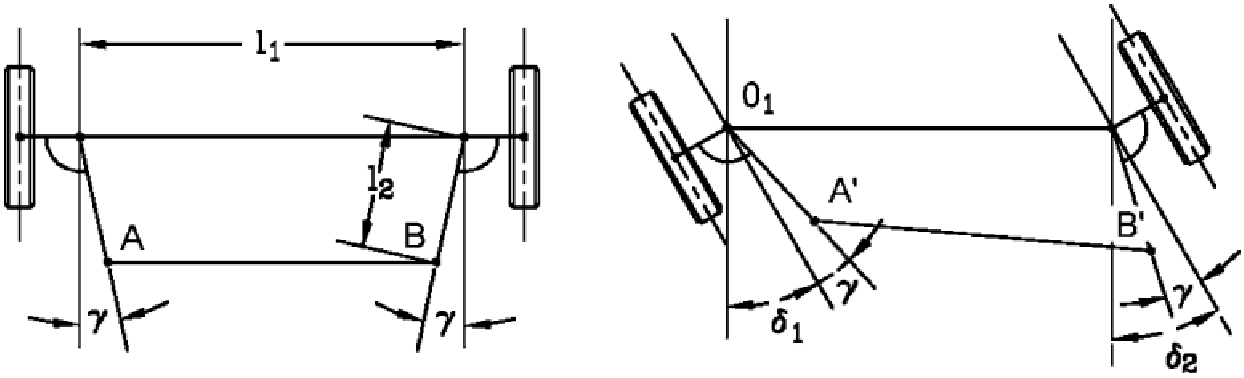

Figure 2.8 Steering system [11]

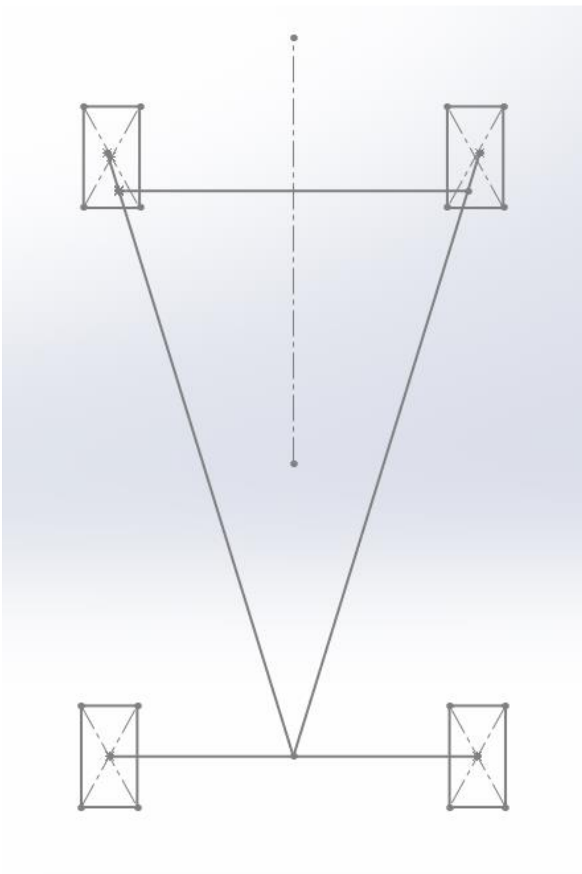

Figure 2.9 Jeantaud condition for the designed suspension

Considering figure 2.6, the following relations can be used:

$$R^2 = b^2 + {R_1}^2 \tag{3.4}$$

$$cot\delta = \frac{cot\delta_1 + cot\delta_2}{2} \tag{3.5}$$

$$cot\delta = \frac{R_1}{l} \tag{3.6}$$

The turn radius of the real vehicle used like example is known. Using the previous relations is it possible to compute the steer angle of each wheel at the maximum angle of the steering wheel in the ideal condition of Ackermann.

Table 2.9

Turning circle	11.3 [m]
Turn radius	5.65 [m]
δ_1	29.63 [deg]
δ_2	22.91 [deg]
b	1.36 [m]
l	2.66 [m]
t	1.656 [m]
R_1	5.48 [m]

During the body roll and the Bump and droop, the stirage linkage is subjected to traction or compression force depending on the position of the external ball joints leading to the following effects:

- Bump steer

  The independent layout decouples the two wheels allowing them to have a different vertical motion. Bump steer concerns changes of steer for a single wheel.

- Roll steer

  Regardless the independent layout, the body roll influences the two wheels simultaneously, hence the whole axle.

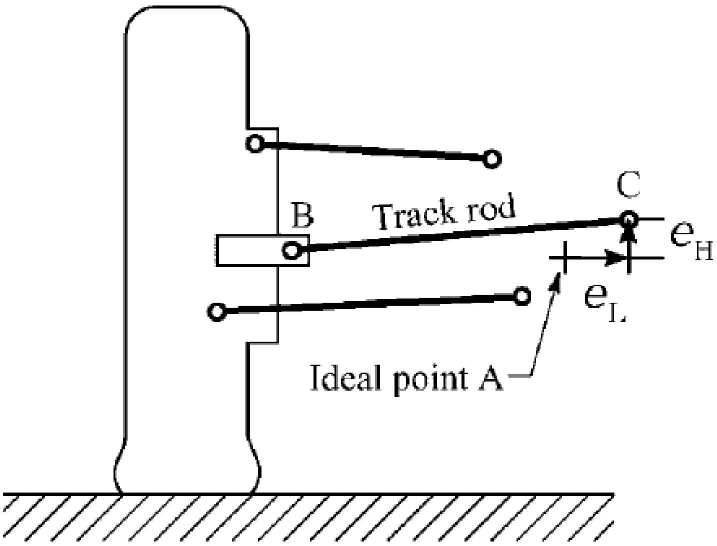

Figure 2.10 Tie-rod Geometry [9]

To design properly the tie-rod system is necessary to consider:

- The inclination of the track rod
- The length of the track rod

The geometric construction of the instant center and, hence, of the Roll center is made in two dimensions not considering the tie-rod. The motion of the wheel can be considered like a rotation about the kingpin axis and about the Instant axis. To consider the wheel rotating just about the instant axis, the extension of the tie rod should pass through the instant center setting the tie rod inclination.

In figure 2.10 is shown the ideal position of the inner ball joint of the relay linkages for a certain geometry of the suspension arms. Is considered to design the relay linkage rear the wheel center. During the bump, the correct track rod varies greatly with the change of arms inclination. If point C is inner than the ideal point A, the track rod is pushed making that wheel turn inwards. On the contrary, if the point C is outer than the ideal point A ,the track rod is pulled making the wheel turning outwards.Similarily if the point C is upper respect the ideal point A ,during the bump the track rod is pushed and the wheel turns inwards while if the point C is below the ideal point ,during the droop, the track rod is pulled and the wheel turns outwards. To reduce this influence, the following geometrical construction has been followed.

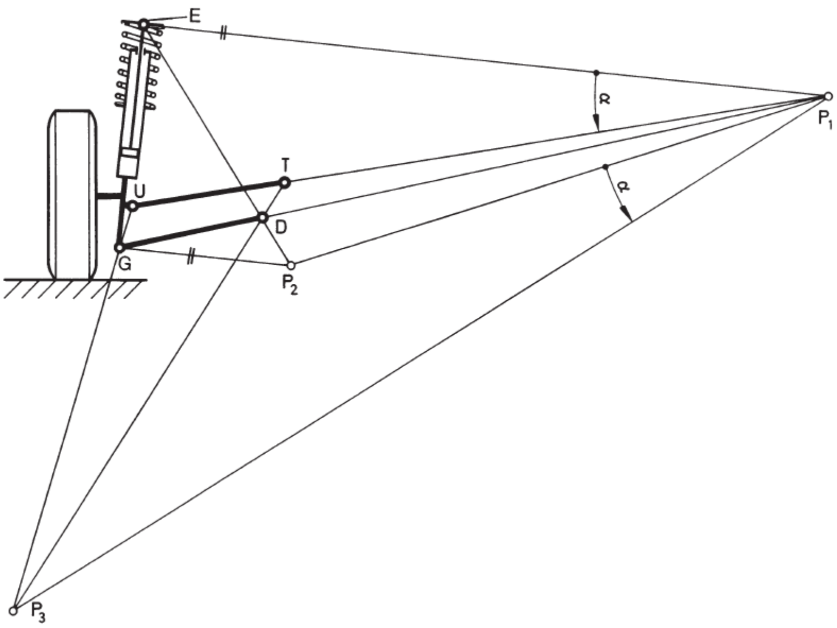

Figure 2.11 Geometric construction for tie-rod [10]

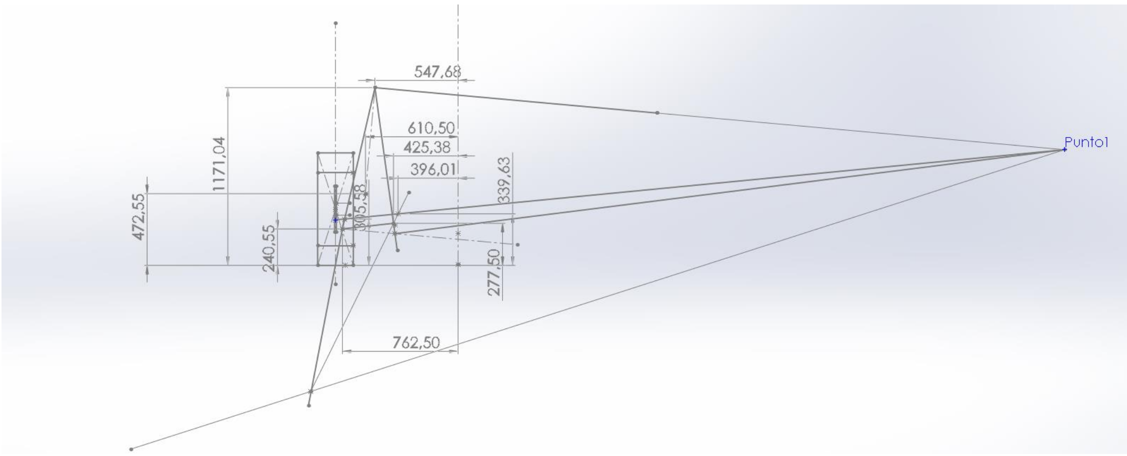

Figure 2.12 Geometric construction in Solidwork

2.3 Elastic Components

The elastic components mounted on a vehicle are the springs and the dampers. They are necessary to ensure proper handling and comfort. The springs support the total weight of the vehicle reaching the static equilibrium setting the proper preload. Compressing and extending, the springs allow the vehicle to adapt to the external unevenness, ensuring to restore the static configuration thanks to the elastic properties. The dampers are in charge to limit the noisy vibrations which affect the dynamics of the car and stress the vehicle components. The elastic components are fundamental to improve the comfort of the passengers limiting the bounce, the pitch and the yaw moment. The design of the elastic components starts from the comfort criteria as stated by Olley's criteria.

2.3.1 Olley's criteria

The most annoying vibration modes affecting the vehicle are the bounce, vertical motion of the chassis, and the pitch, concerning a rotation of the chassis about the Y axis, the axis that comes out from the paper in figure 2.13.Many studies have demonstrated that for human's beings the frequency close to 1 Hz is comfortable. The pitch mode is more annoying than the bounce, so it is necessary to reduce it, especially for the driver. For this reason, the design follows the following rules:

- Both natural frequencies must fall in the range 1.0-1.5 Hz;
- The pitch mode should have its node located at about the front seat.

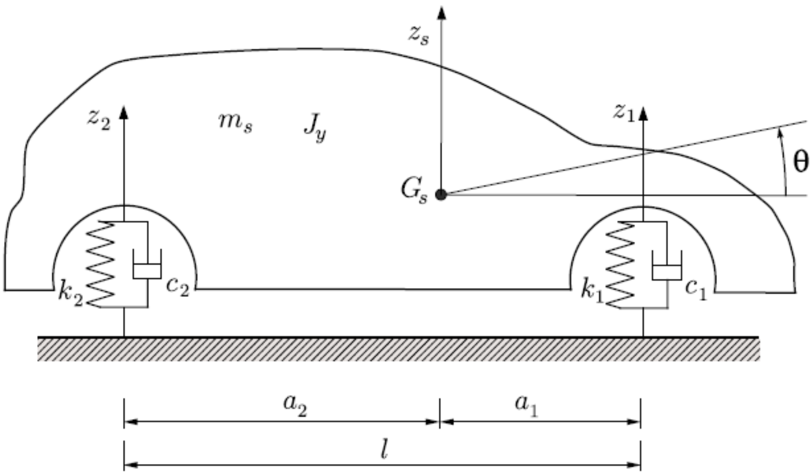

Figure 2.13 Two-degree-of-freedom system for bounce and pitch analysis [2]

Bounce degree of freedom

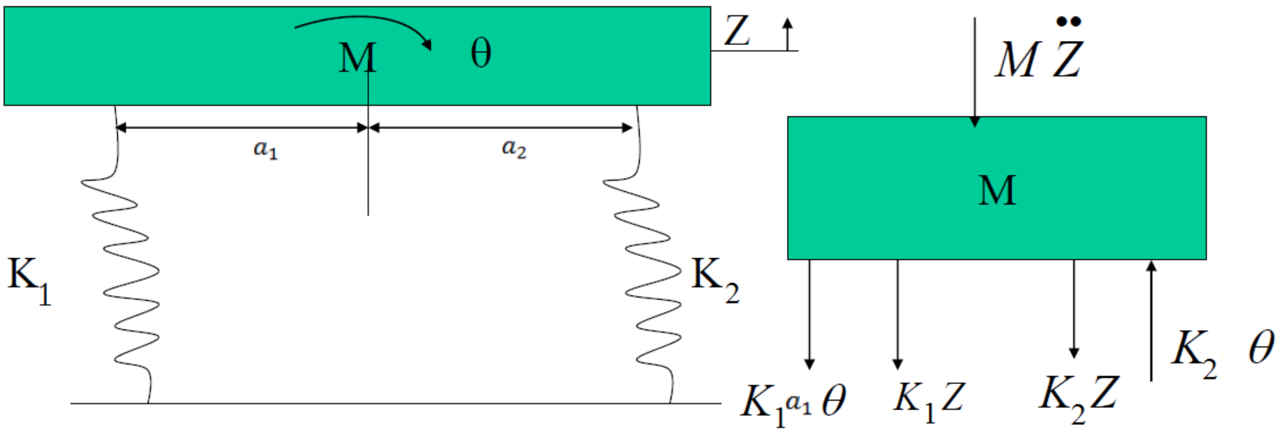

Figure 2.14 Freebody diagram for the bounce mode [11]

From the Freebody diagram shown in figure 2.14, the equilibrium equations follow:

$$M\ddot{z} + (K_1 + K_2)z + (K_2a_2 - K_1a_1)\theta = 0 \tag{3.1}$$

$$\ddot{z} + \frac{(K_1+K_2)z}{M} + \frac{(K_2a_2-K_1a_1)\theta}{M} = 0 \tag{3.2}$$

Considering the following writing simplifications, the (3.2) can be written like (3.3):

$$\alpha = \frac{(K_1 + K_2)}{M}$$

$$\beta = \frac{(K_2a_2-K_1a_1)}{M}$$

$$\Gamma = \frac{(K_1{a_1}^2-K_1{a_2}^2)}{M}$$

$$\ddot{z} + \alpha z + \beta\theta = 0 \tag{3.3}$$

Pitch degree of freedom

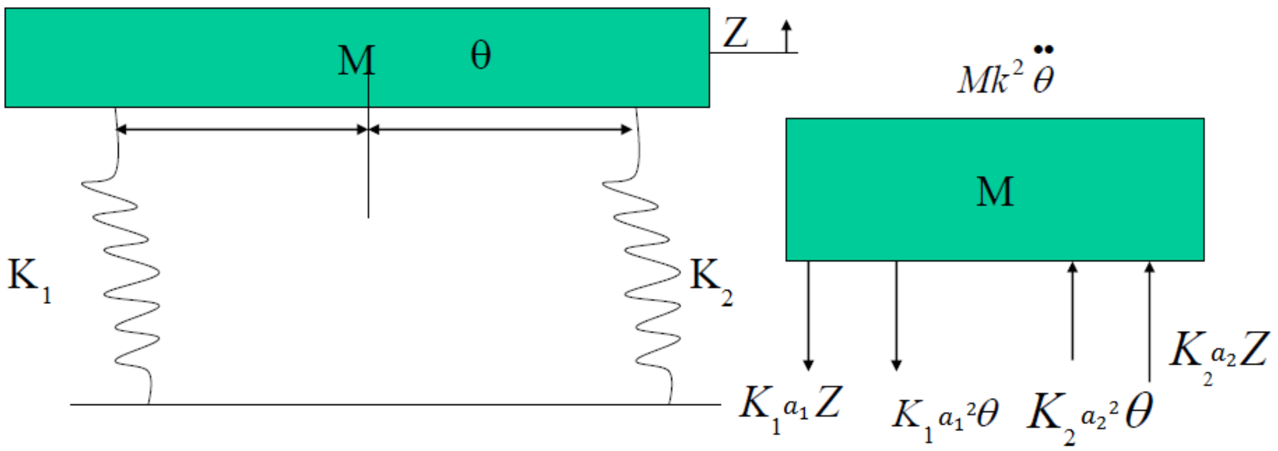

Figure 2.15

$$Mk^2\ddot{\theta} + (K_1{a_1}^2 + K_2{a_2}^2)\theta + (K_2a_2 - K_1a_1)z = 0 \tag{3.4}$$

$$\ddot{\theta} + \frac{(K_1{a_1}^2+K_2{a_2}^2)}{Mk^2}\theta + \frac{(K_2a_2-K_1a_1)}{Mk^2}z = 0 \tag{3.5}$$

$$\ddot{\theta} + \gamma\theta + \frac{\beta}{k^2}z = 0 \tag{3.6}$$

Where:

- K_1 is the front axle stiffness
- K_2 is the rear axle stiffness
- a_1 is the distance from the front axle to the center of gravity
- a_2 is the distance from the rear axle to the center of gravity
- I_y is the Pitch moment of Inertia
- $k = \sqrt{\frac{I_y}{M}}$ is the Radius of gyration

Resuming, the equilibrium equations are:

$$\ddot{z} + \alpha z + \beta\theta = 0 \tag{3.3}$$

$$\ddot{\theta} + \gamma\theta + \frac{\beta}{k^2} z = 0 \tag{3.6}$$

In both equations there is the coefficients β that couples both the equations and therefore is called coupling coefficient. When $\beta = 0$ there is not coupling. For this condition, a vertical force applied in the center of gravity produces only bounce motion and similarily a torque applied to the chassis produces only pitch motion.

Neglecting the damping, the solutions of the differential equations have sinusoidal shape:

$$z = zsin(\omega t) \tag{3.7}$$

$$\theta = \theta\sin(\omega t) \tag{3.8}$$

Substituting (3.7) and (3.8) respectively in (3.3) and in (3.6):

$$-z\omega^2 sin(\omega t) + \alpha z\sin(\omega t) + \beta\theta sin(\omega t) = 0 \tag{3.9}$$

$$-\theta\omega^2 sin(\omega t) + \gamma\theta\sin(\omega t) + \frac{\beta}{k^2} zsin(\omega t) = 0 \tag{3.10}$$

Simplifying the $sin(\omega t)$ and bracketing the similar variables (3.9) and (3.10) can be written like:

$$(\alpha - \omega^2)z + \beta\theta = 0 \tag{3.11}$$

$$(\gamma - \omega^2)\theta + \frac{\beta}{k^2} z = 0 \tag{3.12}$$

Rearranging the previous equations:

$$\frac{z}{\theta} = -\frac{\beta}{(\alpha - \omega^2)} \tag{3.13}$$

$$\frac{z}{\theta} = -\frac{k^2(\gamma - \omega^2)}{\beta} \tag{3.14}$$

Equation (3.13) and (3.14) are the modes of the system. To get the natural frequencies at which the system vibrates is necessary to equate the previous equations and solve them for ω.

$$(\alpha - \omega^2)(\gamma - \omega^2) = \frac{\beta^2}{k^2} \tag{3.15}$$

$$\omega^4 - (\alpha + \gamma)\omega^2 + \left(\alpha\gamma - \frac{\beta^2}{k^2}\right) = 0 \tag{3.16}$$

Solve the (3.16) for ω^2 the natural frequencies are obtained:

$$(\omega_{1,2})^2 = \frac{(\alpha+\gamma)}{2} \pm \sqrt{\frac{(\alpha+\gamma)^2}{4} - \left(\alpha\gamma - \frac{\beta^2}{k^2}\right)} \tag{3.17}$$

Rearranging the previous equation:

$$(\omega_{1,2})^2 = \frac{(\alpha+\gamma)}{2} \pm \sqrt{\frac{(\alpha-\gamma)^2}{4} + \left(\frac{\beta^2}{k^2}\right)} \tag{3.18}$$

$$\omega_1 = \sqrt{\frac{(\alpha+\gamma)}{2} + \sqrt{\frac{(\alpha-\gamma)^2}{4} + \left(\frac{\beta^2}{k^2}\right)}} \tag{3.19}$$

$$\omega_2 = \sqrt{\frac{(\alpha+\gamma)}{2} - \sqrt{\frac{(\alpha-\gamma)^2}{4} + \left(\frac{\beta^2}{k^2}\right)}} \tag{3.20}$$

Using the computed natural frequencies in (3.13) and (3.14) can be found the amplitude ratio of the two motions. When the ratio is positive it concerns that z and θ are simultaneously both positive or both negative. The oscillation center is in the first case in ahead the center of gravity while behind it in the second case. One distance is large enough to lies outside the wheelbase and the other one lies within the wheelbase. In the first case the motion is bounce and the related frequency is the bounce frequency while in the second case the motion is pitch and the related frequency is called pitch frequency as shown in figure 2.16.

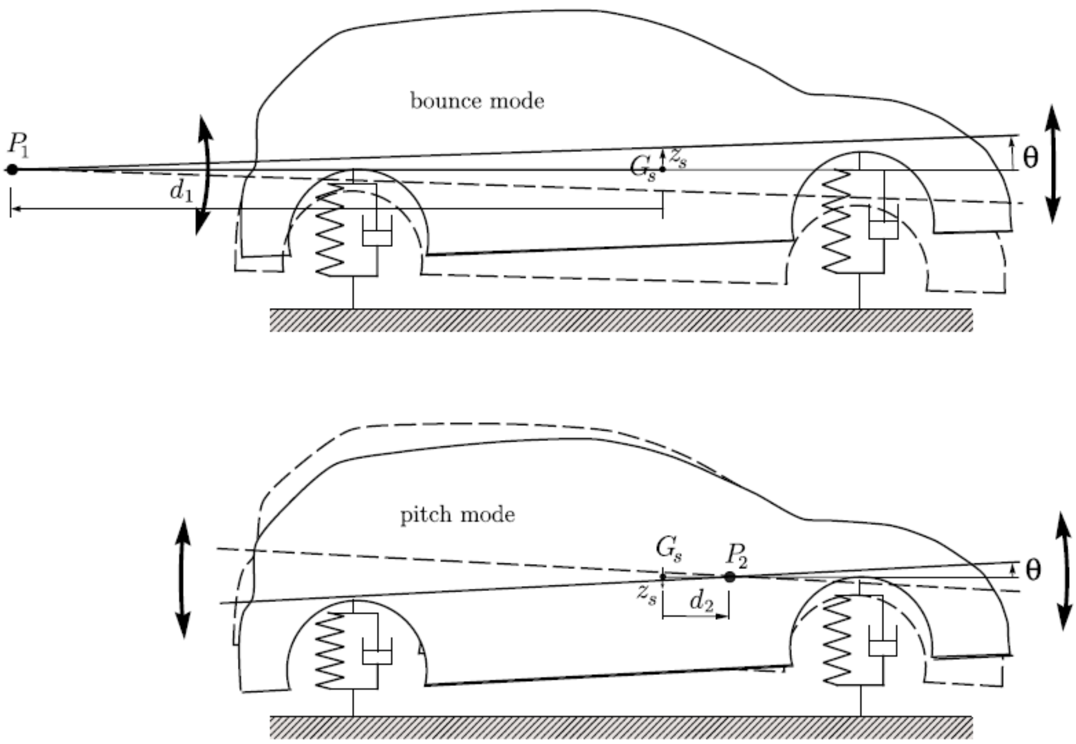

Figure 2.16 Vibration modes

The location of the motion centers are linked to the natural frequencies of each axle.

$$f_f = \frac{1}{2\pi}\sqrt{\frac{K_f g}{W_f}} \tag{3.21}$$

$$f_r = \frac{1}{2\pi}\sqrt{\frac{K_r g}{W_r}} \tag{3.22}$$

Where:

- Kf is the stiffness of the front axle
- Kr is the stiffness of the rear axle
- g is the gravitational constant
- Wf is the weight at the front axle
- Wr is the weight at the rear axle

Olley recognized that a lower front frequency makes the bounce center lie behind the rear axle and the pitch center near the front axle. This condition provides good ride. The Olley criteria state that:

- The rear suspension should have 30% higher ride rate compared to the front suspension
- The pitch and the bounce frequencies should be close together
- The pitch and the bounce frequencies should be smaller than 1.3 Hz

2.3.2 Design of the Springs

In accordance with what stated before, a trial and error methodology has been used trying different combination of front and rear spring stiffness to make the natural frequencies lie within the desired range.

Table 2.10

Front axle stiffness Kf	45000 [N/m]
Front rear stiffness Kr	50000 [N/m]
ω_f	6.11 [rad/s]
ω_r	6.59 [rad/s]
α	40.33 [1/s^2]
β	4.03 [m/s^2]
γ	66.7 [1/s^2]
k	1.035 [m]
ω_1	1.3 [Hz]
ω_2	1 [Hz]
$Z/_{\theta} \mid \ \omega_1$	0.15 [m] (Pitch)
$Z/_{\theta} \mid \ \omega_2$	-7.16 [m] (Bounce)

- The Ride rate is defined as vertical force per unit vertical displacement of the tire ground contact with respect to chassis.

The ride rate can be computed as the half of the axle stiffness. To choose the proper spring to install on the vehicle, is it necessary to considering a fundamental parameter, the installation ratio.

- The installation ratio is the ratio of the displacement of the wheel center respect to the displacement of the spring.

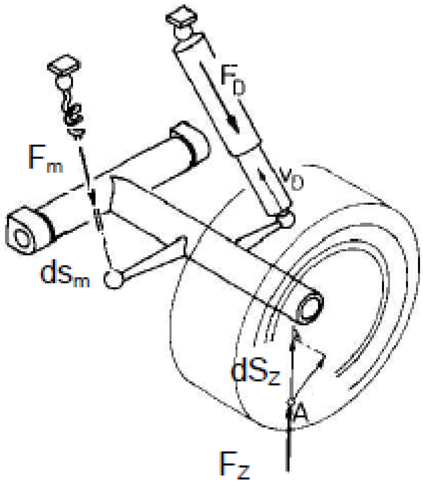

Figure 2.17 Suspension system [8]

Considering figure 2.17, the suspension system is subjected to the force F_z exterted by the ground to the tire at the contact patch and to F_m,the force exerted by the spring. From the principle of virtual work:

$$F_z ds_z = F_m ds_m \quad (3.23)$$

Where ds_z is vertical component of the tire displacement and ds_m is the compression of the spring. Formula 3.23 can be rearranged and written as:

$$F_z = F_m \frac{ds_m}{ds_z} = F_m i_m \quad (3.24)$$

i_m is the installation ratio and represents both the ratio between the displacement of the wheel and the spring and the displacement of the forces:

$$i_m = \frac{ds_m}{ds_z} = \frac{F_z}{F_m} \tag{3.25}$$

Considering the definition of stiffness:

$$k_a = \frac{dF_z}{ds_z} = \frac{\partial F_z}{\partial F_m}\frac{dF_m}{ds_z} + \frac{\partial F_z}{\partial i_m}\frac{di_m}{ds_z} \tag{3.26}$$

Is it possible to consider the following terms:

$$\frac{\partial F_z}{\partial F_m} = i_m \tag{3.27}$$

$$\frac{\partial F_z}{\partial i_m} = F_m \tag{3.28}$$

$$\frac{dF_m}{ds_z} = \frac{\partial F_m}{\partial s_m}\frac{ds_m}{ds_z} = \frac{\partial F_m}{\partial s_m} i_m = k_m i_m \tag{3.29}$$

The formula 3.26 can be written in the following way:

$$k_a = k_m {i^2}_m + \frac{F_m}{i_m}\frac{di_m}{ds_z} \tag{3.30}$$

The previous equations relate the stiffness of the spring to the ride rate through a geometric squared parameter, that is the installation ratio, and through a kinematic term which evaluate the variation of the installation ratio during the bump. For the choice of the necessary spring the kinematic terms are neglected.

For the Macpherson strut the installation ratio, as simplification, can be considered close to the cosine of the inclination of the strut. As first attempt is considered the kingpin angle equal to 14 degrees.

When a vehicle is in a turn is subjected to two forces that produce the body roll:

- Lateral or centrifugal force exerted on the center of gravity in outwards direction respect to the turn
- Lateral forces exerted on the wheel in opposite direction respect to the centrifugal force

Considered the weight of the vehicle and defined in steady state the distance H of the roll axis from of the center of gravity, shown in figure 2.18, the total roll moment acting on the vehicle is:

$$Mr = W a_y H \tag{3.31}$$

- The roll sensitivity is the value of body roll in radians per acceleration g and is defined like following:

$$\frac{\varphi}{a_y} = \frac{-WH}{K_f+K_r} = K_\varphi \tag{3.32}$$

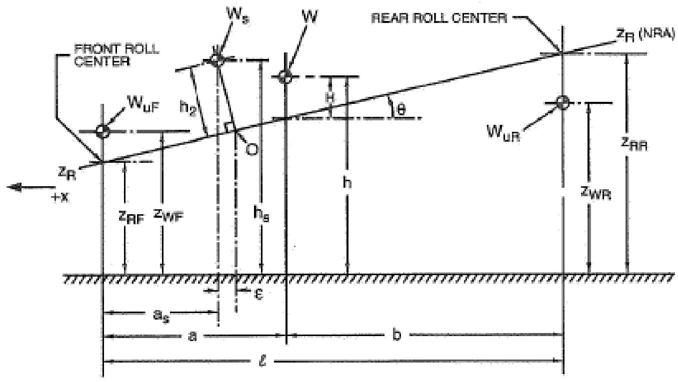

Figure 2.18 Roll axis [3]

It was chosen the value of 5 degree/g as roll sensitivity. To reach this value, the elastic elements need to be designed properly.

- The suspension roll rate is the value of the torque produced by the lateral force to make the body roll of one degree. Springs and anti-roll bars counteract the body roll.

In the equation (3.34), $(K_f + K_r)$ concerns the total contribution to the body roll from both springs and anti roll bars and is the desired roll stiffness to achieve the desired roll sensitivity. The influences of the springs on the body roll depends on the track of the vehicle.

$$k_\varphi = k_a \frac{t^2}{2} \tag{3.33}$$

Table 2.11

Front ride rate	22500 [N/m]
Rear ride rate	25000 [N/m]
Installation ratio	0.97
k_{mf}	23898 [N/m]
k_{mr}	26554 [N/m]
$k_{\varphi f}$	29378.88 [Nm/rad]
$k_{\varphi r}$	32643.2 [Nm/rad]
Mr	11539 [Nm]
Roll angle	5 [degree]
Roll sensitivity	0.0872 [rad/g]
H	490 [mm]
$k_{\varphi desired}$	132300 [Nm/rad]
Δk_{φ}	70277.91 [Nm/rad]

The stiffness of the front and rear springs is related to the Olley's criteria and cannot be changed, hence, the contribution to the suspension roll rate is defined. The difference between the desired roll stiffness and the sum of the front and rear roll stiffness must be covered by the anti-roll bars.

2.3.3 Anti-Roll bar

The anti-roll bar is an elastic element that twists about its own axis, hence its characteristic is the torsional stiffness. The function of the anti-roll bar is to reduce the body roll during cornering and influences the under/oversteer behaviour of the vehicle. During the bump and droop, when the both wheels moves simultaneously, the anti-roll bar doesn't influence the vertical motion or the natural frequencies.

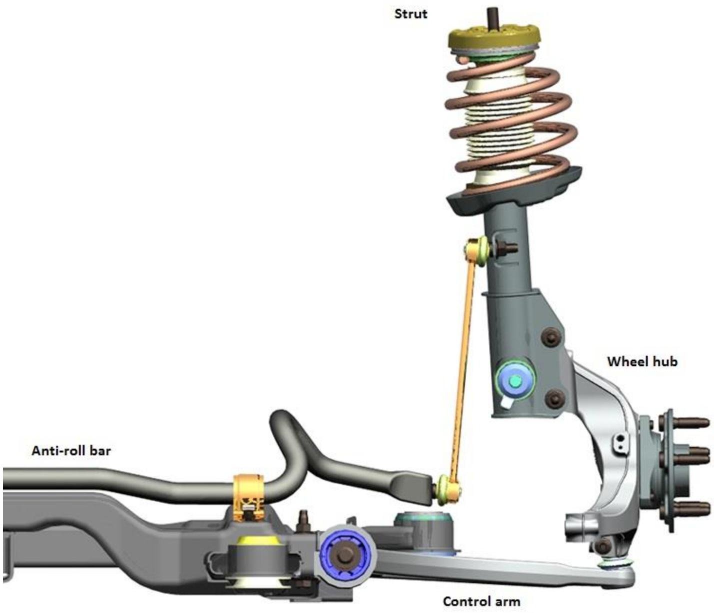

Figure 2.19 Anti roll-bar on Macpherson layout

To explain clearly how the anti-roll bar influences the handling of a vehicle is necessary to introduce the concept of lateral load transfer.

2.3.4 Lateral Load Transfer

In a steady-state turn the vehicle, as previously stated, is subjected to a centrifugal force applied at the center of gravity that makes the chassis roll outwards. During the body roll the outer wheels are more loaded than the inner wheels, this is called lateral load transfer. It depends only on the geometry of the vehicle, hence, track and center of gravity height.

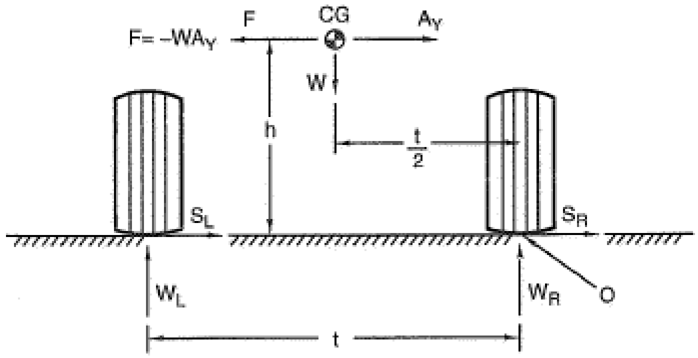

Figure 2.20 Total lateral load transfer [3]

Computing the rotational equilibrium equations, the lateral load transfer is:

$$LLT = \frac{A_Y h}{t} \tag{3.34}$$

Where:

- LLT is the total lateral load transfer over the total weight
- A_Y is the lateral acceleration
- h is the height of the center of gravity
- t is the track of the vehicle

From equations (3.33) is clear that total lateral load transfer is always the same for a given vehicle for a given lateral acceleration. The total lateral load transfer is influences by two aspects:

- Elastic members stiffness
- Height of the Roll center at the front and rear axle

Considering the front and the rear axle, the lateral load transfer on each axle can be varied, adjusting the ratio of the torsional stiffness between front and rear axle. The anti-roll bar influences the torsional stiffness of each axle, so it affects the lateral load transfer on each axle. Considering the previous equations (3.33) and (3.35) the following relations are obtained:

$$\frac{\Delta W_f}{a_y} = \frac{W}{t_f}\left[\frac{HK_f}{K_f+K_r} + \frac{b}{l} z_{Rf}\right] \tag{3.35}$$

$$\frac{\Delta W_r}{a_y} = \frac{W}{t_r}\left[\frac{HK_r}{K_f+K_r} + \frac{a}{l} z_{Rr}\right] \tag{3.36}$$

Equating the equations (3.36) and (3.37), the value of the anti-roll bars roll rate is obtained. This condition leads to the same lateral load transfer on each axle.

Table 2.12

	Roll rate [Nm/rad]
Front Anti-roll bar	48394
Rear Anti-roll bar	21883

2.3.5 Design of The Anti-roll bar

The previous values are the request roll rate contribution from the anti-roll bar. To know the proper torsional stiffness and design the anti-roll bar is necessary to consider the how it is installed on the suspension system. The contribution of the anti-roll bar to the total roll rate is:

$$K_{\varphi} = K_{\theta} I^2 \left(\frac{T^2}{L^2}\right) \tag{3.37}$$

Where:

- K_{θ} is the torsional stiffness in [Nm/rad];
- I^2 is the installation ratio of the bar
- T^2 is the track width
- L^2 is the anti-roll lever arm

Known the desired roll rate, the installation ratio is supposed for the first attempt to be the same of the one considered for the spring, as the anti-roll bar, is attached to the strut and considered a value for the lever arm, the torsional stiffness is computed.

Table 2.13

T	1616 [mm]
L	300 [mm]
I	0.97
K_{φ}	844206.5 [Nmm/deg]
K_{θ}	30921.8 [Nmm/deg]

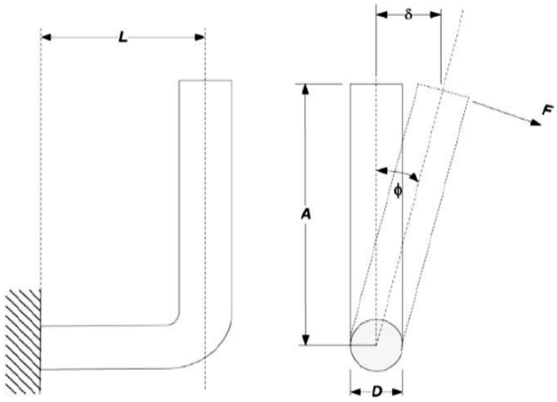

Figure 2.21 Anti-roll bar scheme

Considering figure 3.18:

$$K_{bar} = \frac{F}{\delta} = \frac{F}{A\varphi} \tag{3.38}$$

For a torsion bar the twist is:

$$\varphi = \frac{32LFA}{\pi G D^4} \tag{3.39}$$

So:

$$K_{bar} = \frac{\pi G D^4}{32LA^2} \tag{3.40}$$

The anti-roll bar can be thought like two stiffness in series, the bar itself and the lever arm, so the total stiffness is:

$$\frac{1}{K_{arb}} = \frac{1}{K_{bar}} + \frac{1}{K_{arm}} \tag{3.41}$$

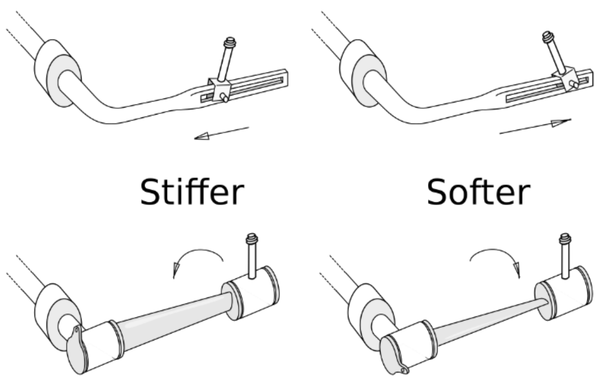

Figure 2.22 Anti-roll bar lever arm length

2.3.6 Dampers

The damper is a mechanical component which function is to reduce the amplitude of the vibrations exerted from the tire and spread to chassis. Dampers improve the comfort reducing the vertical motion of the chassis and improve the handling of the vehicle reducing the amplitude of the force exerted from the ground to the tire, allowing the tire to have always the best condition to copy the road profile. The quarter car model is used to focus the study on the single system spring, damper, wheel. The chassis, the passenger and part of the suspension architecture is suspended mass. The wheel, the brake disc, the knuckle and part of the suspension is non-suspended mass.

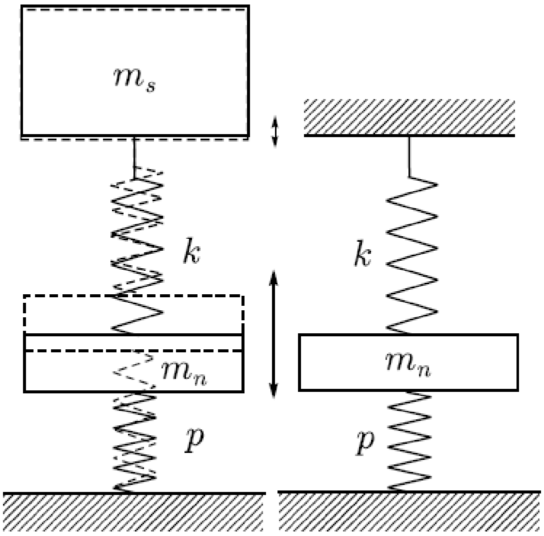

Figure 2.23 Quarter car model [2]

For road cars, the interest of the design is to limit the vibration of the chassis to improve comfort. As studied and suggested by Guiggiani, the optimal damping coefficient is the one that provide a horizontal tangent at point A, as shown in figure 3.21. The value of the optimal damping coefficient is:

$$c_{opt} = \sqrt{\frac{m_s k}{2}}\sqrt{\frac{p+2k}{p}} \tag{3.42}$$

The second term is close to one, so negligible. Considering for each axle the mass loading on it and the value of the stiffness, the optimal damping for each axle is computed.

Table 2.14

c_1	5204 [Ns/m]
c_2	5364 [Ns/m]
c_{fwheel}	2602 [Ns/m]
c_{rwheel}	2682 [Ns/m]
$c_{fdamper}$	2710 [Ns/m]
$c_{rdamper}$	2793 [Ns/m]

In the same way is possible to relate the damping value at the wheel center and at the damper itself through the same consideration:

$$c_{fdamper} = c_{fwheel} {i^2}_m \tag{3.43}$$

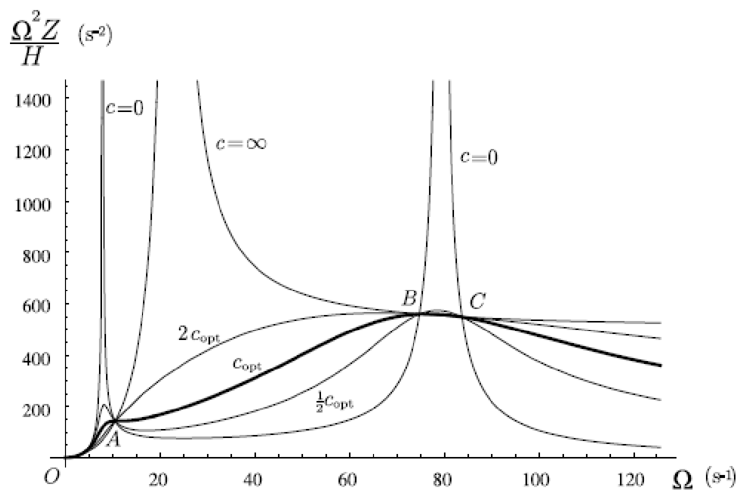

Figure 2.24 Amplitude of the sprung mass of a road vehicle [2]

3.MODELLING AND ANALYSIS OF THE MACPHERSON IN ADAMS\CAR

3.1 Introduction to Adams\Car

Adams\Car is a suite of the well-known multibody dynamics software Adams. The Multibody Dynamics concerns the study of multiple rigid bodies connected through joints that limit the motion of the bodies. The goal of the analysis is, imposing an external force on the system or a forced motion, understand how the whole system moves and how the strain is shared between the rigid bodies. For complex system, like a car suspension, the final motion is often unpredictable because of the geometry, therefore a powerful tool is necessary to investigate the influence of each body on the whole motion.

3.2 Approaching Adams

Adams\Car is composed of two environments:

- Template builder
  In this area is it possible to create your own templates, starting by the geometric definition of the hardpoints. The steps to follow to create a model are:

1) Define the position of the hardpoints, figure 4.1
2) Define the parts, hence a rigid entity, assigning coordinate references and mass properties
3) Define a geometry to the parts
4) Assign joints or bushing that connect the parts
5) Define force elements like springs and dampers

Once completed the model, in Adams\Car is necessary to define the communicators. When the template is used in the standard interface in a suspension or full-vehicle assembly, each subsystem swap information about location or role. There are output communicators, like camber angle and toe-angle, that provides information on the respective parameters during the simulation and input communicator, like wheel center location, that inform the test rig where it must relate to the template.

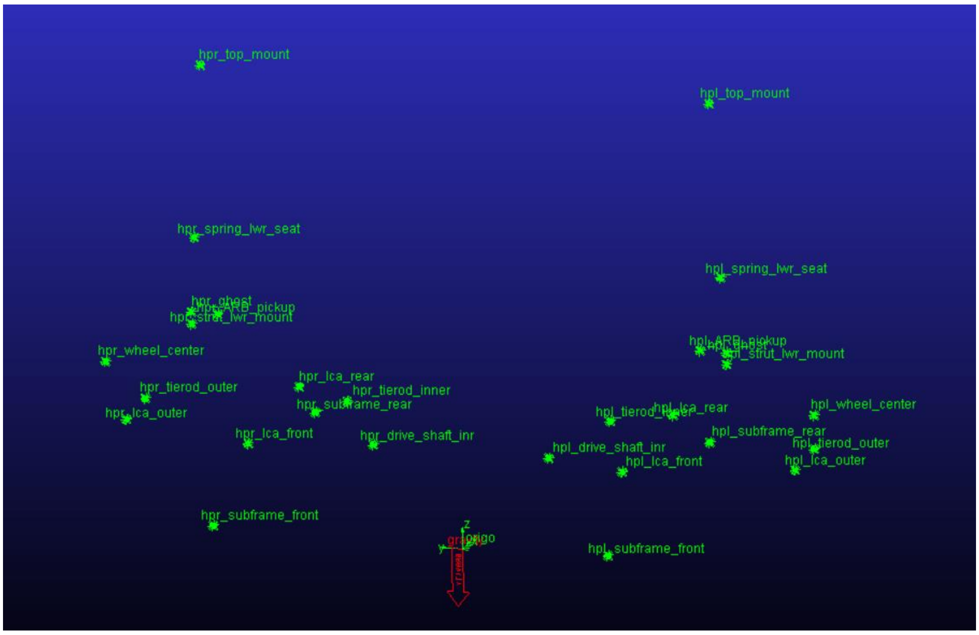

Figure 3.1 Hardpoints setting

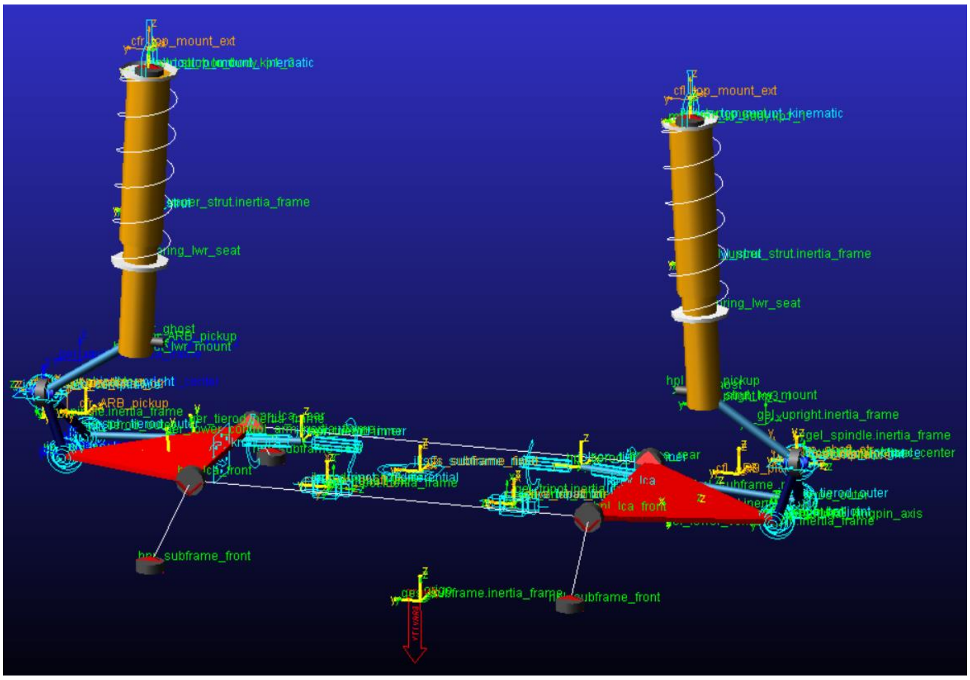

Figure 3.2 Macpherson template

- Standard user interface:
  In this area, the user can lead several kinds of simulation on the system: kinematic, quasi-static, static and dynamic. Is it possible to conduct simulation on a single component like a tire or on a suspension system or on a full-vehicle thanks to the test-rig, a subsystem that forces the motion of the wheel of the suspension system or exerts forces at the contact patch. The suite provides a user-friendly post-processor which has many already defined requests ready to be plotted.

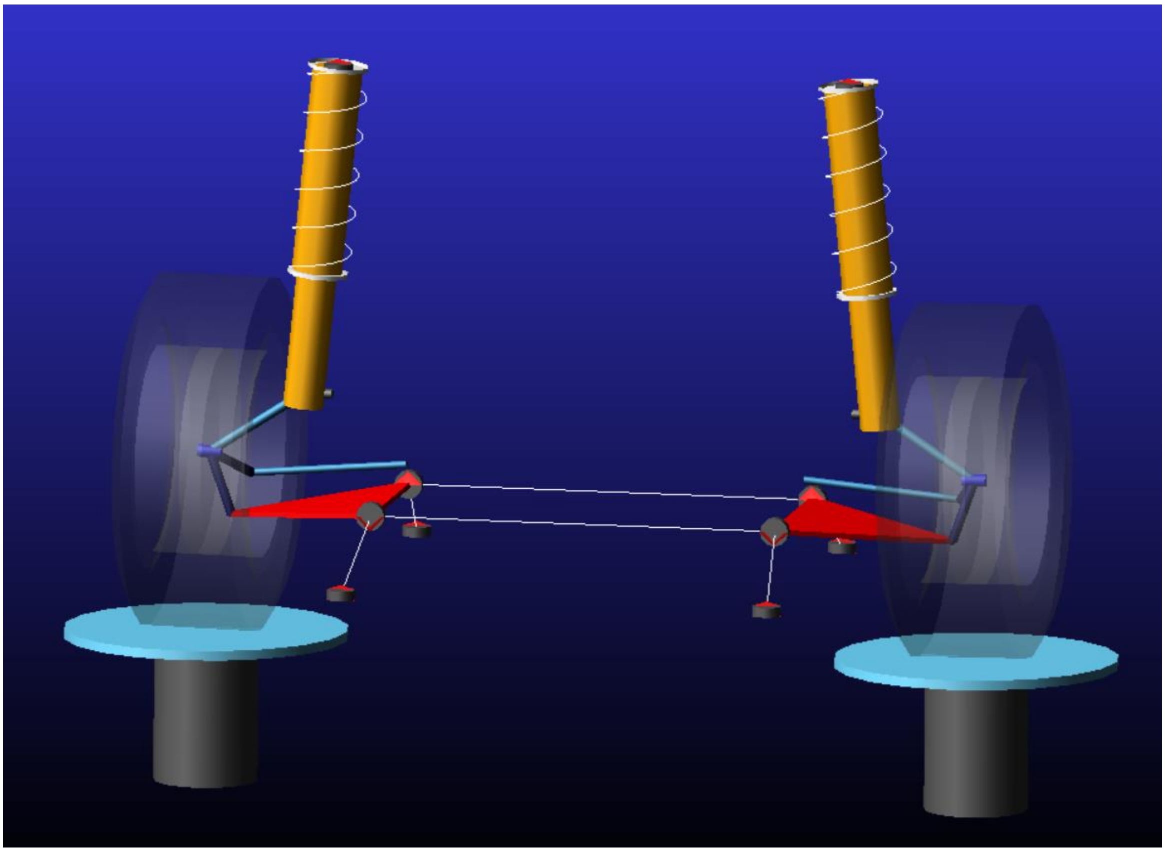

Figure 3.3 Suspension assembly and test rig

In the stand-alone simulation on the suspension assembly, the top mount of the strut, the chassis side of the lower control arm and the inner side of the tie-rod are connected on a fixed frame while the wheel is moved vertically.

3.3 Simulations

Spring stiffness and damping coefficient have been set like the value computed in the previous chapter, no preload has been set. The coordinates used are the one found in the previous chapters and defined as the best one, computed with SolidWorks. The simulation conducted on the suspension system is the Parallel Wheel Travel. The test rig, moves the wheels up and down, keeping fixed the top mount of the strut and the inner side of the lower control arm. In figure 4.4 are shown the inputs given for the simulation.

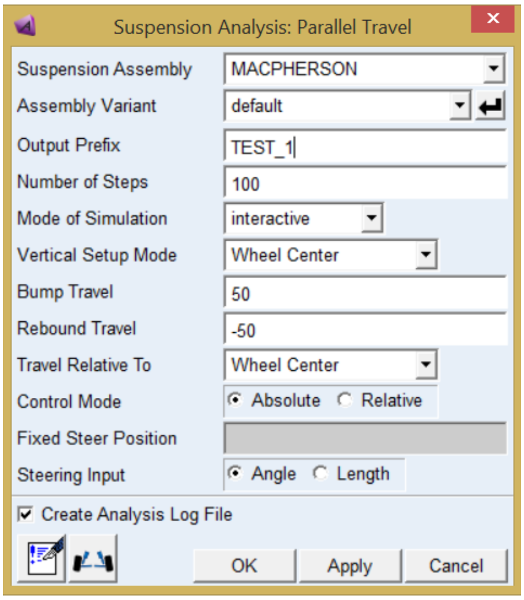

Figure 3.4 Input Window

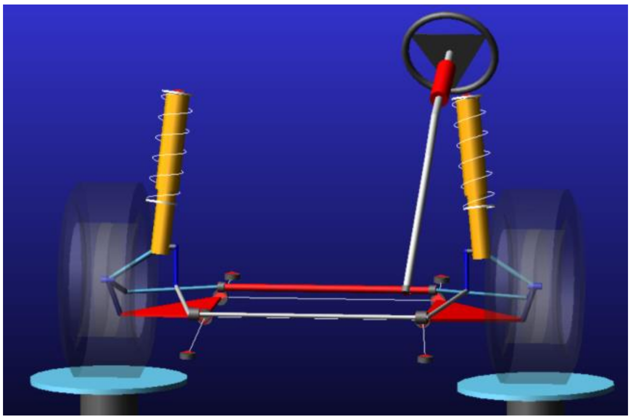

Figure 3.5 Bottom position of the wheel

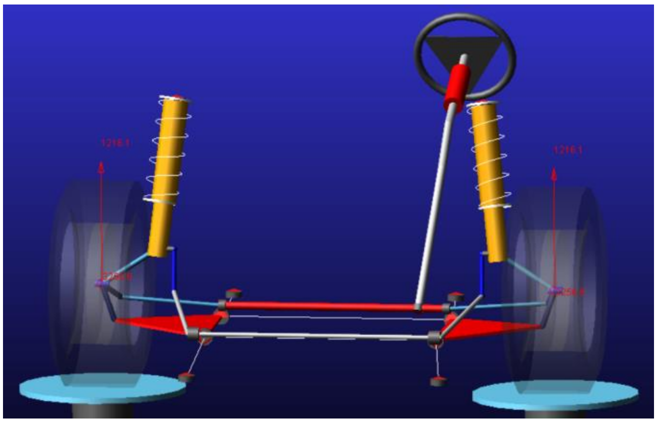

Figure 3.6 Upper position of the wheel

The post-processor is the area where the user can plot different curves representing a specific suspension parameter. The first step is to plot the relevant parameters to validate the architecture designed using Solidworks.

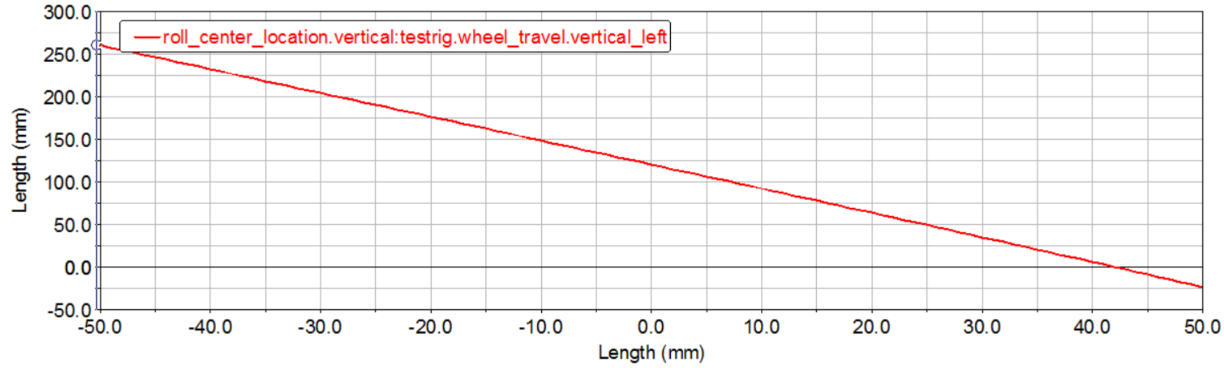

Figure 3.7 Roll Center Height

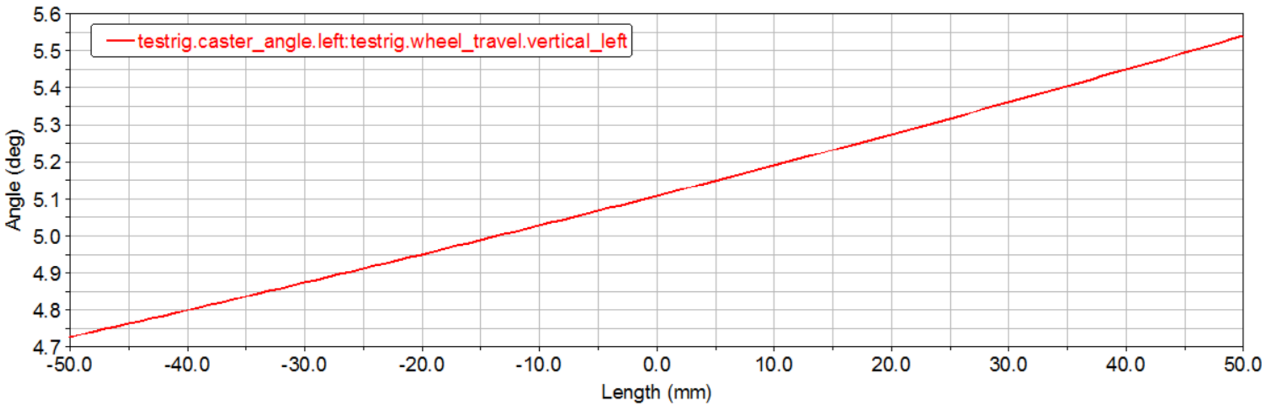

Figure 3.8 Caster angle

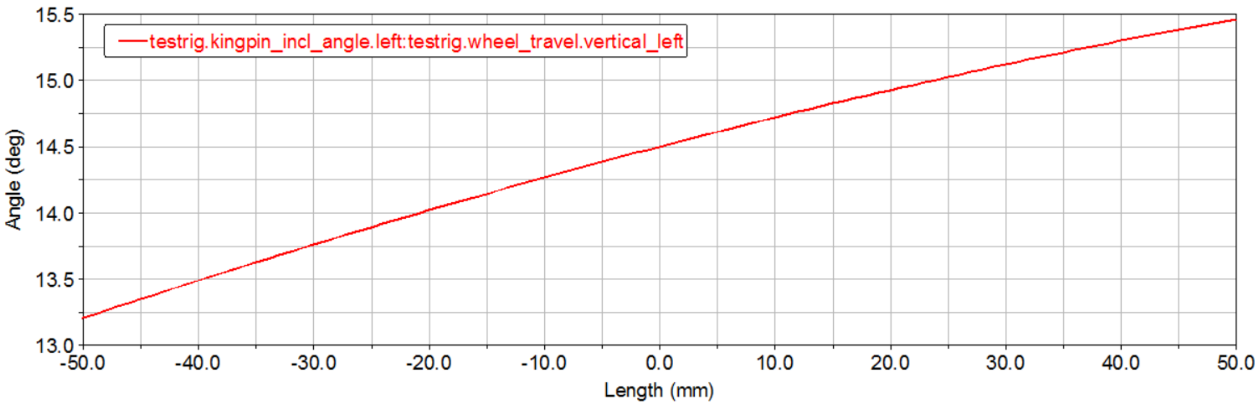

Figure 3.9 Kingpin Inclination Angle

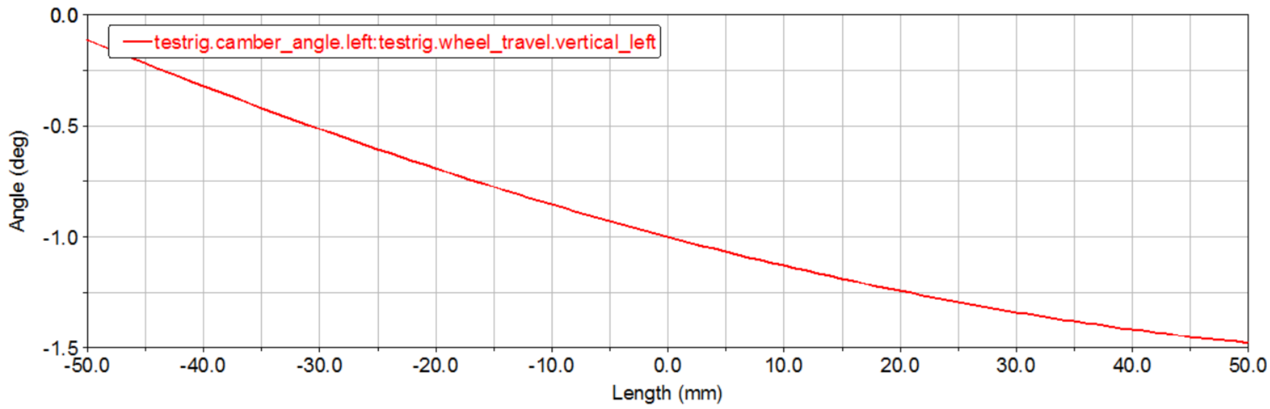

Figure 3.10 Camber Angle

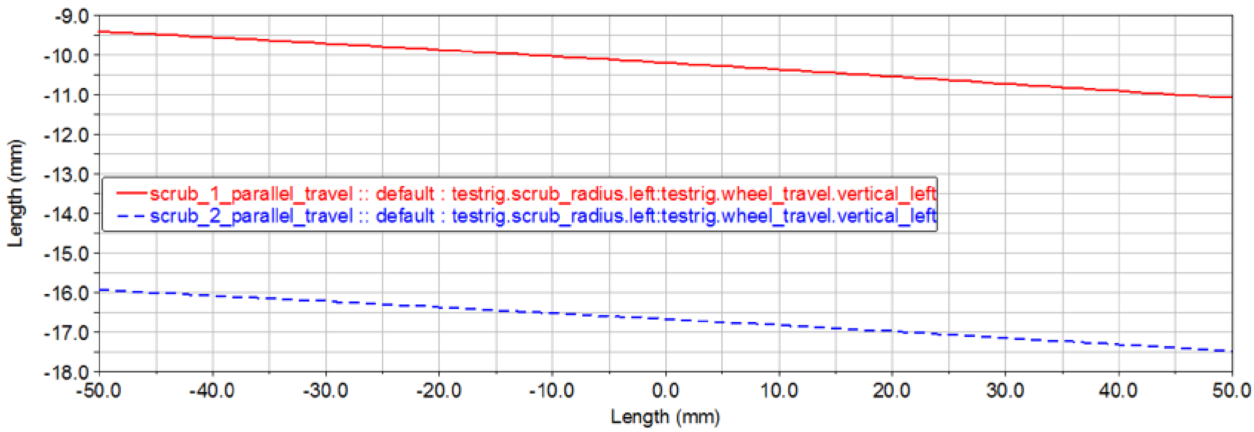

Figure 3.11 Scrub Radius

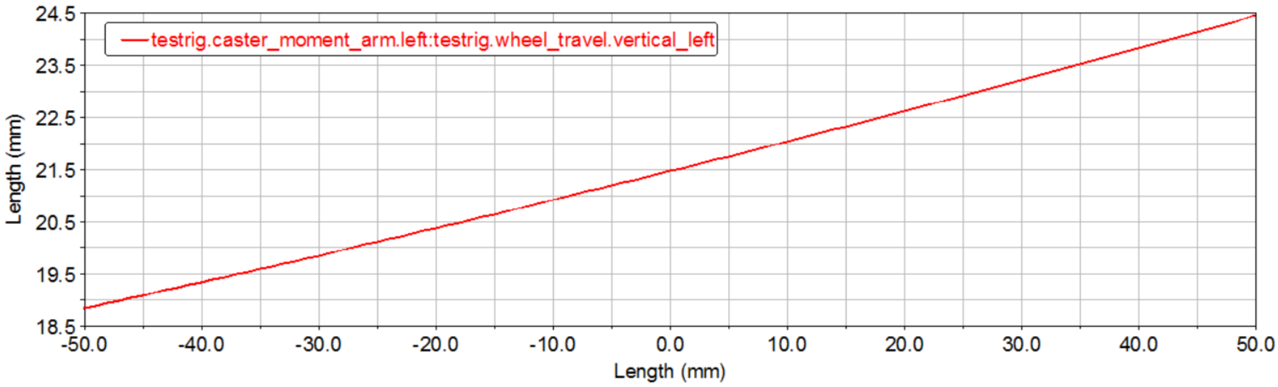

Figure 3.12 Caster trail

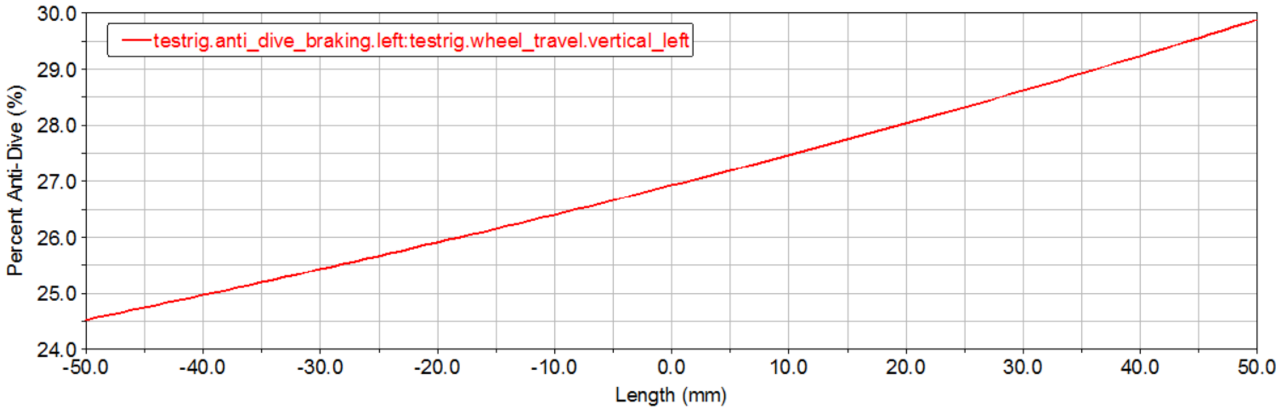

Figure 3.13 Anti-dive Property

Looking at the previous plots, the value of the parameters computed at the static condition is the same of the one computed with SolidWorks. The only parameters that differs from the one computed in SolidWorks is the scrub radus,as visible in figure 11.This is difference is the consequence of having set the camber angle at -1 degrees. This software, to compute the instant center position, uses the *force-based method.* The rig applies a unit force on the wheel, recording the compliance on the vertical and lateral direction, it computes the resultant of the force and its direction. The intersection of this directions is the roll center. For suspension system like the Macpherson or the Double Wishbone the geometrical approach leads to the same results of Adams\Car. For the Multi-link layout this doesn't work, and another analytical method needs to be used. Figure 4.13 shows the variation of the total track during the wheel travel. The value at the static condition is of 1628 mm, slightly different from the designed value. This is due to the application of the static camber value which is -1 degrees.

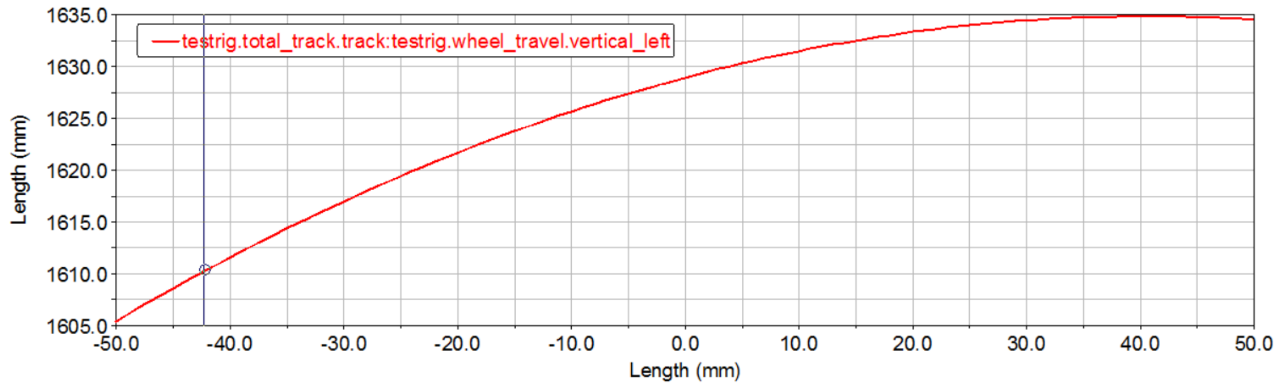

Figure 3.14 Total track

Following the geometrical construction, introduced in the previous chapter, the right length for tie-rod follows. The coordinates are listed in the following table. In figure 4.14 it can be seen clearly that the magnitude of the toe-angle is close to the zero, it confirms that following the geometrical construction, the tie rod doesn't influence the kinematics of the wheel.

Table 4.1

	X [mm]	Y [mm]	Z [mm]
Tie rod inner	**143**	**-396**	**339.63**
Tie rod outer	**149**	**-720**	**305.38**

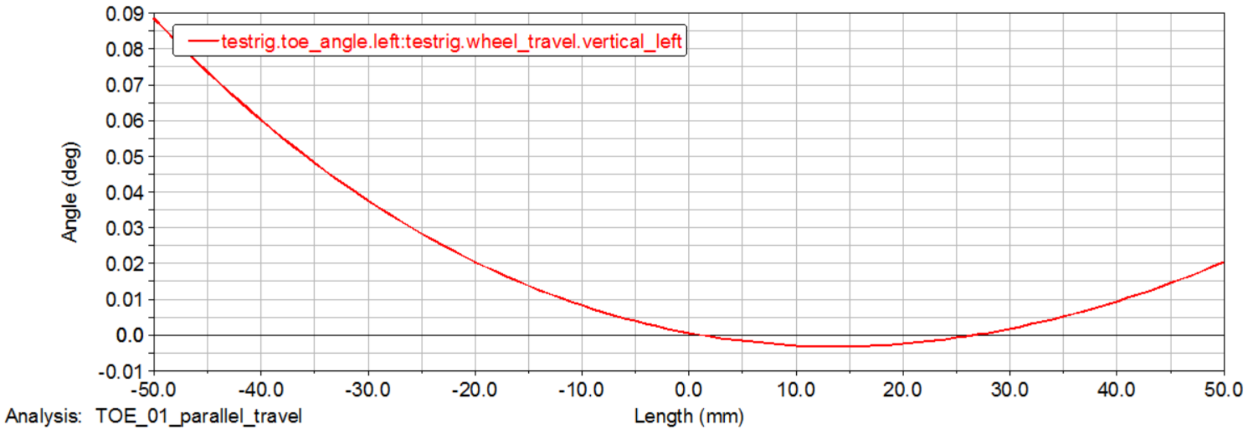

Figure 3.15 Variation of the toe angle with the wheel travel

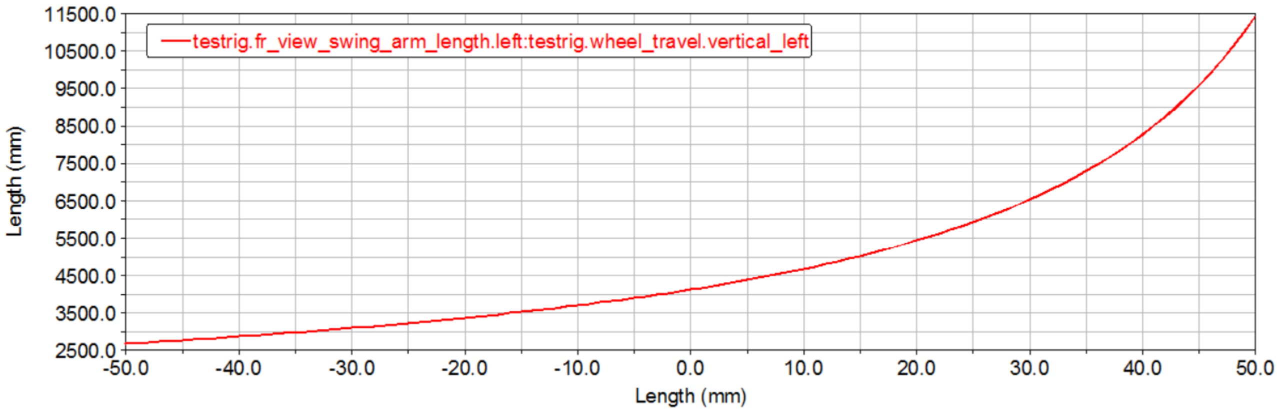

Figure 3.16 Front view swing arm length

3.4 Comparison with empirical data

The design of the suspension in this thesis started from the desired of roll center height. From the simulations made with SolidWorks, several options have been considered for the right positions of the hardpoints. Therefore, the data of real cars contained in 'The Automotive Chassis' by Reimpell have been used for validate the results of the simulations.

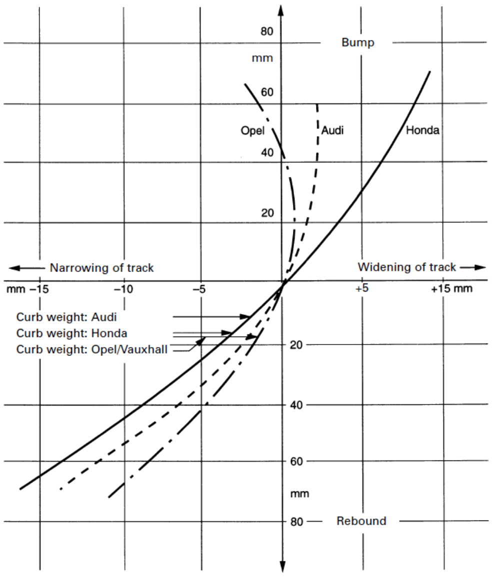

Figure 3.17 Track variation during the wheel travel

In the figure above are shown the curves of the variation of the track during the wheel travel for different kind of suspension system. Honda has a Double Wishbone suspension. This layout, as explained in the chapter about the Multi-link, has many advantages. The Audi has a Macpherson layout. The variation of the track is linked to the variation of the roll center height.

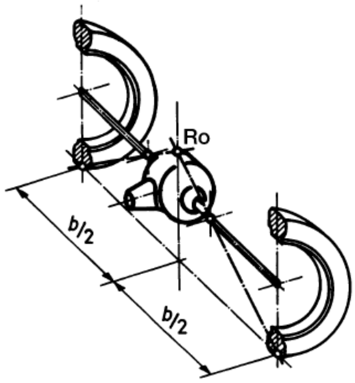

Figure 3.18 Sketch of the suspension geometry [5]

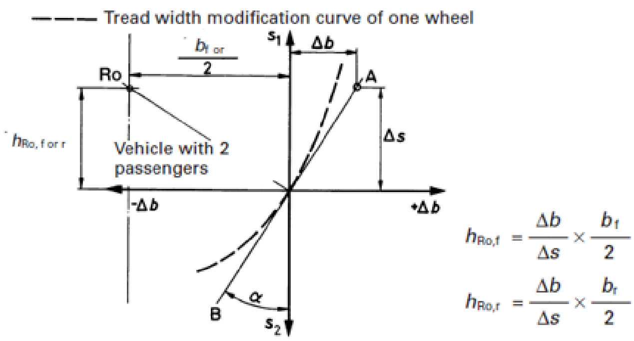

Figure 4.19 Variation of the track during the wheel travel [5]

Looking at figure 4.18, the roll center height can be computed as the following:

$$\frac{\Delta b}{\Delta s} = tan\alpha \tag{4.1}$$

$$h_{Ro} = \frac{\Delta b}{\Delta s} * \frac{b}{2} \tag{4.2}$$

The tangent of the curves, hence the trend, gives information about the variation of the roll center height. In figure 4.14, similarly in figure 4.19, the curves of the variation of the track tends to be parallel to the wheel travel axis. Considering equation 4.2, if the track remains constant and the wheel travel varies, the roll center height decreases. This is a characteristic of the Macpherson strut. The variation of the roll center height influences the body roll. As stated previously, the greater the distance between the center of gravity and the roll center height, the greater the body roll. Is it possible to anticipate that a vehicle in which is installed a Macpherson strut tends to roll more than a vehicle in which a Double Wishbone is installed.

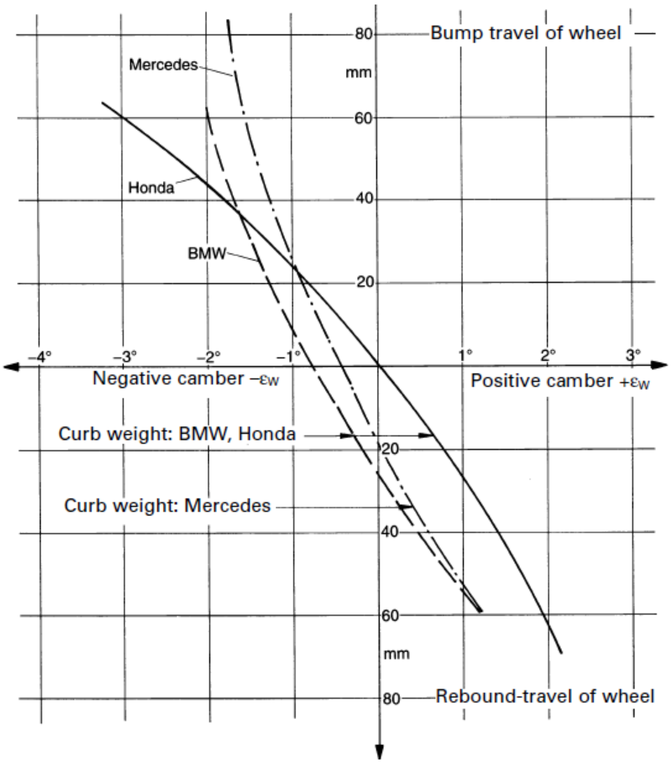

Figure 3.20 Camber variation with the wheel travel

In figure 4.20 are shown the curves representing the variation of camber angle during the wheel travel. The BMW and the Mercedes models are provided with the MacPherson strut. The static camber angle is set to a value close to -0.8 degrees, the maximum value reached is -1.7 degrees for the Mercedes model and -2 degrees for the BMW model. Looking at figure 4.10, the static camber for the designed suspension has been set at -1 degree and the highest value reaches is -1.5 degrees. The camber variation is close to the real car curves. The cars considered in the Reimpell book have a roll center height lower than the one designed in this thesis and this leads to a greater camber gain for first two models. The variation of the camber angle is important for the handling because counteract the variation of the wheel angle due to the body roll.

3.5 Ackermann Geometry

In the third chapter, was introduced and discussed the topic about the Ackerman Geometry. Considered the Jeantaud construction ,it was found as first attempt a position for the outer joint of the tie-rod and the ideal steer angle for each wheel to allow the vehicle to meet the desired turn radius. Figure 4.21 shows the steer angle of each wheel for the design layout for a turn to the right. The right wheel is the inner one and the left is outer. Looking at the figure there are two things that don’t match: the right wheel steer angle is smaller than the outer and the difference is not the one computed. This is due to the computed position of the outer tierod.Therefore,it was decided to move it inner at 720 mm from the middle plane of the car.

Figure 4.22 shows the result of the previous changes. In this case the right wheel is properly more steered than the left one and their difference is close to the one desired. Figure 4.23 shows the turn radius for both the configurations, figure 4.24 is the zoom of the previous figure and allows to seize better the difference. The turn radius for the first configuration is of 6110 metres while the turn radius for the second configuration is 5500 metres. Figure 4.25 shows the Ackerman error for the two configurations, the second one is under the four percent at the maximum steering.

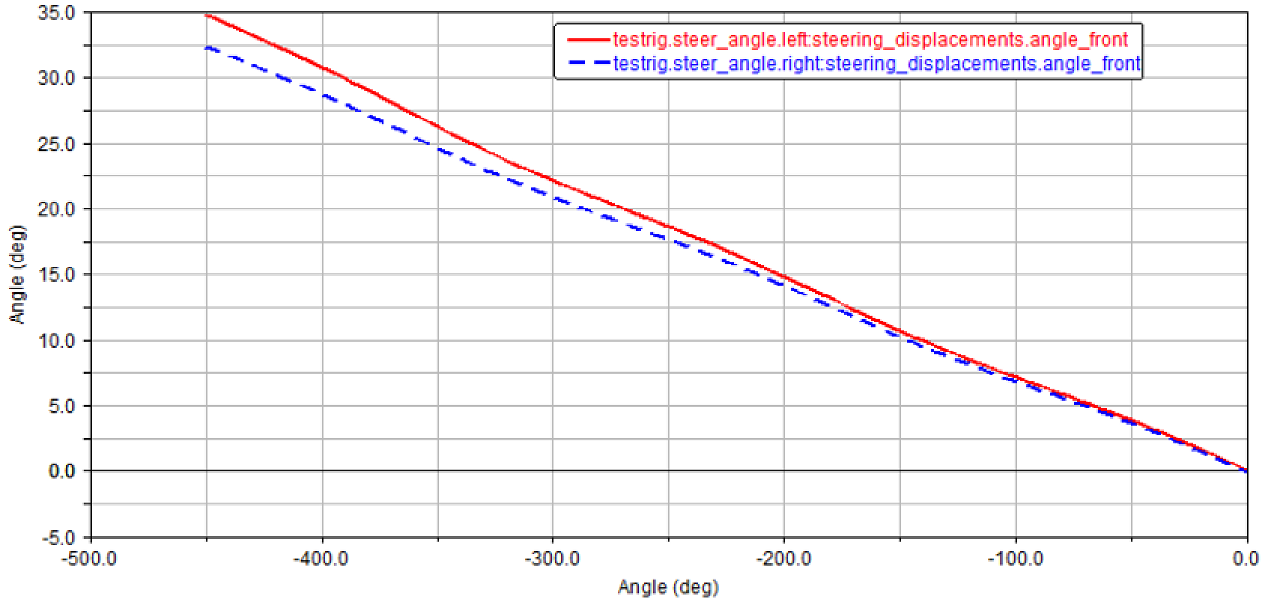

Figure 3.21 Steer angle against the steering wheel angle

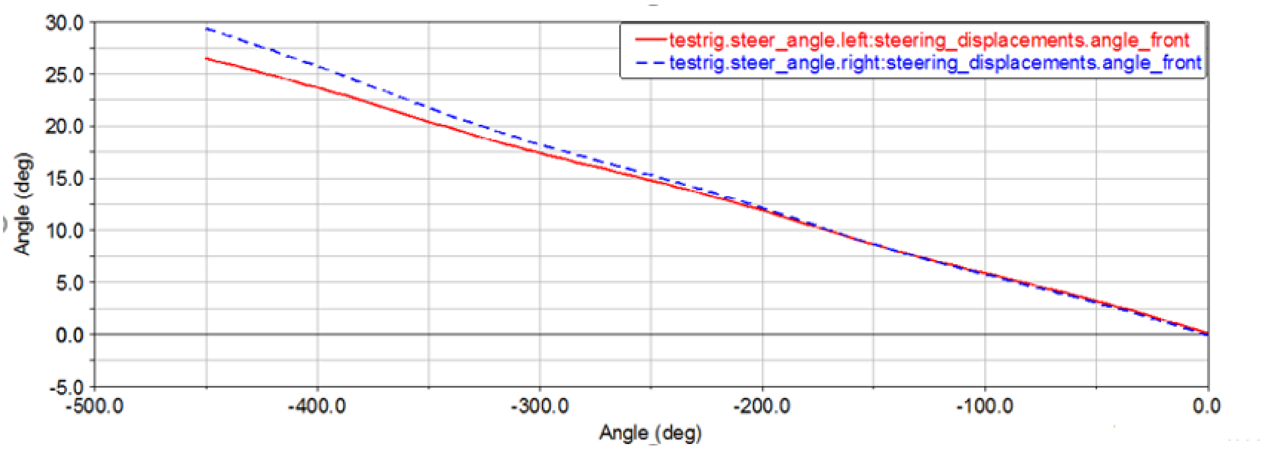

Figure 3.22 Steer angle against the steering wheel angle

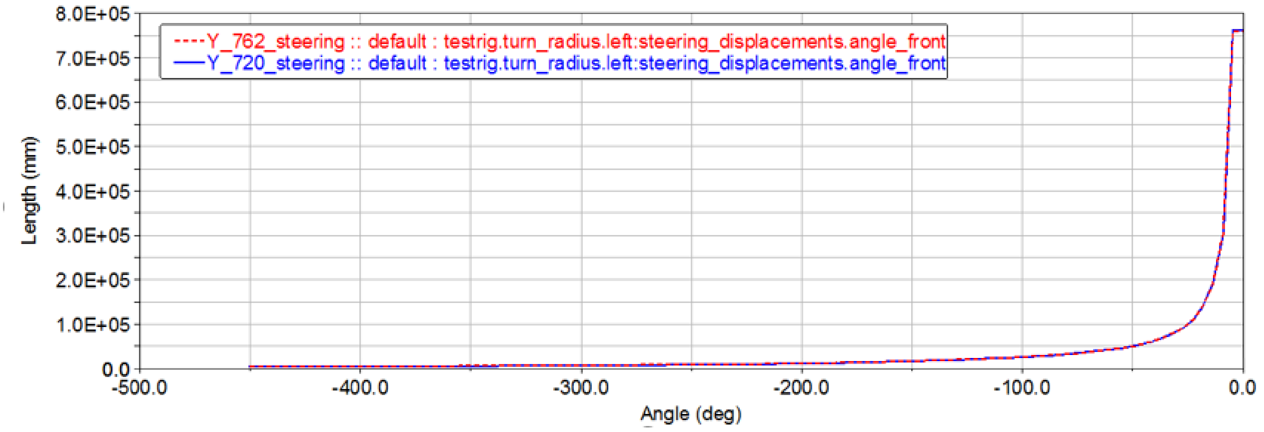

Figure 3.23 Turn radius

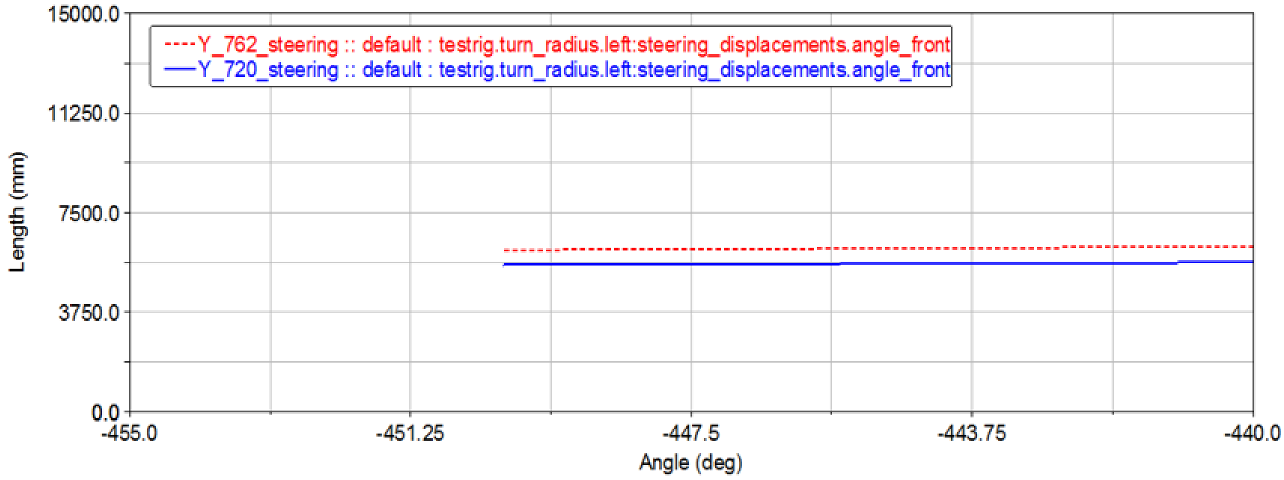

Figure 3.24 Zoom of the previous picture

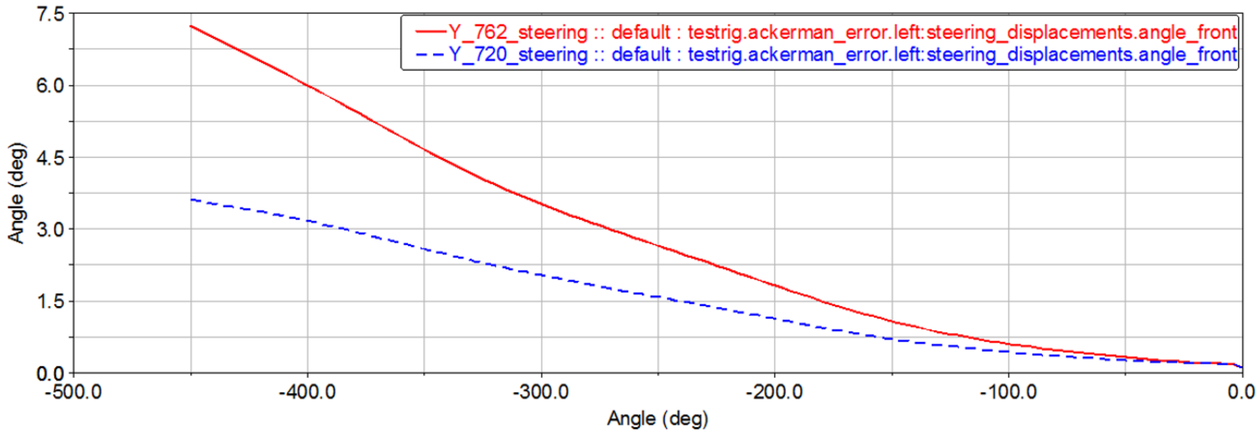

Figure 3.25 Ackerman error

3.6 Optimization of the Camber gain during Parallel Wheel Travel

It is important to remember to the reader that the camber gain is important because leads to have a wider contact patch and higher forces as consequences. Following, the study focuses on the suspension parameters like caster angle and kingpin inclination angle that affect the camber gain and is investigated the influences of the position of the lower strut. Considering the influence of the kingpin angle, from the default configuration, two different configurations have been tested. The top mount of the strut is moved along the y direction. In figure 4.21, the distance considered is referred to the distance from the center of the vehicle. For the second configuration, the top mount is moved outer, hence the kingpin angle decreases, and the camber gain is reduced. For the third configuration the top mount is moved inner, the kingpin angle increases, and the camber gain becomes greater. The influences of the kingpin angle on the camber gain is related to the distance of the instant center from the center of the wheel. Considering the same inclination of the lower control arm, increasing the inclination of the strut, hence increasing the kingpin angle, the instant center moves closer to the wheel and the camber gain increases. Wider kingpin angle involves greater scrub radius affecting the handling of the vehicle and tire wear.

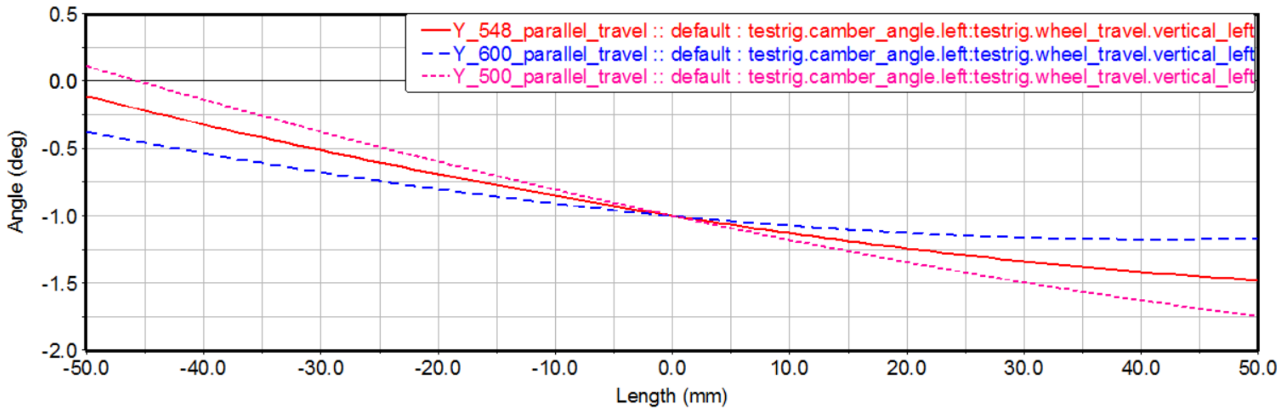

Figure 3.21 Camber variation for different kingpin angles

Considering the influence of the caster angle, for test the top mount is moved along the x directions respect the default position which coordinate is 74 mm rear from the center of the wheel. From figure 4.22 it is possible to state that caster angle during this simulation doesn't have strong influences on the camber gain. Figure 4.24 shows that the change of the position of the lower strut along the y direction has strong influences on the camber gain even though the neither the kingpin angle or the caster angle are changed. Changing the position of the lower strut leads to a different inclination of the strut. In so doing, the orthogonal plane passing through the top mount changes inclination and the instant center position is changed, so as the position of the roll center height. As previously stated, if the instant center is closer to the wheel center the camber gain is increased.

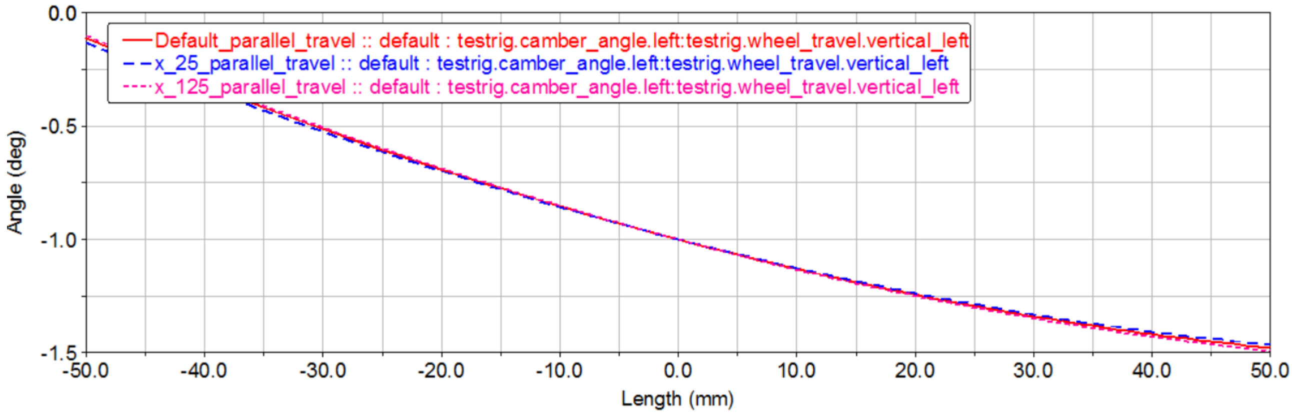

Figure 3.22 Camber variation for different caster angles

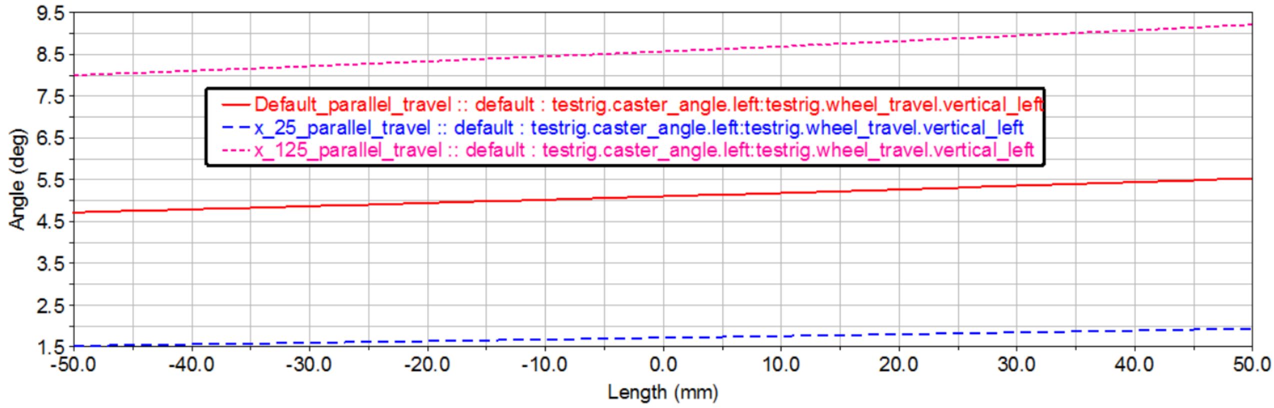

Figure 3.23 Caster angle values for the different configurations

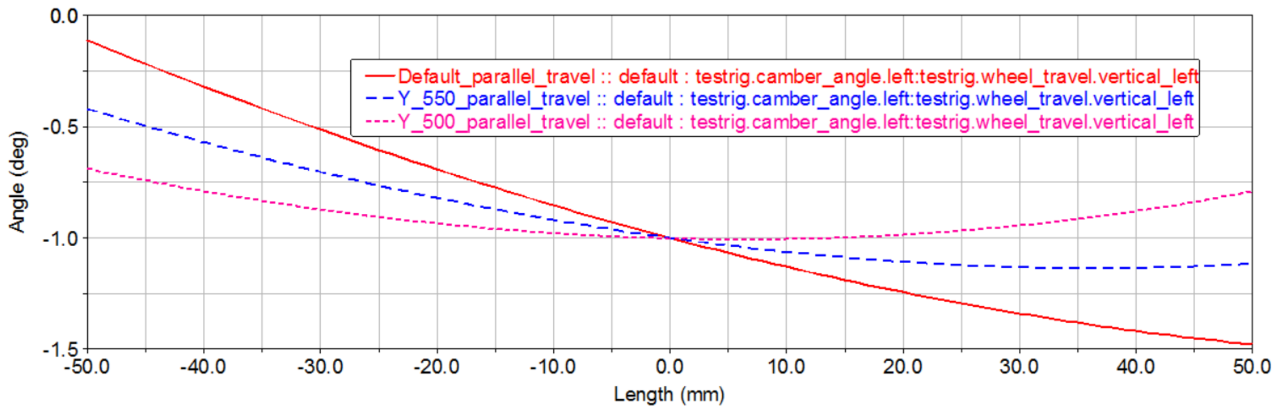

Figure 3.24 Camber angle during wheel travel for different positions of the lower strut

3.7 Camber gain during steering

The Camber angle varies strongly during steering and kingpin angle and caster angle have strong influences on the camber variation. For this test a steering input is used. In figure 4.25 and 4.26 the positive part of the steering wheel angle refers to a left turn. In this maneuver the right wheel is the outer and the left wheel is the outer. To improve the handling of the vehicle is interesting improving the camber gain on the outer wheel. Figure 4.25 refers to the camber variation changing the caster angle. As visible in the bottom right hand corner, increasing the caster angle the camber variation is wider for the right wheel. Looking at the upper right-hand corners, the left wheel, the inner one, has a positive variation of the camber angle that concerns reduce the contact patch worsening the handling. For the handling of the car is important have the bigger contact patch on the outer wheel. Figure 4.26 shows the variation of the camber angle for the change of the kingpin angle. As visible, increasing the kingpin angle, the camber angle variation is smaller compared to the default configurations on the outer wheel worsening the handling. The camber angle of the inner wheel reduces too. Resuming, considering the effect of the caster angle and kingpin angle on the camber gain during steering, the caster angle has a positive effect while the kingpin angle has a negative effect. Figure 4.27 shows that the position of the lower strut doesn't have any effect on the camber variation during steering simulation.

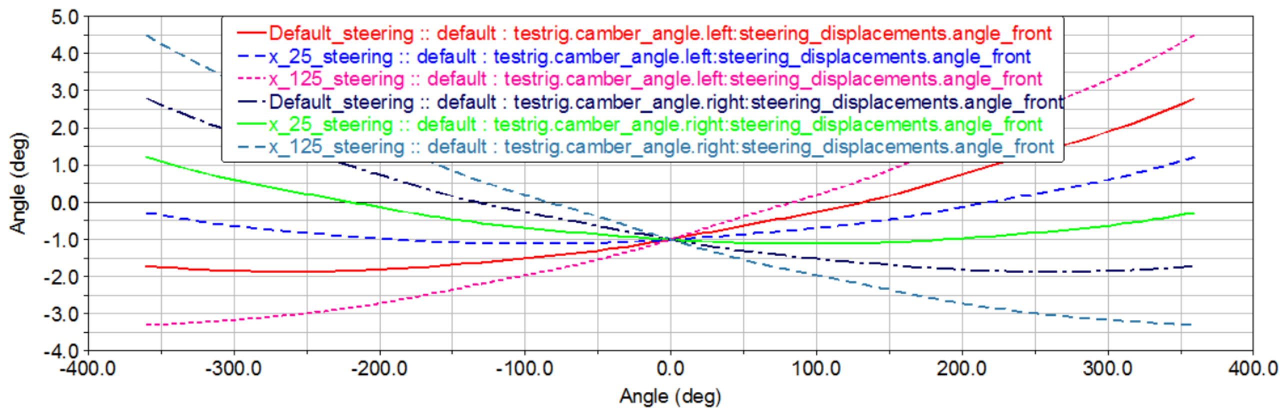

Figure 3.25 Camber variation for caster angle change

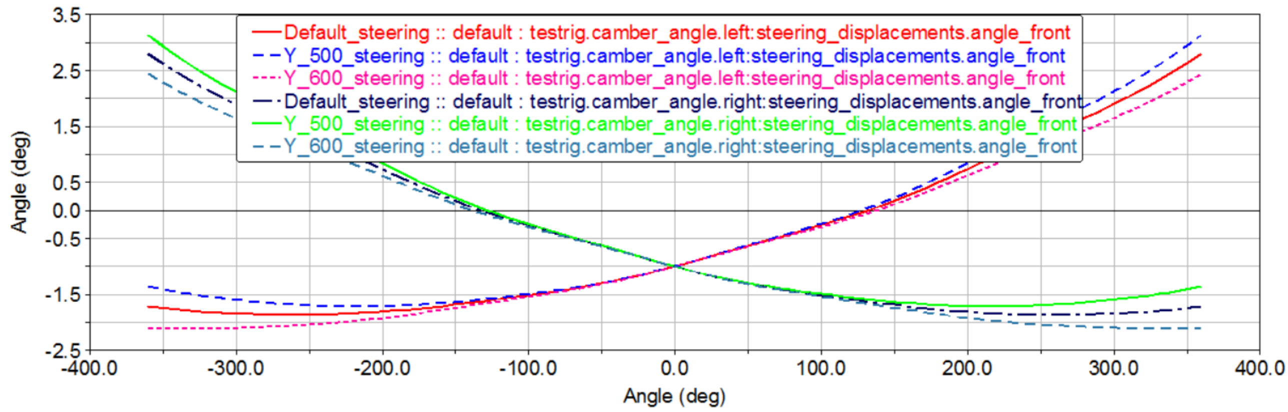

Figure 3.26 Camber variation for kingpin angle change

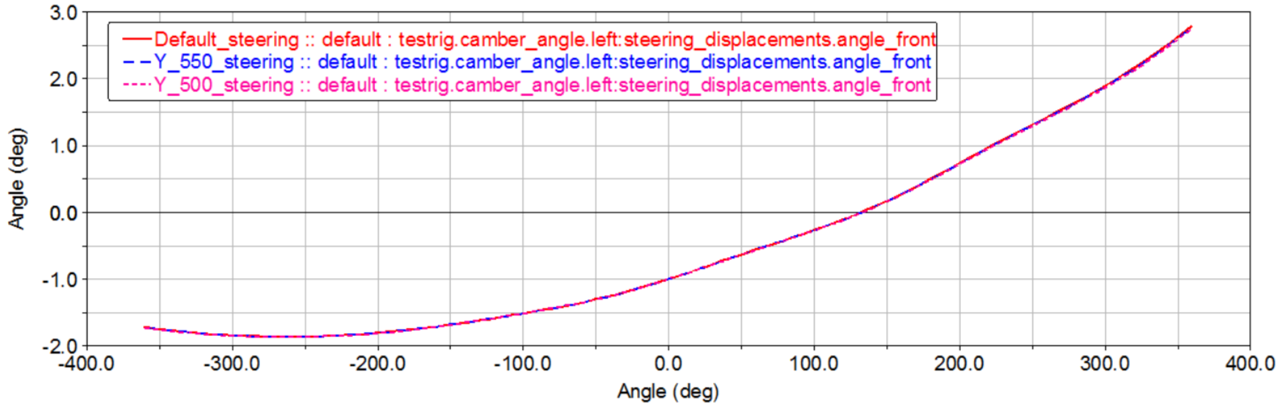

Figure 3.27 Camber variation during steering for different lower strut position

3.8 Analysis of the Anti-roll bar

For the analysis the already made template of Adams\Car has been used. It is the simple model of anti-roll bar. There is a torsional stiffness concentrated in the middle of the bar, therefore the wide of the anti-roll bar or the section doesn't influence the torsional stiffness. The lever arm, as defined in the previous chapter affects strongly the global suspension roll rate. The anti-roll bar is attached to the subframe through the bushing that have elastic properties. The anti-roll bar is linked to the strut through the droplinks. The main parameters to be set are the concentrated torsional stiffness and the lever arms. It is necessary to specify that depending on the position of the lower point of the drop link the installation ratio of the anti-roll bar changes. Therefore, many simulations have been made to analyse the possible variation on the suspension roll rate.

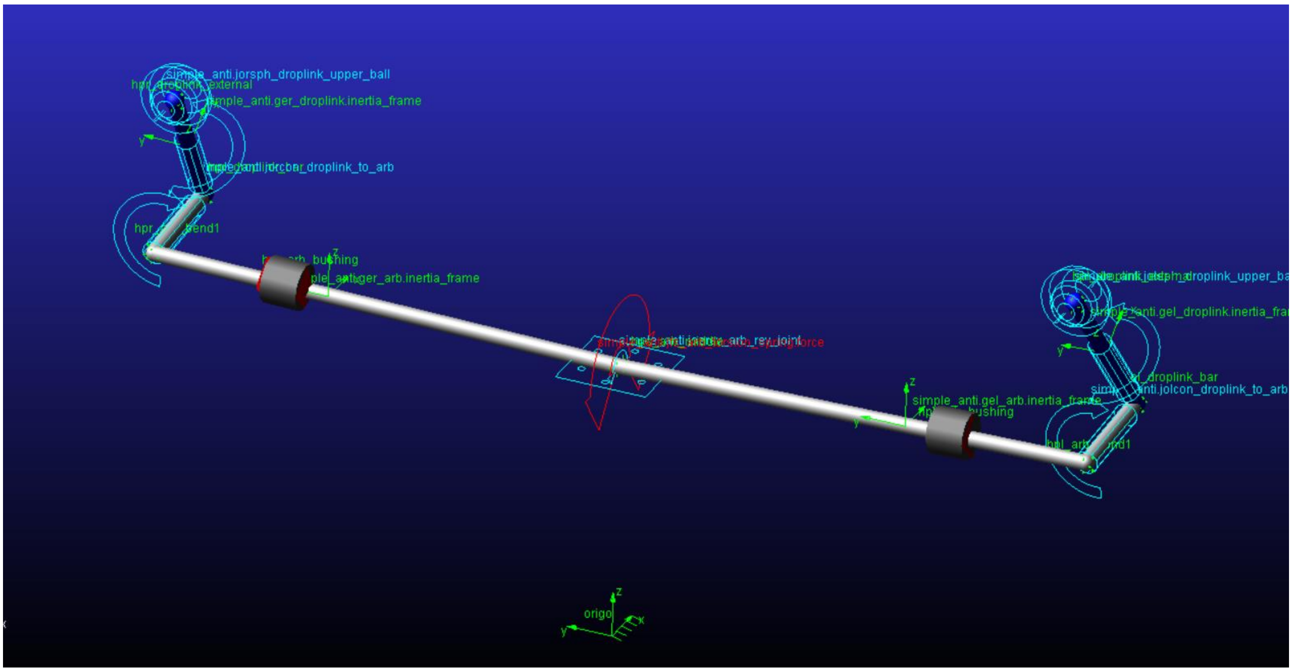

Figure 3.28 Anti-roll bar template

From the computation made previously the desired roll rate values due to the springs contribution and to the anti-roll bar contribution are:

Table 4.2

	[Nm/rad]	[Nmm/deg]
Spring roll rate	29378	512498,24
ARB roll rate	48394	844206,5
Total suspension roll rate	77772	1356704,7

The coordinates of each component of the anti-roll bar for the first attempt are listed in table. The first test is aimed to verify the suspension suspension roll rate for the springs. As visible in figure 4.29, the value of the roll rate due to the spring contribution is quite close to the one computed analytically order to study the contribution of the anti-roll bar , the value of the spring stiffness has been set to zero. In figure 4.20 is shown the vertical displacement of the lower point of the droplink against the wheel travel. The slope of the curve in each line corresponds to the installation ratio. For the considered configuration, the installation ratio is close 0.97.

Table 4.3

T	1616 [mm]
L	300 [mm]
IB	0.97
KϕB	844206,5 [Nmm/deg]
KθB	30921,82 [Nmm/deg]
Pickup x|y|z	0,-500,500 [mm]
Droplink	0,-517.7,325 [mm]
Arb bend1	-300,-600,325 [mm]
ARB height	325 [mm]

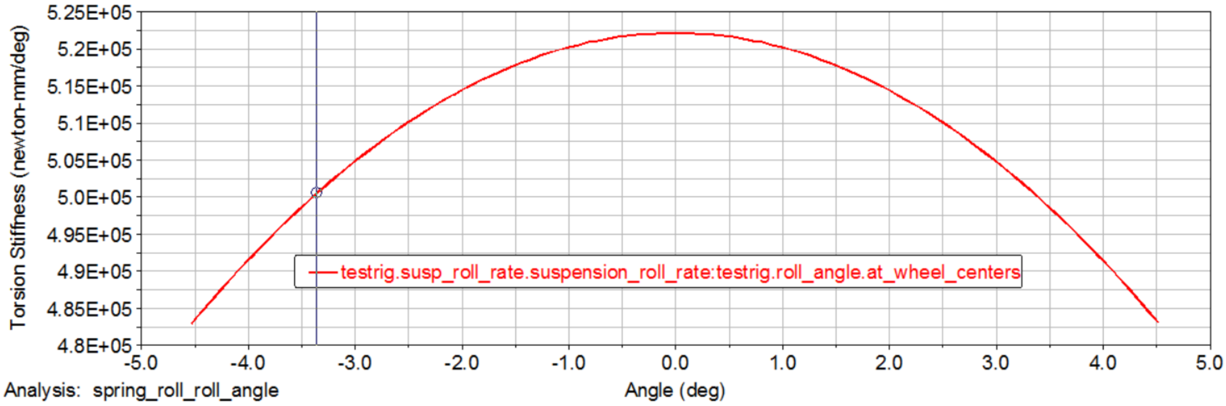

Figure 3.29 Roll rate due to spring contribution

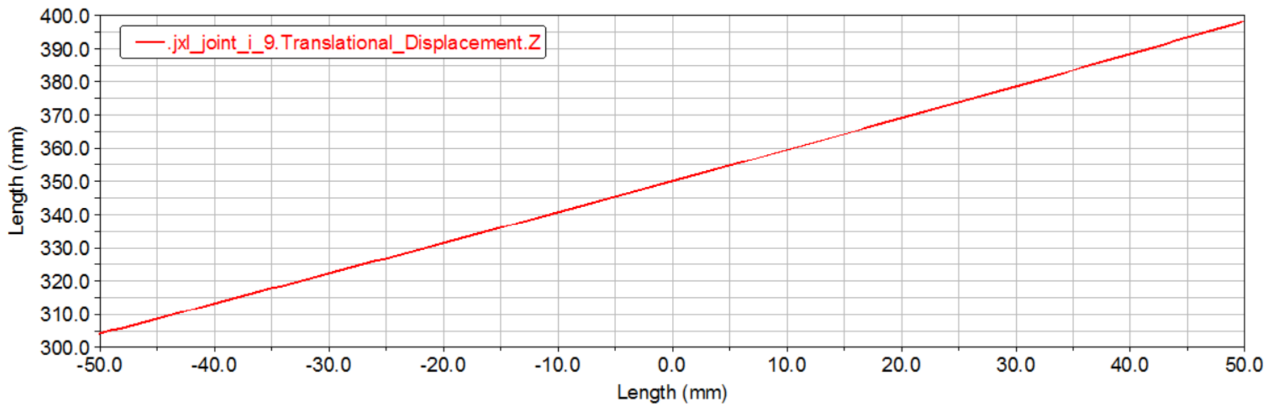

Figure 3.30 Vertical displacement of the droplink against the wheel travel

To lead the simulation and verify the value of the suspension roll rate due only to the anti-roll bar, the value of the spring stiffness has been set to zero. Figure 4.31 shows the value of the suspension roll rate during the roll. The value recorded for the initial condition is 786000 [Nmm/deg],slightly different from the value computed. Differently from the theoretical formula, in Adams\Car there are many reason for which the two values don’t match, for example the elastic of the bushings.

To better understand the contribution real contribution given by the anti-roll bar, many different configurations have been investigated:

- Height of the anti-roll bar
- Height of the pickup point to the strut
- Width of the droplink bar lower point

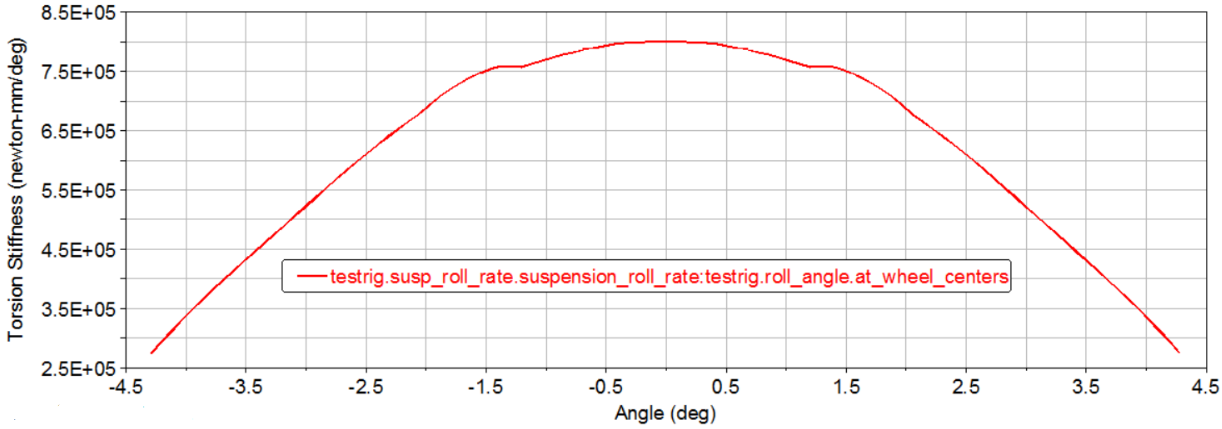

Figure 3.31 Suspension roll rate due to the Anti-roll bar contribution

From the initial height, listed in table 2, the height of the anti-roll bar has been rised up to 400 mm.As visibile in figure 4.32 the value of the suspenion roll rate doesn't change in a relevant way at the initial condition but ,during the roll, the suspension roll rate in the second configuration decreases strongly.Similarily,in figure 4.33 , it is shown the influences of the position of the pickup point to the stut on the suspension roll rate.The height of the pickup point has been increased from 500 mm to 550 mm.

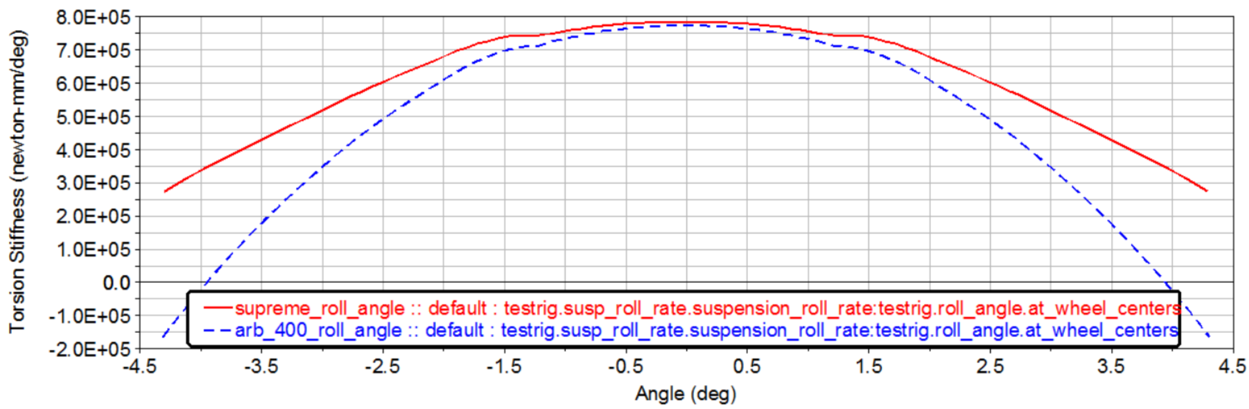

Figure 3.32 Roll rate for different anti-roll bar height

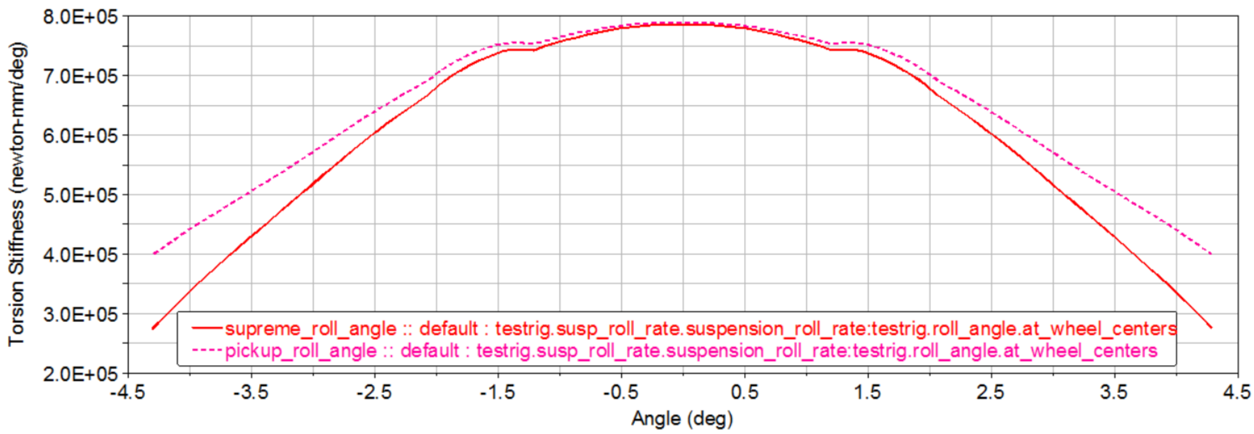

Figure 3.33 Roll rate for different positions of the pickup

It has been moved the lower point of the droplinks in order to detect any influences on the installation ratio of the anti-roll bar.The point is moved in two different positon from the default one, as visibile in figure 4.34.Leading a parallel wheel travel analysis on the suspension, the motion of the droplink has been recorded.Figure 4.35 shows the results for the configuration C.The red cuves refers to the upper part of the droplink that is directly linked to the strut and as consequences has the same installation ratio. The blu line refers to the lower part of the droplink.In table , the results for each configuration are listed.Also a small differences in the installation ratio leads to big differences in the total suspension roll rate.

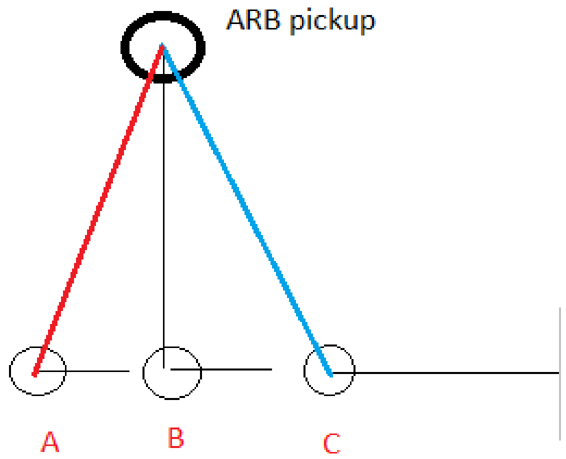

Figure 3.34 Positions of the lower point of the droplink

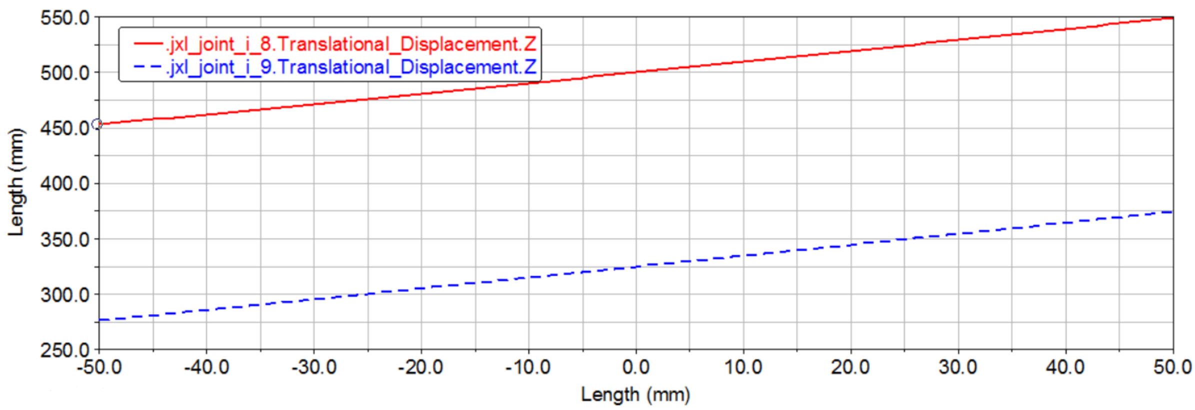

Figure 3.35 Vertical motion of the extreme points of the droplink against the wheel travel

Table 4.4

	Y-coordinate [mm]	Slope (Installation ratio)
A	517.7	0.9529
B	500	0.96
C	400	0.9828

4.DESIGN OF THE MULTI-LINK LAYOUT

The Multi-link layout, as already introduced in chapter 2, is composed by five independent links that connect the wheel to the chassis .In the Macpherson strut the kingpin axis passes through the upper ball joint , where there is the connection of the strut to the chassis, and the outer lower ball joint, through which the lower control arm connects to the wheel carrier. The kingpin axis in so doing is physically constrained to the real geometry of the strut and the lower control arm. The main peculiarity of the Multi link layout is the possibility to split the upper and lower ball joint in two ball joints each, figure 5.1. The extension of the connection rods meets in two virtual points through which the imaginary kingpin axis passes. During the bouncing, the connection rods move, and the imaginary kingpin axis moves too, figure 5.2. In so doing its possible to make the kingpin axis lie close to the wheel center and obtain a null or small kingpin offset ,the scrub radius, figure 5.3.The infinite possibility of positioning of each link allow to match the desired roll center height and the swing arm length at the same time. Moreover, allows to design properly the inclination of the kingpin axis and its offset. The design of the Multi-link is more complicated and less intuitive compared to the Double Wishbone or Macpherson layout. For the latter is it possible to use a geometrical approach because the instant center of rotation is well defined in the space by two planes whose intersection produces the instant axis. Intersecting the instant axis with the vertical plane passing through the axle, the instant center is obatined.Considering the Multi-link, if each link has different direction, is not possible to define an upper and a lower plane, hence, is not always possible to find geometrically the instant center of rotation and therefore the roll center height.

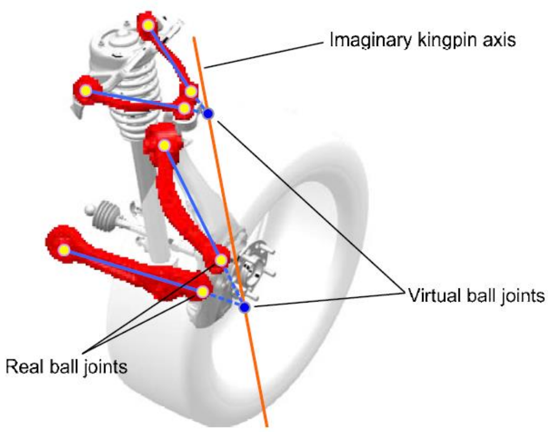

Figure 4.1 Imaginary kingpin axis of a Multilink

The method used to analyse the kinematics of the multilink suspension are :

- Adams\Car: computes the kingpin axis by analysing the displacement of the wheel under small forces and torques in the x, y, and z directions .However, these methods require precise suspension geometry data and even deformations of compliant parts for every steered position. In the meantime, measuring those data in a real vehicle requires much expense, time, and effort. As a result, there is no method to compute or measure the kingpin axis of real vehicles yet. The position of the roll center is computed thanks to a force-based method. Similarly , the kingpin axis can be computed or in a geometric way, assigning two physical ball joints or thanks an instant axis. To compute the instant axis , the spring is kept still while a torque is applied at the wheel carrier. The displacement and the rotation lead to the computation of the position of the kingpin axis suspension points. All suspension measurements are taken from wheel orientations (toe, camber, spin), wheel center location (x, y, z), and tire contact patch movement (x, y). The K&C machine software then calculates other suspension parameters from the available measurements. The kingpin axis calculation is since the direction of the angular velocity of the wheel is its axis of rotation. A 4th order polynomial is fitted to each of toe, camber, and spin against handwheel steer angle and then differentiated.

- Screw Axis: the aim of this method is to use suspension- parameter-measuring device (SPMD) data. Based on the suspension characteristics data such as displacement of the wheel center and changes in toe, camber, and side view angle, is possible to use them to create the displacement matrix. The displacement matrix consists of a rotational part and a translational part. The rotational part can be defined using the screw axis. Thanks to this method it’s not necessary having a test rig and moreover it seems to be more successful to explain the behaviour of the vehicle during high lateral acceleration or transient behaviours.

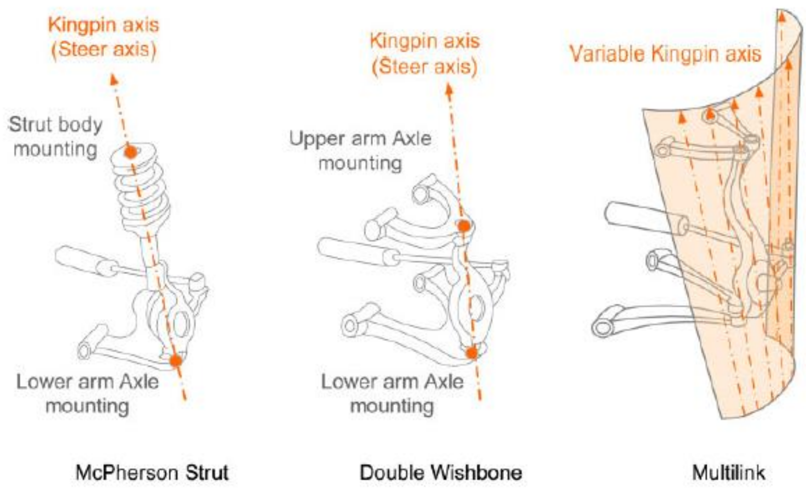

Figure 4.2 Kingpin axis for different layout

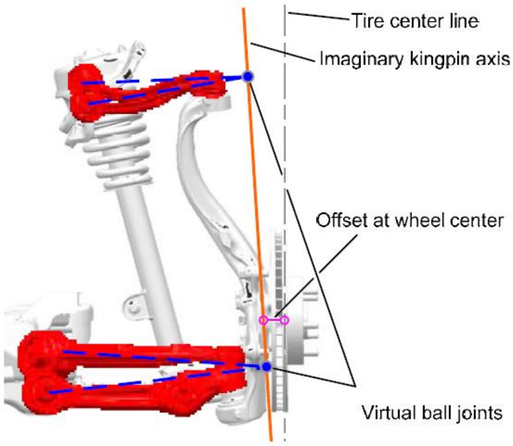

Figure 4.3 Kingpin axis off-set

4.1 Geometry Design

To use the geometric approach to the design, the layout of the Multi-link is thought like the Double Wishbone one: an upper control arm, contained in plane three, a lower control arm, contained in plane four and a tie-rod, figure 5.4. In this way, the main differences with a double wishbone is the possibility to design properly the inclination of the kingpin axis and its offset. Figure 5.5.On each plane, the two rods are designed with the possibility of being inclined of respectively of different angles.

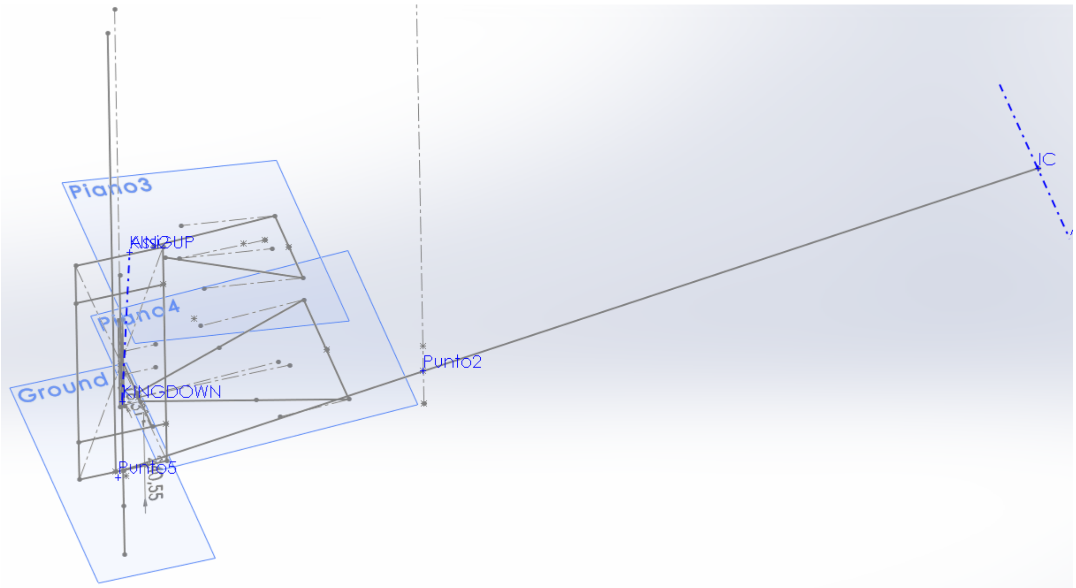

Figure 4.4 SolidWorks model

Similarly, to the Macpherson, the first attempt was aimed to match the desired roll center height. Using the Excel suite contained in SolidWorks, several configurations have been tested until the proper one was matched. The main suspension parameters are listed in table 5.1.

Table 5.1

Roll center height [mm]	Kingpin angle [degree]	Caster angle [degree]	Scrub radius [mm]	Antidive%
120	8.33	5.02	-6.71	27.32

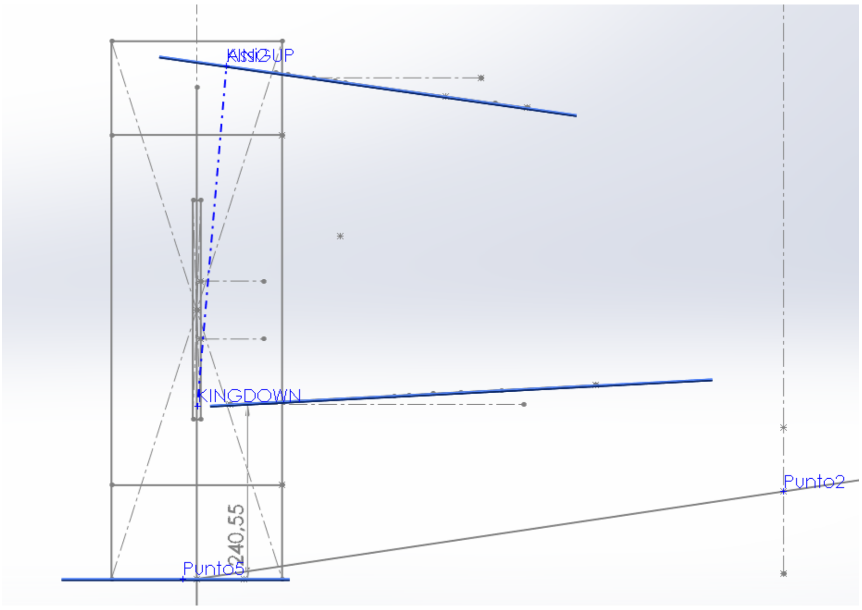

Figure 4.5 Kingpin axis and Scrub radius

Similarly, for the Macpherson, it was necessary to design properly the position of the inner tie-rod ball joint and hence its length. It was followed a geometric construction useful to obtain the minimum effect of the tie-rod on toe-angle variation, figure 5.6.

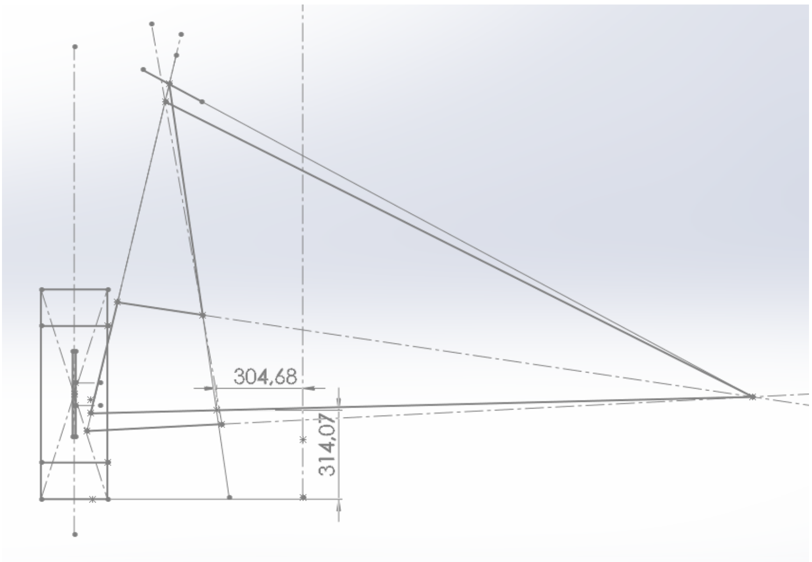

Figure 4.6 Tie-rod length

Table 5.2

	x	y	z
Tie-rod outer	149	-720	303
Tie-rod inner	130	-304.68	314.07

4.2 Elastic components

The design of the elastic components concerns the same consideration considered for the design of the MacPherson. The Olley's criteria are still valid and the value of the stiffness required is the same as well as the value of the damping. In the Macpherson layout the spring is coaxial to the strut and the installation ratio of the spring is the same of the strut which, as stated in the previous chapters ,is linked to the cosine of the kingpin angle. In the Multi-link layout, the spring can be attached in many point on the rods, changing the installation ratio. The installation ratio is the ratio between the vertical motion of the spring and the vertical motion of the wheel. As visible in figure 5.6, the installation ratio for a Multi-link can be computed as the ratio between the distance of the point where the spring is linked and the inner joint of the rod. It was decided to link the spring in a position that would have led to an installation ratio of 0.75.

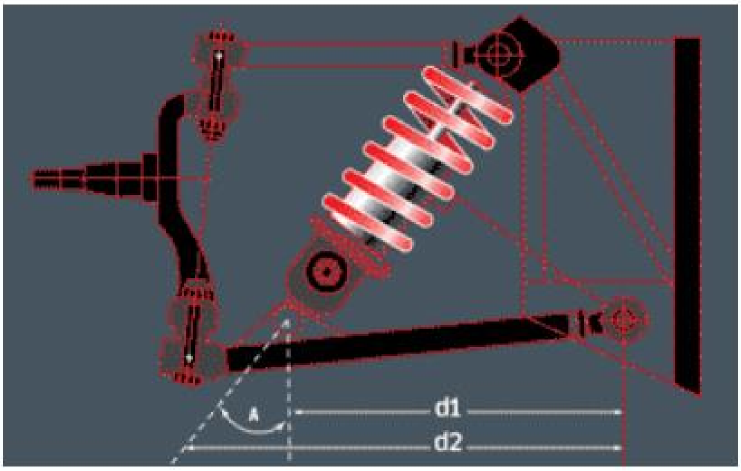

Figure 4.6 Installation ratio

Table 5.3

IR	0.75
K_{fwheel} [kN/mm]	22.5
$K_{fspring}$[kN/mm]	40
c_{fwheel}[Ns/mm]	1.9
$c_{fdamper}$[Ns/mm]	3.2

The design of the anti-roll bar is the same of what done for the Macpherson strut. The difference is the installation ratio between the torsional stiffness of the bar and the global roll rate. In table 5.4 is listed the necessary torsional stiffness of the anti-roll bar.

Table 5.4

T	1616 [mm]
L	300 [mm]
IB	0.75
$K\varphi B$	844206,5 Nmm/deg
$K\theta B$	51723.24 Nmm/deg

5.ANALYSIS OF THE MULTI-LINK IN ADAMS\CAR AND COMPARISON WITH THE MACPHERSON STRUT

For this study, the template of the Multi-link has been created by zero by the user. In figure 6.1 is shown the assembly with the steering subsystem and the test-rig with which apply the motion and the force to the wheel to run the simulations on the assembly. Three different kind of simulation are done on the assembly to investigate the main suspension parameters, offering the comparison with Macpherson layout:

- Parallel Wheel Travel

  The first attempt of simulation is aimed to confirm the suspension parameters designed with SolidWorks, the Parallel wheel travel simulation is run. Looking at the following plots , the value of each parameter at the initial condition is quite perfectly the same of the ones computed with SolidWorks. The only value that is farther from the computed one is the Scrub radius. This difference is due to the static camber angle imposed in Adams\Car .Running the simulation with zero static camber angle, the scrub radius values matches perfectly. For each plot, is offered the comparison with the MacPherson strut to see the advantages of the five-link layout. It is interesting to focus on figure 6.4.It shows the curves of the scrub radius. The Multi-link layout allows to have small scrub radius and its variation during the wheel travel is limited, this reduces the vibration of the wheel improving the handling of the vehicle, reducing the tire wear too.

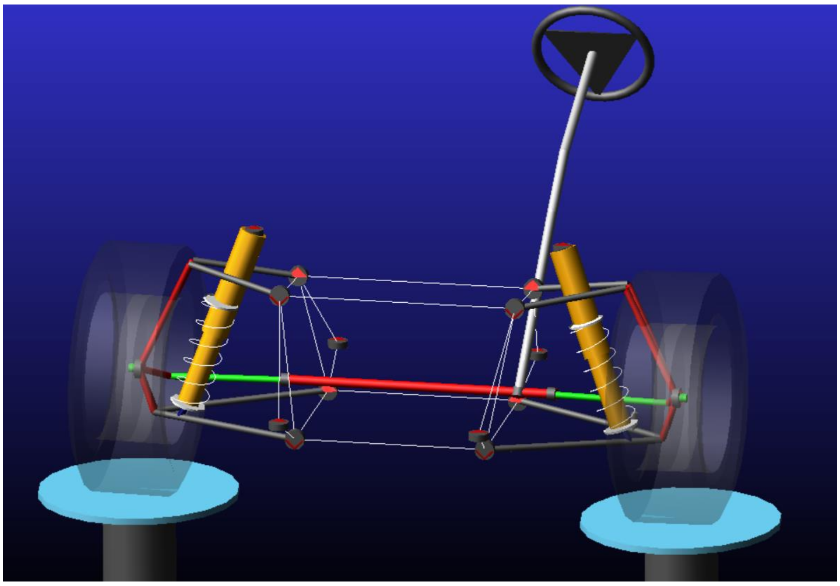

Figure 5.1 Multi-link assembly

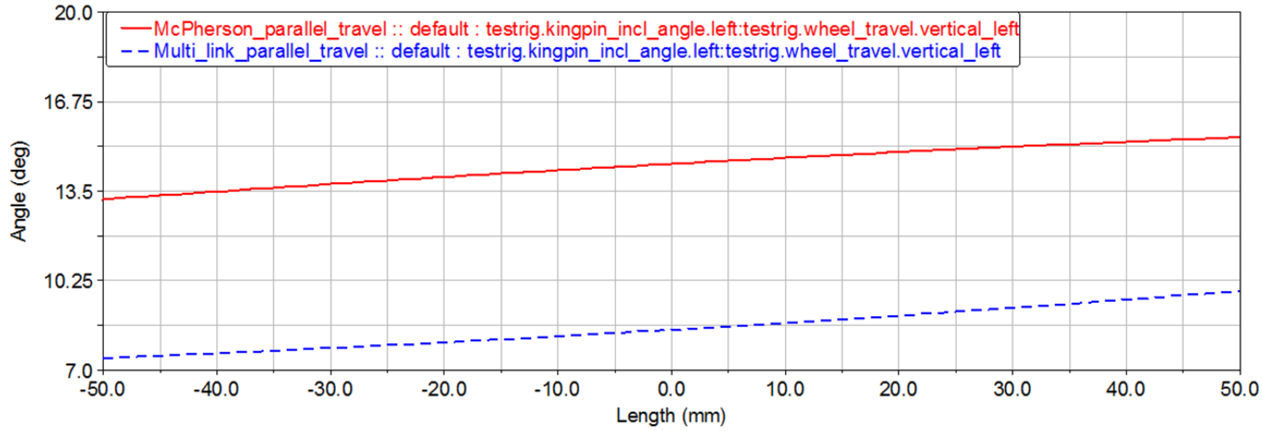

Figure 5.2 Kingpin inclination angle with wheel travel

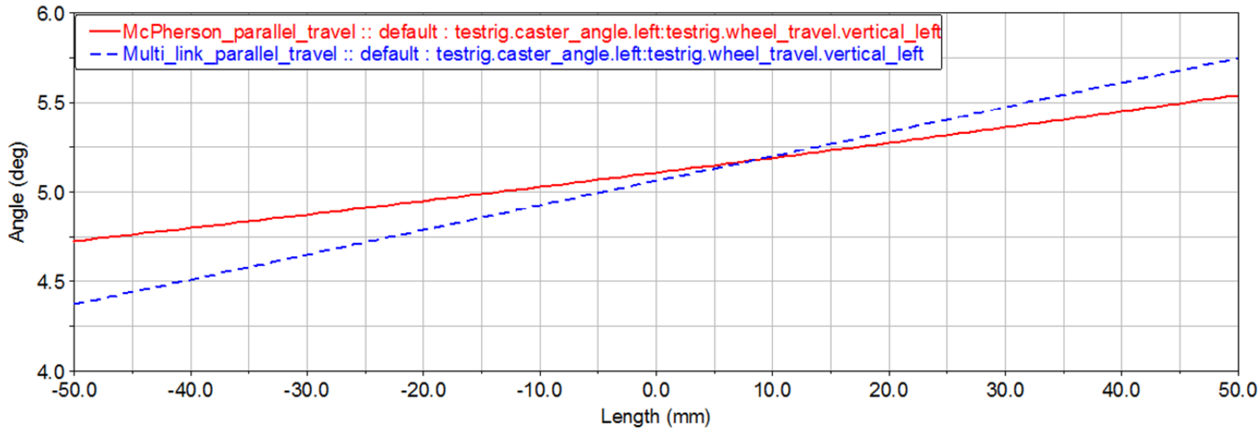

Figure 5.3 Caster angle with wheel travel

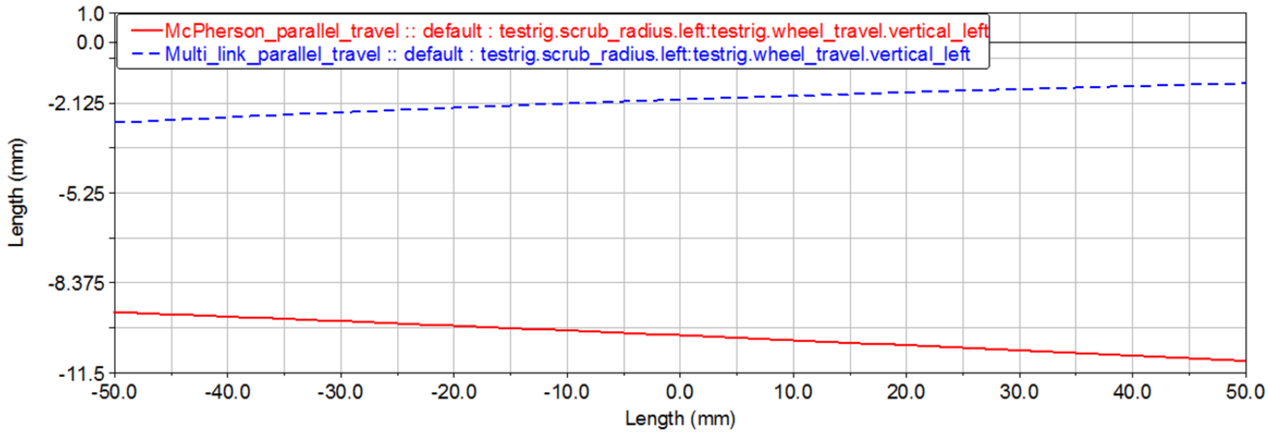

Figure 5.4 Scrub radius with wheel travel

Figure 6.5 shows the variation of the Toe angle with the wheel travel. The variation of the toe-angle for the McPherson strut is wider than the one of the Multi-link. Moreover, during the wheel travel the McPherson strut shows a variation of the sign of the toe, this affects the handling of the vehicle strongly. The advantages of the Multi-link are the narrow range of variation and the constant of the sign. For riding is desirable to have a Toe-in behaviour during breaking, during which bump occurs. As seen in chapter 4,the variation of the track is directly linked to the roll center height change. In figure 6.6 is clearly visible a different trend for the two curves. The red curves, referring to McPherson ,during the bump, tends to be parallel to the wheel travel axis while the blue curve, referring to the Multi-link layout, keep growing with the bump travel. This trend has effect on the roll center height ,as visible in figure 6.7.At the initial condition, both the curves have the same roll center height value, as fixed at the beginning of the design. During the wheel travel, the range of variation of the roll center height of the Multi-link is narrower than for the McPherson. This has big influence on the handling of the vehicle. Higher roll center height involves less body roll.

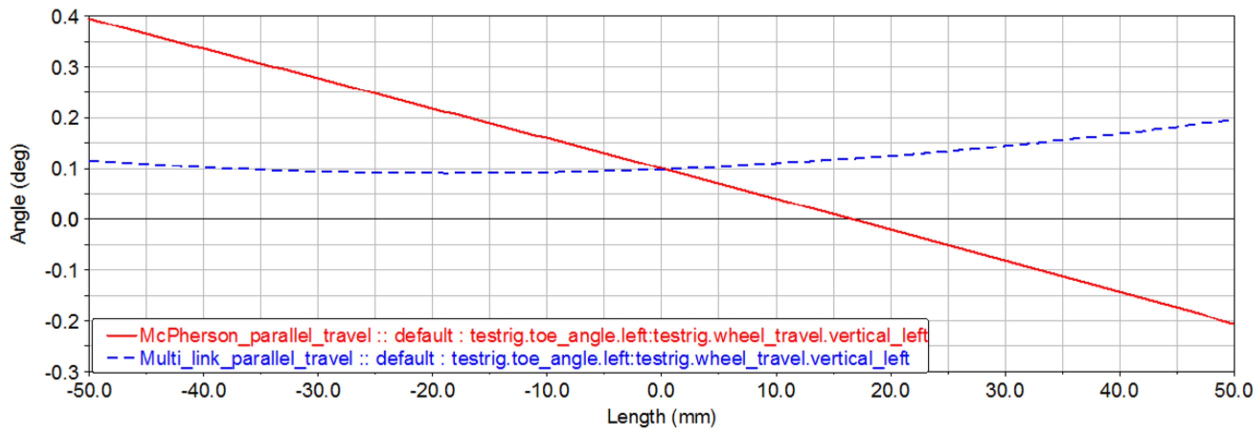

Figure 5.5 Toe angle with wheel travel

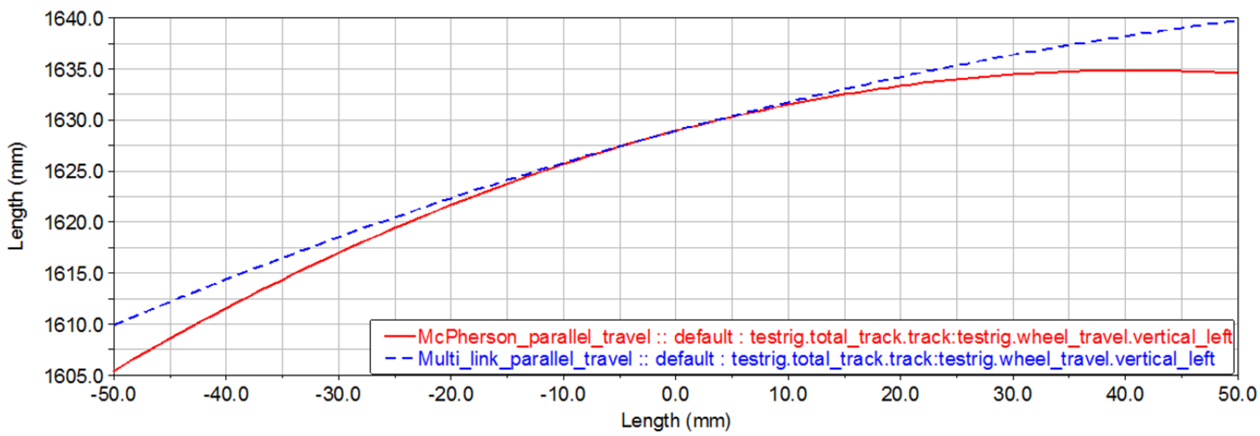

Figure 5.6 Track with wheel travel

One of the main advantages of the Multi-link layout is the wider camber gain as shown in figure 6.8 .The camber gain is useful to counteract the body roll, therefore the vehicle is more stable and the handling, as much as comfort, is improved. The reason of the different camber gain is linked to the different length of the virtual swing arm.Figure 6.9 shows that, for the same roll center height, the swing arm, or the distance of the instant center from the wheel center, is shorter for the Multi-link at the initial condition. Moreover, the growth of the red line is monotonous.

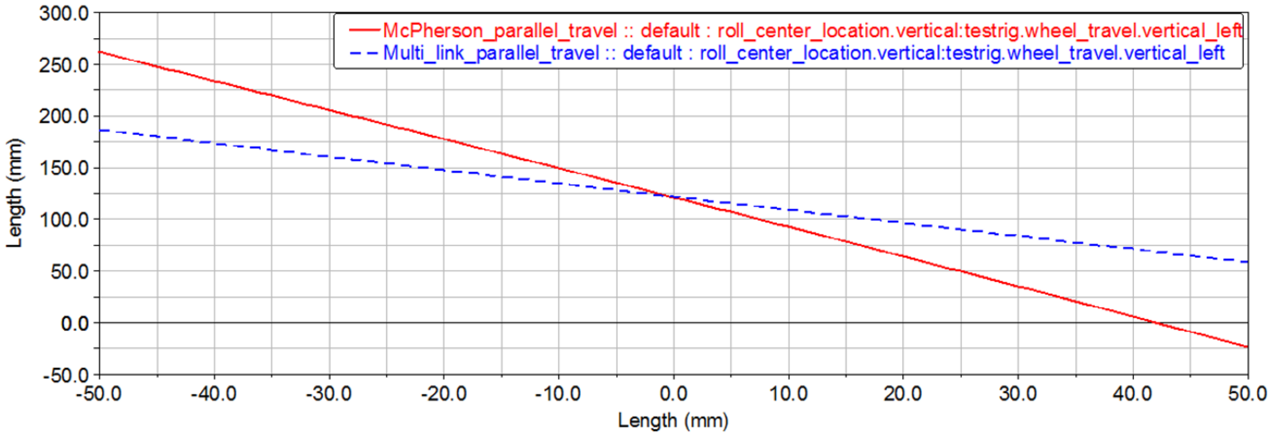

Figure 5.7 Roll center location with wheel travel

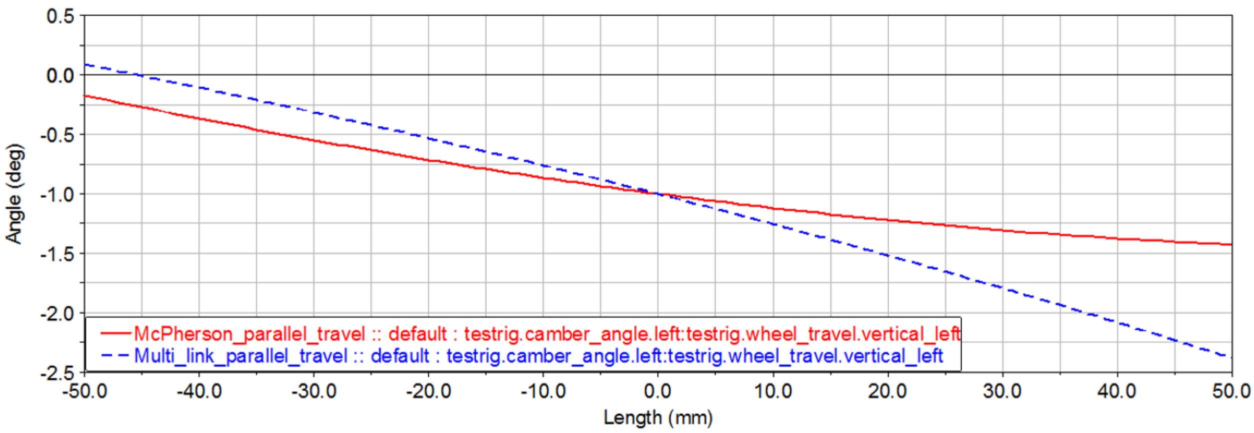

Figure 5.8 Camber angle with wheel travel

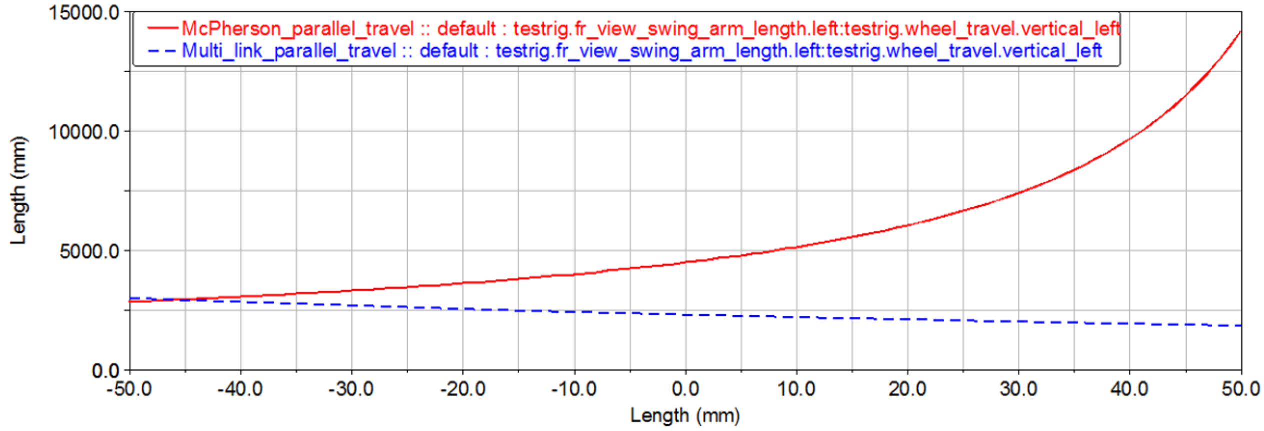

Figure 5.9 Virtual swing arm length

- Roll Analysis

The Roll analysis is useful to investigate the roll behaviour of the suspension. The main factor to analyse are :

- Suspension roll rate
- Camber gain
- Toe variation

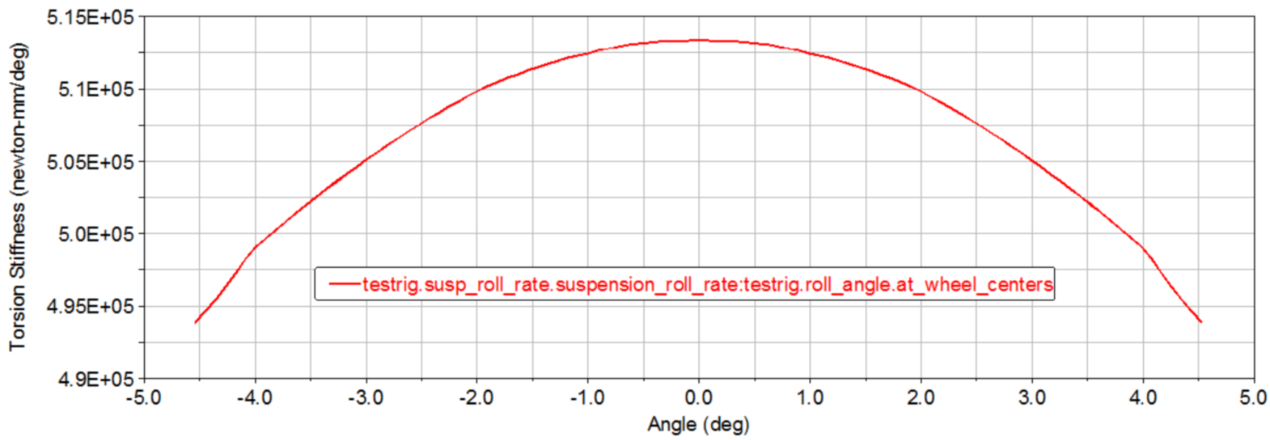

Figure 5.6 Suspension roll rate due to spring contribution

Looking at figure 6.6, the value of the suspension roll rate at the initial condition is the same of the one computed for the Macpherson strut. Doing the same computation made for the Macpherson strut, the value of the necessary anti-roll bar has been computed. The only difference between the two layout is the value of the installation ratio, smaller for the Multi-link layout, therefore the value of the necessary anti-roll bar torsional stiffness needs to be higher as shown in table 6.1.Actually,as visible in figure 6.7, the value of the suspension roll rate is slightly different from the desired one. After several simulations made on the assembly , it was found that the stiffness of the bushing, the length of the drop links and their position influences the results.Therefore,it was chosen to use a stiffer anti-roll bar to match the desired total roll rate.

Table 6.1

T	1616 [mm]
L	300 [mm]
I	0.75
K_{φ}	844206.5 [Nmm/deg]
K_{θ}	51723 [Nmm/deg]

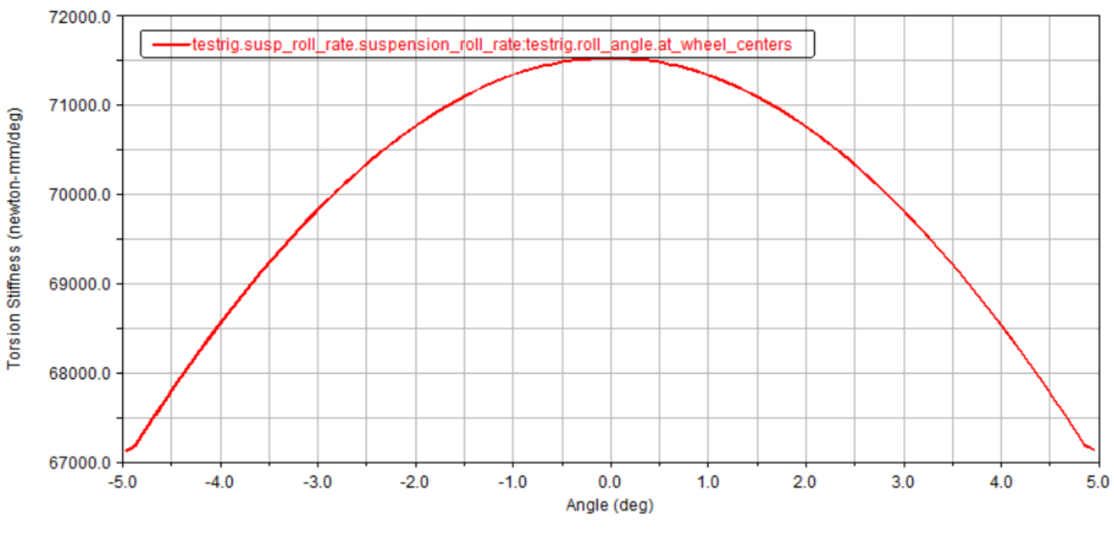

Figure 5.7 Suspension roll rate due to Anti-roll bar

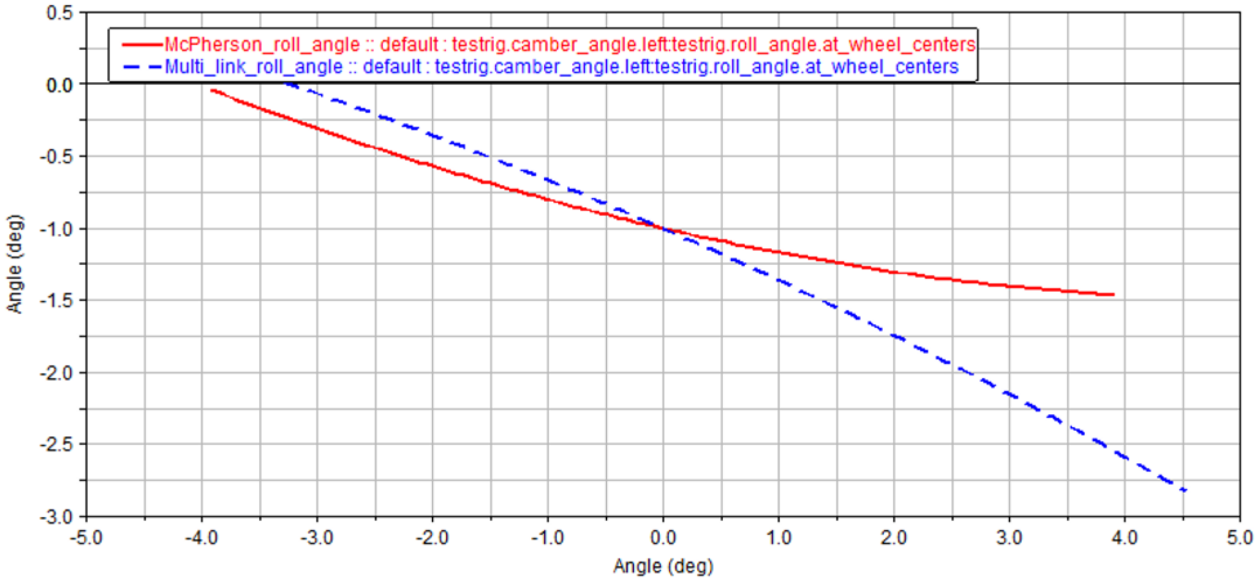

Figure 5.8 Camber angle against roll angle

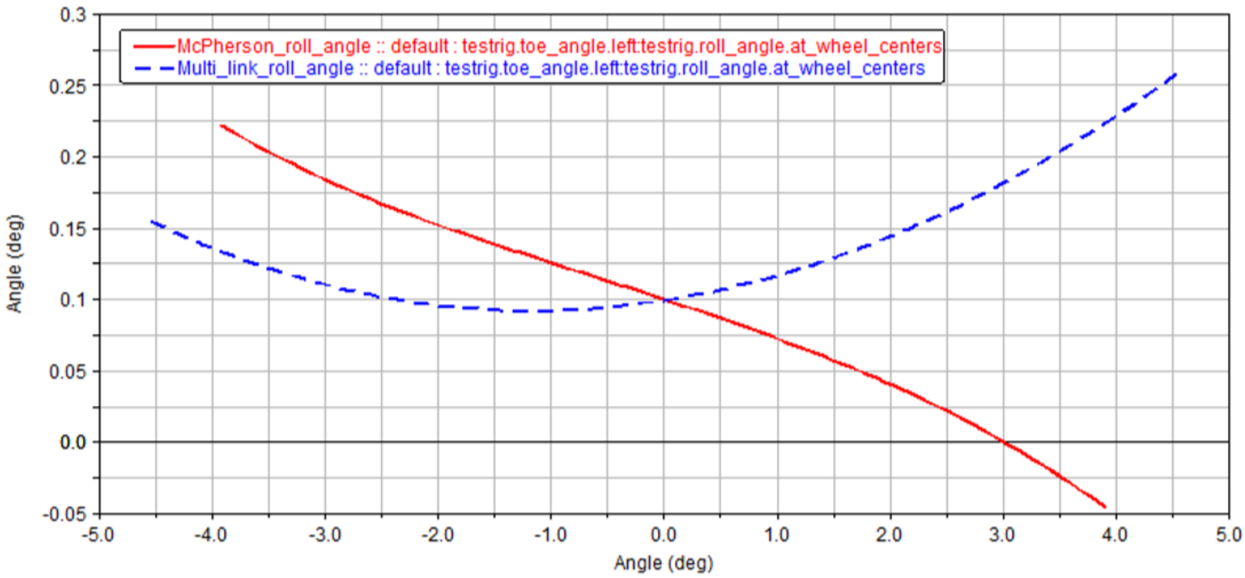

Figure 5.9 Toe variation due to roll

- Static Load Analysis

  The static load analysis allows to impose to the wheel static forces in all directions, mainly the interesting analysis involves:
  - Longitudinal forces during braking or acceleration
  - Lateral forces during cornering

For a good handling, during braking it is desirable to have a toe-in behavior.The McPherson layout doesn’t show quite any variation due to the rigid lower control arm architecture, figure 6.9.The

Multi-link virtual lower control arm can be compared to a deformable quadrilateral that allows the suspension to adapt to the external forces.Similarily,the behaviour of the Multi-link subjected to cornering forces, positive in the left direction, is better than the McPherson. Figure 6.10 shows the behaviour of the both wheel of the two cases. The Multi-link shows a toe-in behaviour while the McPherson a toe-out behavior.Conversely,figure 6.11 shows the variation of the camber on the right wheel that it can be considered the outer wheel compared to the direction of the force applied. The outer wheel tilt outwards. The Macpherson architecture comes out to be more rigid with a benefit for this application of forces.

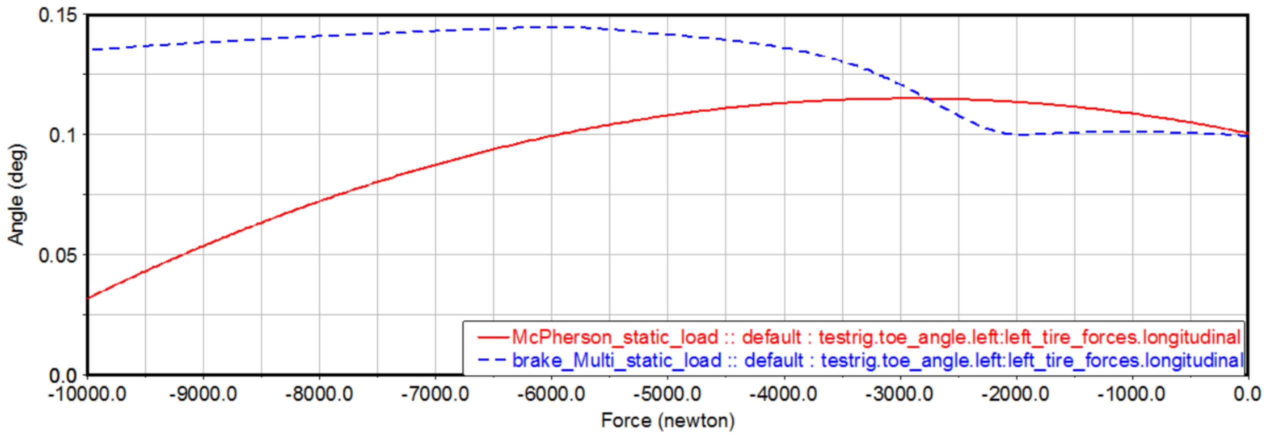

Figure 5.10 Toe variation due to braking forces

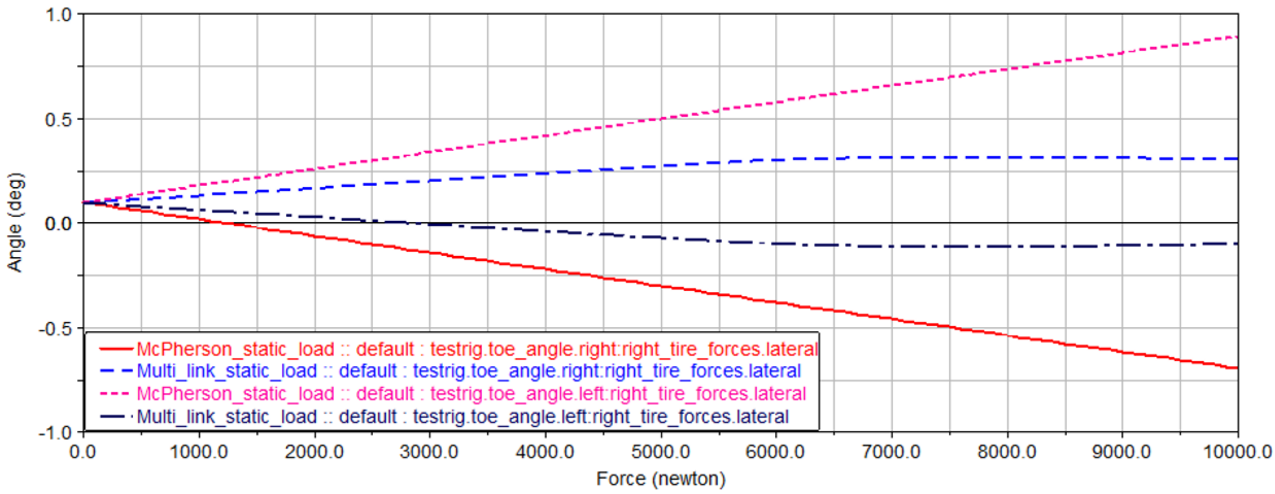

Figure 5.11 Toe variation due to lateral forces

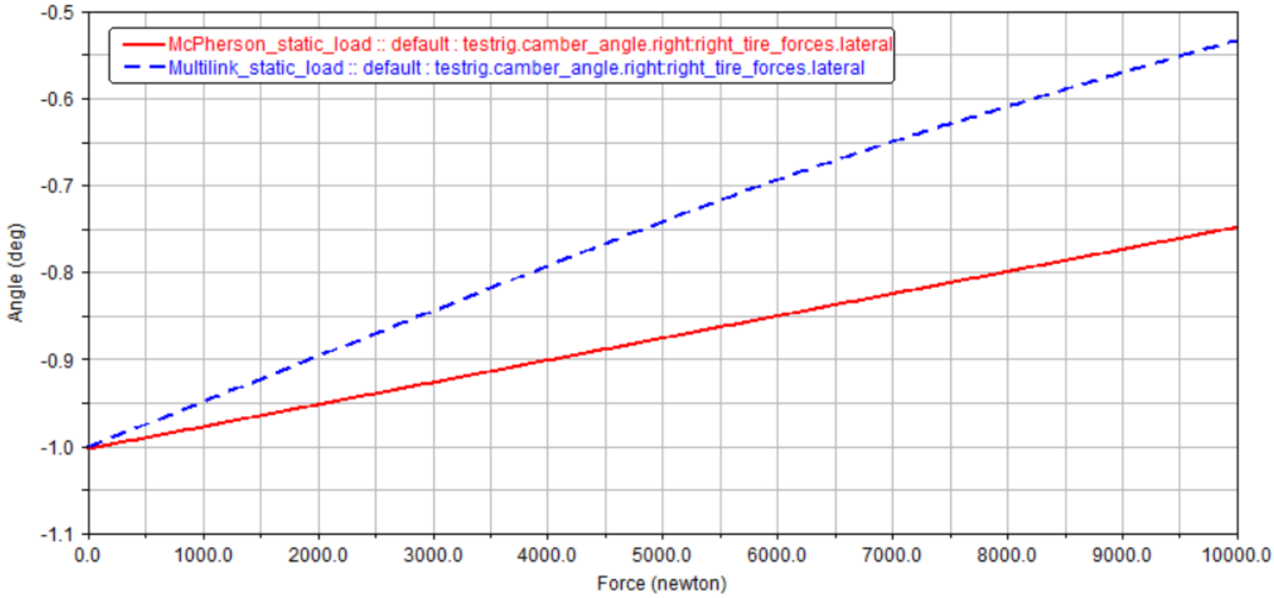

Figure 5.12 Camber variation on the outer wheel due to lateral forces

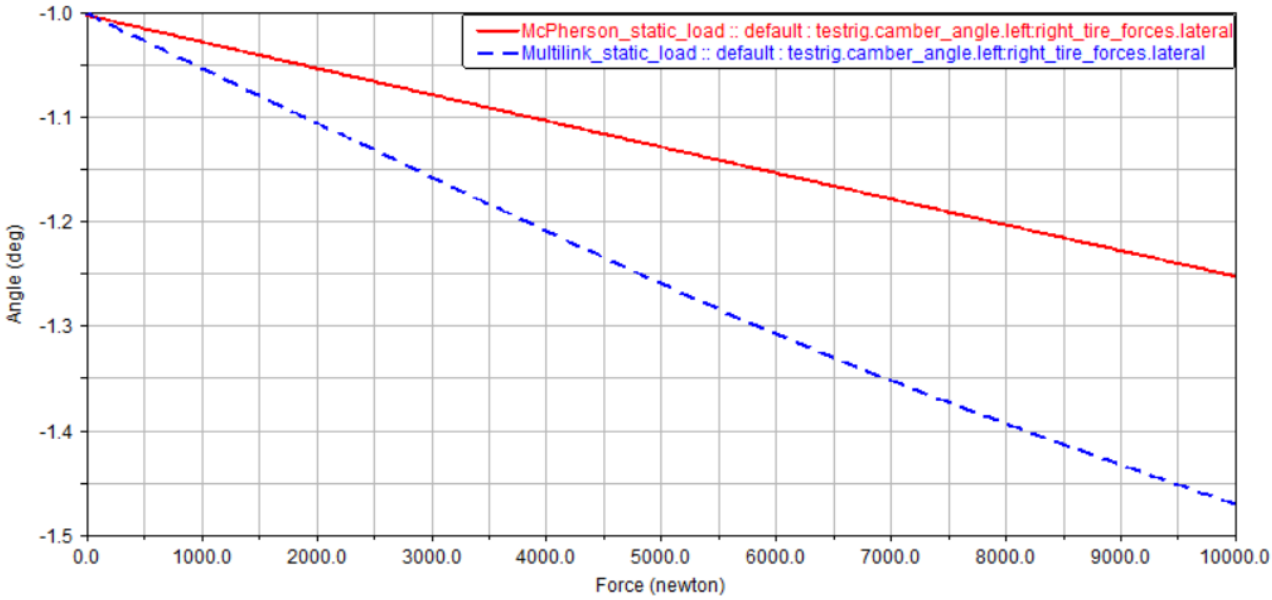

Figure 5.13 Camber variation on the inner wheel due to lateral forces

- Steering simulation

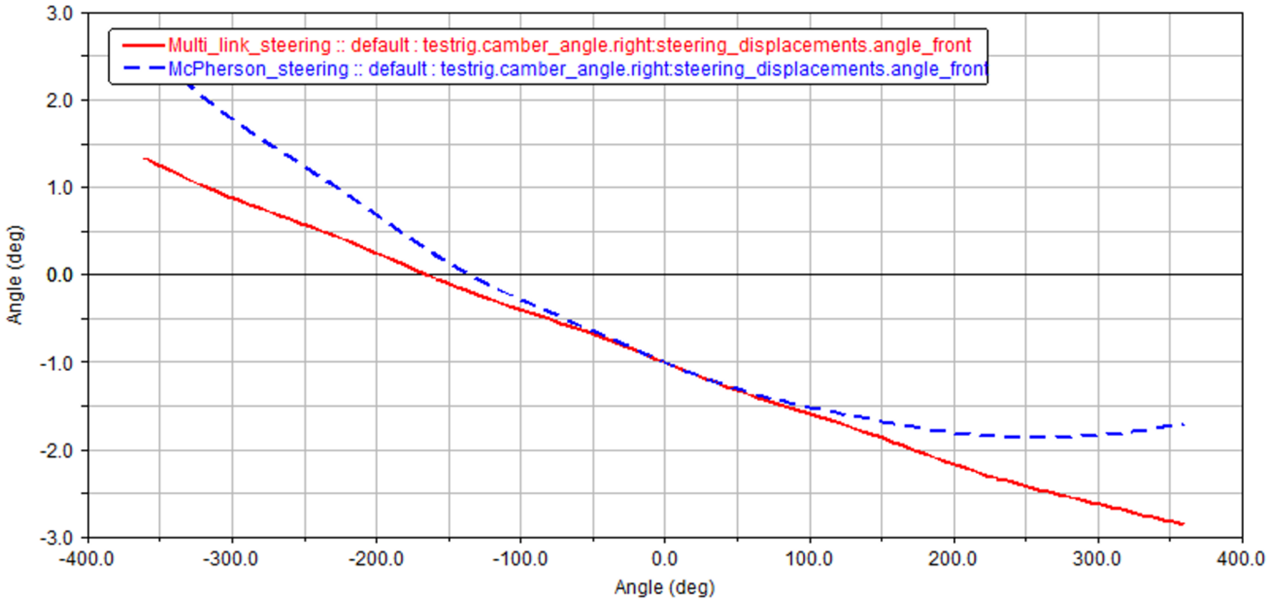

Figure 5.14 Camber variation due to steering input

Figure 6.12 shows the variation of the camber angle of the outer wheel during steering. The Multi-link suspension shows a wider and more linear camber variation.

6.FULL-VEHICLE SENSITIVITY ANALYSIS

The study on the full-vehicle system is aimed to evaluate the performance of the designed suspension on a full-vehicle assembly. More specifically, the study investigates the influence of the elastic elements and of the suspension architecture to the body roll. The car is leading to conduct the Ramp Steer simulation. The Ramp steer concerns to start the ride in longitudinal direction from a fixed velocity since a steering input is given. The full vehicle assembly is made from:

- Front Macpherson suspension subsystem
- Front steering system subsystem
- Front anti-roll bar subsystem
- Rear Double Wishbone suspension subsystem
- Rear anti-roll bar
- Body
- Powertrain

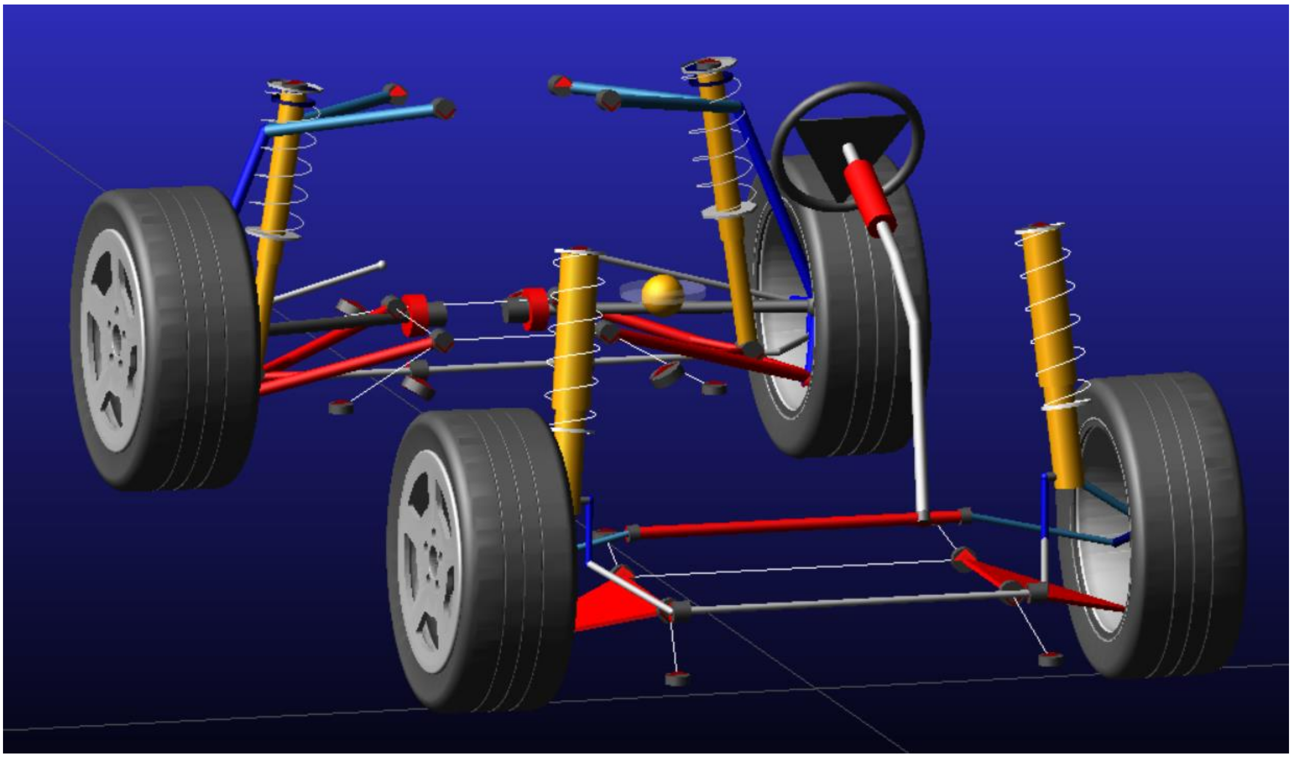

Figure 6.1 Full Vehicle Assembly

Each subsystem, in the design stage in the template builder is provided with communicators. The communicators, input and output, exchange information, as location, between each subsystem. In the standard interface is possible to assemble the subsystems making the full-vehicle assembly automatically using the communicators. Differently from the stand-alone simulations for which the mass of the vehicle doesn't load the suspension, in the full-vehicle study, through the body the sprung mass of the vehicle such as the moments of inertia are applied to the whole system and on the suspensions. To reach the static equilibrium at the initial condition, it is necessary to impose a preload. The powertrain, installed on the rear axle provides the traction forces. The rear suspension used is the Double Wishbone, which template was already available in the Adams\Car library. The suspension hardpoints have been chosen to match the desired roll center height. The first attempt made, matched the desired roll center height but during the simulation with this setting, the suspension showed a strange behaviour of the camber angle curves. The reason was in the distance of the instant center from the wheel travel that influences the camber gain. Considering also this effect, the proper hardpoints setting has been chosen. The tie rod position and length have been decided using the geometrical approach shown in the previous chapter to reduce the influences of the tie rod during the wheel travel and roll. The ramp steer manuever is useful to analyse the variation of the camber angle and the body roll. The sensitivity analysis is lead considering three different configurations:

- Variation of the inclination strut maintaining the same roll center height and same stiffness
- Variation of the anti-roll bar stiffness, maintaining the same layout for each configuration
- Variation of the lower control arm angle

The first analysis involves the variation of the inclination of the strut maintaining the same roll center height and the same stiffness for the different configurations. Moving the top mount point, hence changing the inclination of the strut, the kingpin inclination angle varies and the instant center and the roll center height changes too as consequences.

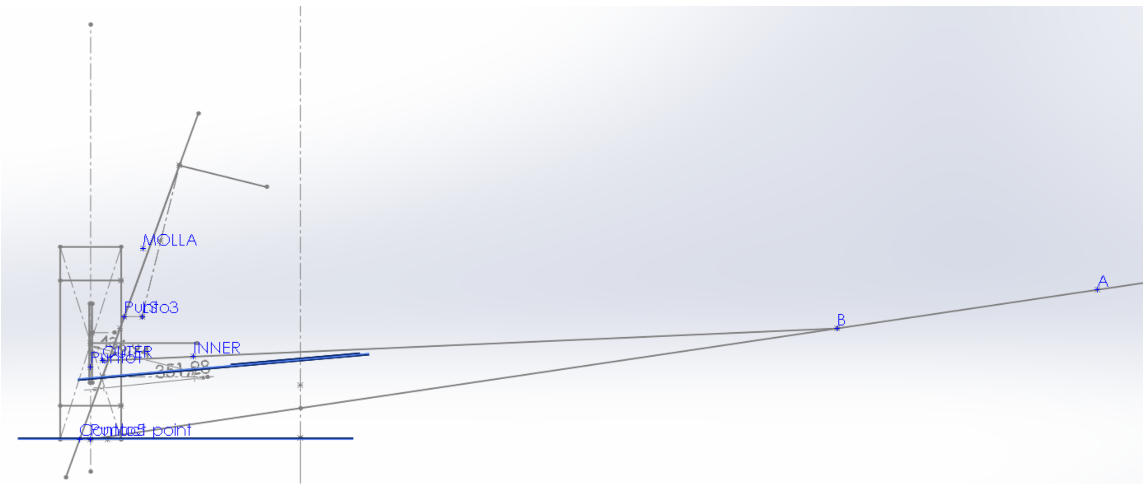

Figure 6.2 SolidWorks sketch

Using SolidWorks, as shown in figure 7.1,the height of the desired roll center height is set. From the wheel center at the ground to the roll center height, in correspondence of the construction line in the middle of the car, a line is drawn. Point B is the intersection of the plane in which the lower control arm lies and the constant roll center height line. Point A is the intersection of the orthogonal plane to the strut and the constant roll center height line. Using the Excel suite contained in SolidWorks, many table data are created in order to , with a trial and error methodology, find the proper values for both the kingpin inclination angle and the lower arm angle that lead to point A and point B to lie on the same position on the constant roll center height line, as visible in figure 7.3.

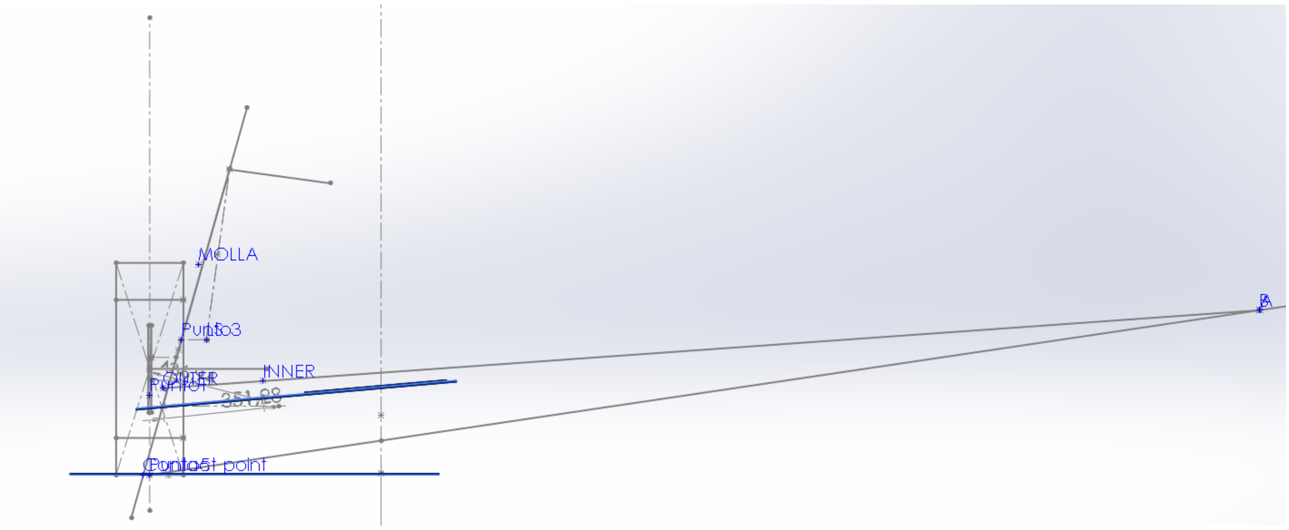

Figure 6.3 Roll center height matching

Five different configurations have been recorded. For each configuration, the position of the instant center changes. The geometrical model allows to vary autonomously the position of the inner tie rod for each case in such a way as to guarantee no influences on the motion of the whole suspension. For each disposition, the coordinates of the hardpoints have been recorded, the main parameters values are listed in table 4.1.

Table 7.1

Configuration	Kingpin angle [degree]	Lower arm angle [degree]	Caster [degree]	Swing arm length [mm]	Strut inclination [degree]
1	26.3	2	5	2103	23.10
2	19.19	4	5	3020	12.75
3	15.76	5	5	3876	7.78
4	12.385	6	5	5431	2.91
5	10.73	6.5	5	6807	0.54

Once got the proper values for the main parameters, for each configuration the simulation is run. The input of the simulation is shown in figure 7.3.The car rides longitudinally with an initial velocity of 70 km/h ,after 4 seconds ,it starts to curve with a rate of change of steering equal to 10 degree/sec.The trajectory of the car is shown in figure 7.4.

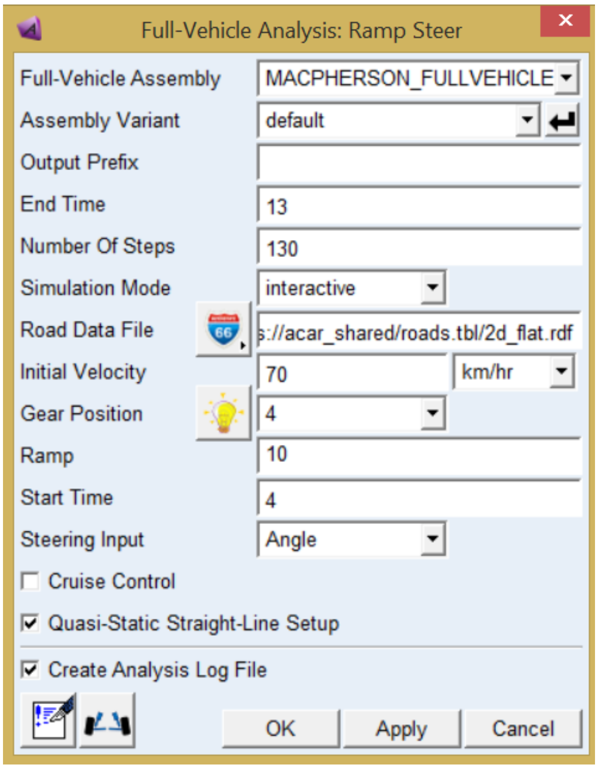

Figure 6.4 Input for the maneuver

This case study is aimed to determine, between the suspension roll rate and the kinematic camber gain, which improves the handling of the vehicle. Looking at table 4.1 it can be seen that ,from the first configuration to the last, while the swing arm length decreases the strut inclination reduces. The swing arm length influences the camber gain, shorter length improves the camber gain that counteracts the body roll. The roll center height for each configuration is the same, hence the distance from the center of gravity, at which the force produced by the lateral acceleration is exerted, is the same. The inclination of the strut affects the magnitude of the vertical component of the force exerted by the springs. Increasing the inclination of the strut, the vertical component reduces, and the suspension roll rate decreases as consequences,favoring the body roll. The value of the lateral acceleration in time is different for each configuration, therefore also the rolling moment would be different at each time. To have a proper comparison, the camber angle and body roll curves are plotted against the lateral acceleration. As expected, in figure 4.42 is clearly visible that for the red line, referring to the first configuration, the camber variation is the smallest.Conversely,the body roll for the first configuration is the greatest as shown in figure 4.43.The difference of camber angle for each configuration is relevant while the difference of the body roll is smaller. It means that for the first case study that increase the strut inclination improves the handling of the car. It need to be noticed in figure 4.40 that with the first configuration the vehicle can curve along a circle which radius is smaller compared to the last configuration.

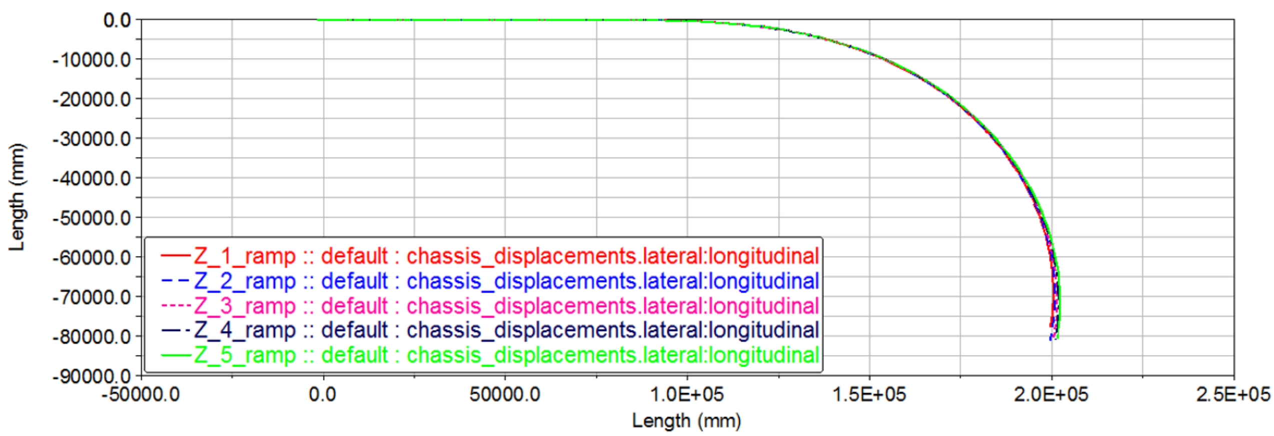

Figure 6.5 Trajectory of the car

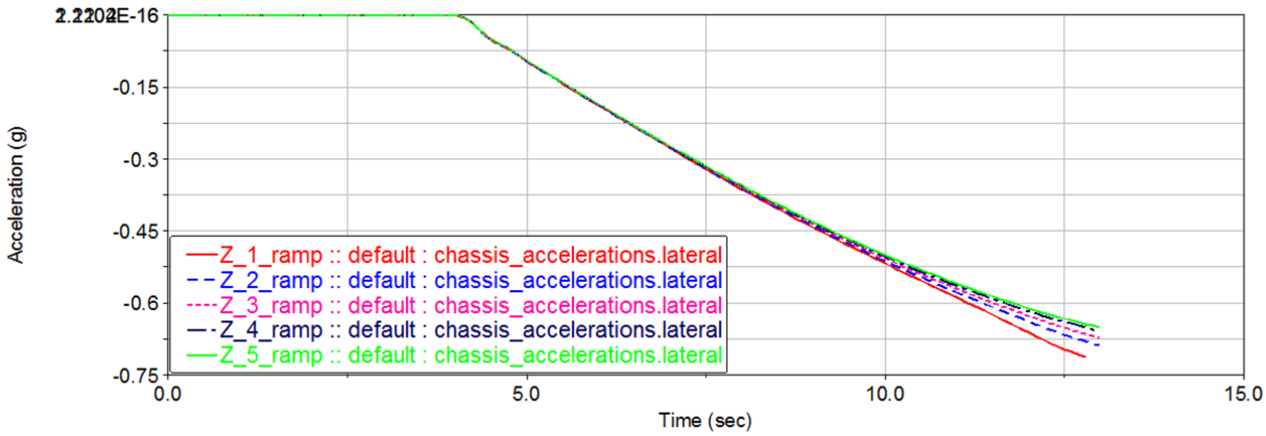

Figure 6.6 Camber angle on the right front wheel

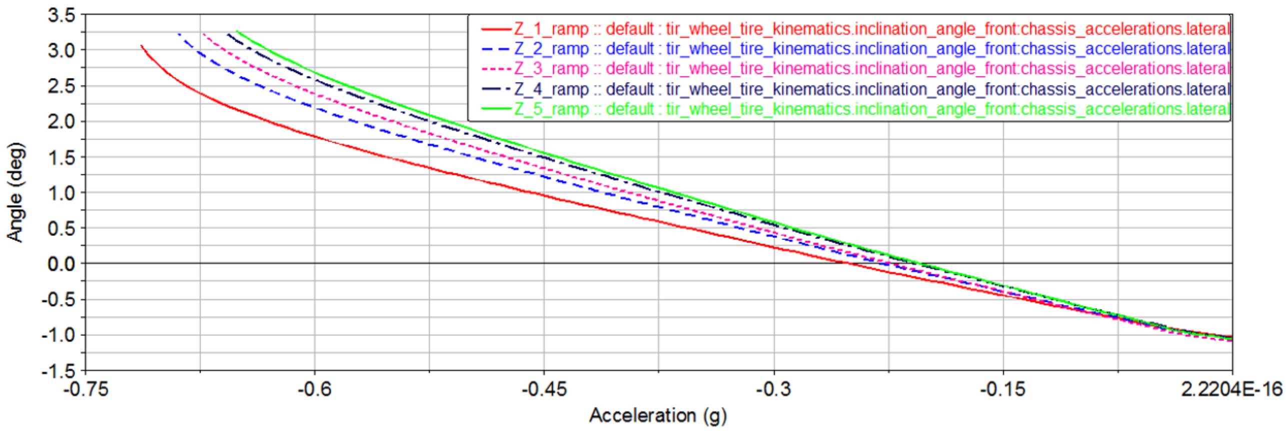

Figure 6.7 Camber angle on the right front wheel

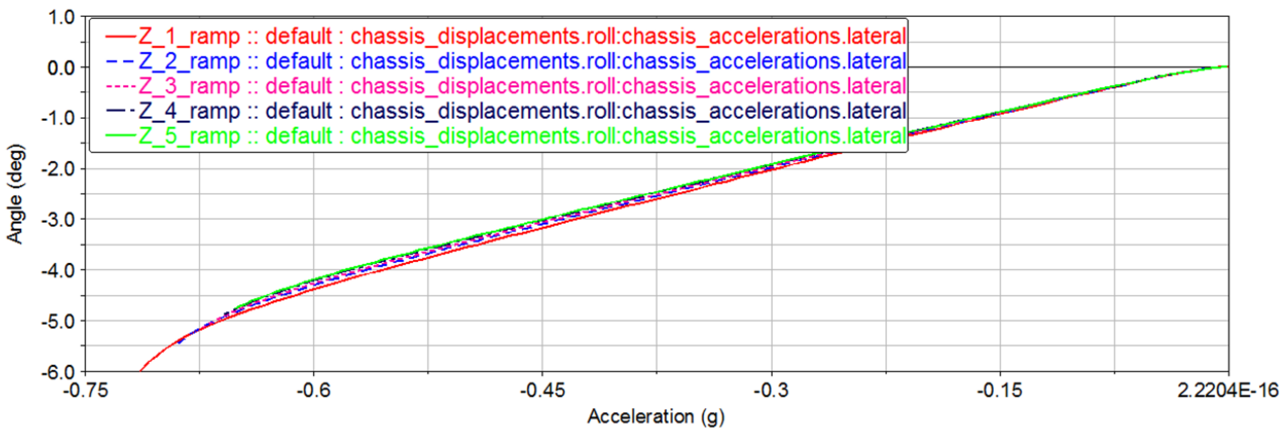

Figure 6.8 Lateral acceleration against time

The second case study involves the variation of the stiffness for each configuration maintaining the same roll center height and the same inclination of the strut. To not moves far from the Olley's criteria, the spring stiffness is not changed. For each configuration the anti-roll bar stiffness is varied, the values are listed in table 4.2.The instant center of rotation in this case study is maintained at the same position, therefore there is no difference camber gain between the different configurations. As expected, figure 7.8 proves that increasing the stiffness, the roll angle is reduced, and the camber angle is reduced as consequence. Looking at figure 7.10, it is interesting to highlight that for the first seconds of the curve maneuver the configuration with the greatest torsional stiffness leads the shortest curve, almost 2 metres, compared to the weakest stiffness configuration while at a certain point, the trajectory becomes wider. To explain this behaviour factors, need to be considered. Increasing the torsional stiffness at the front axle, the stiffness ratio between front and rear axle increases. This allows more lateral load transfer at the front axle and the front right wheel is more loaded. The total lateral force is reduced because the tire goes into saturation and the understeer behaviour increases. This means that to do the same curve, the vehicle with the highest torsional stiffness should lead a wider trajectory.Meanwhile,as shown in figure 7.9, increasing the torsional stiffness ,the camber variation is smaller and it allows to produce higher lateral forces that make the vehicle to go along a narrower curve.Resuming,for the first part of the maneuver the camber angle has a bigger influence on the trajectory, after a certain value of body roll, the lateral load transfer becomes predominant.

Table 7.2

Configurations	Anti-roll bar torsional stiffness [kN/mm]
1	40
2	45
3	50
4	55
5	60

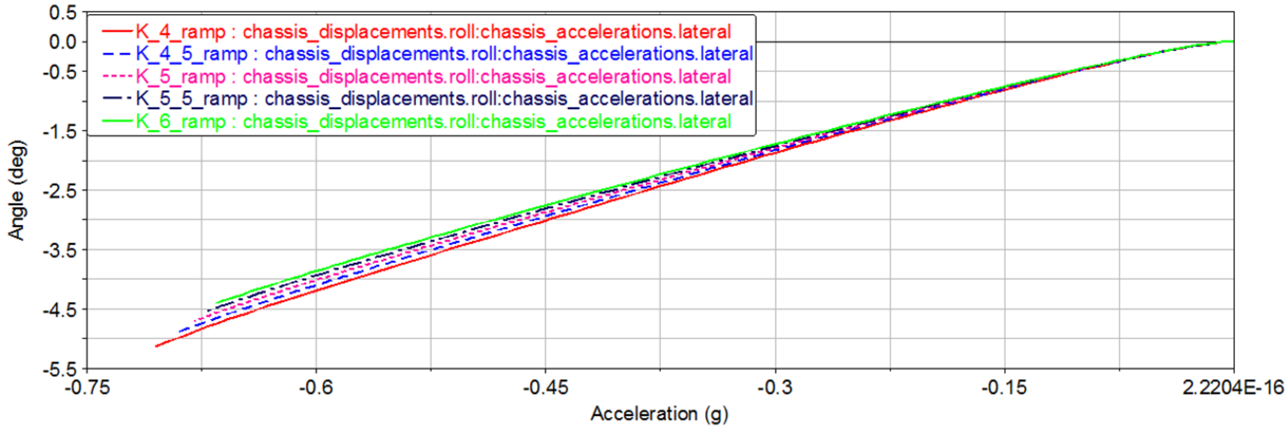

Figure 6.9 Roll against lateral acceleration

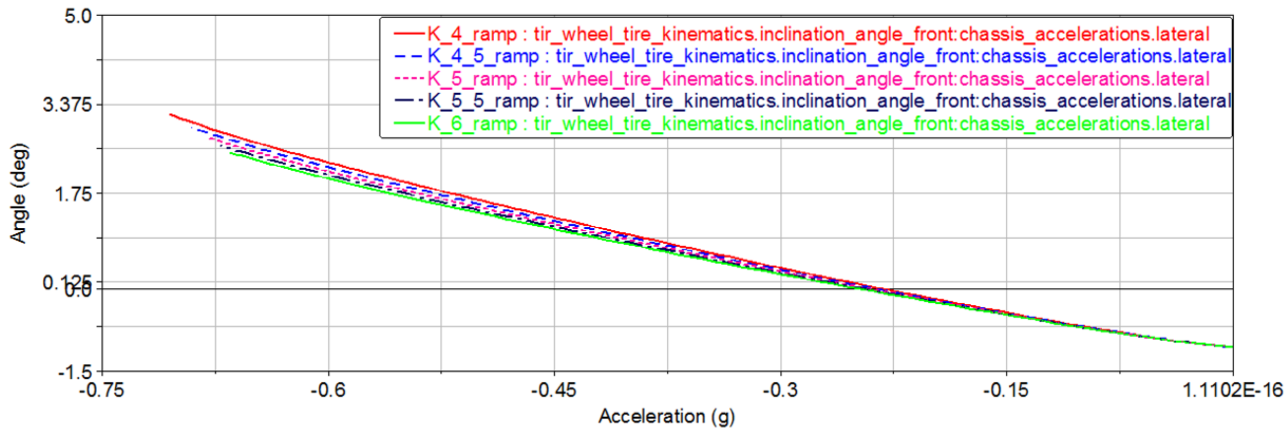

Figure 6.10 Camber angle against lateral acceleration

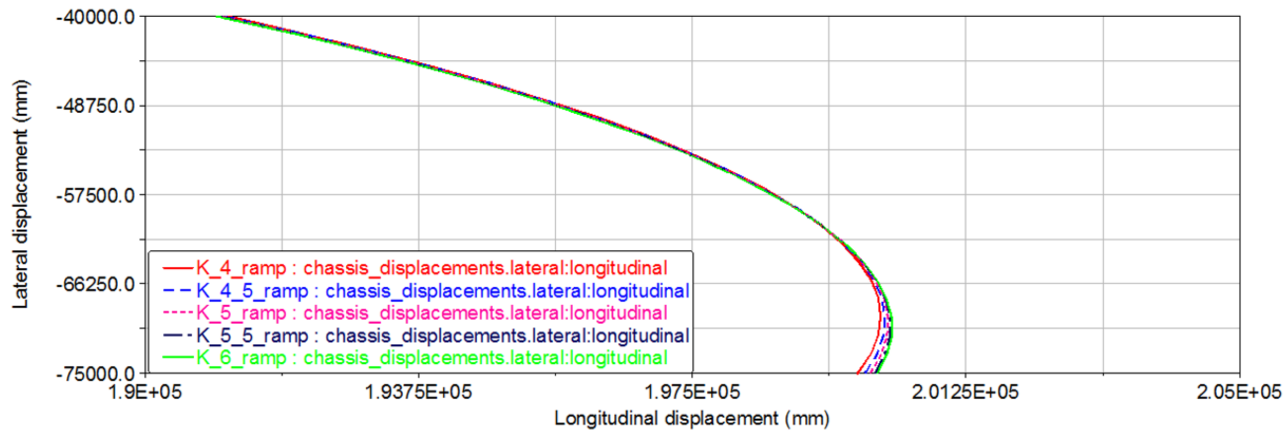

Figure 6.11 Trajectory of the car

The third case study involves maintaining the same stiffness and the same strut inclination for each configuration. The outer ball joint of the lower control arm is moved vertically, making the lower arm inclination change. Changing the lower arm inclination, the instant center and the roll center height change. The different configurations values are listed in table 4.3.Looking at the third column ,the value of the roll center height increases. This make the vehicle roll less and is confirmed by figure 7.12.Looking at the fourth column, the instant center distance from wheel center decreases. It improves the camber gain as proved by figure 7.11.Both effects improve the handling of the vehicle. The results are ,looking at figure 7.14, a narrower curve made by the car with the last configuration.

Table 7.3

Configuration	Outer ball joint height from ground [mm]	Roll center height [mm]	Instant center distance from wheel center [mm]	Kingpin angle [degree]
1	295.55	-48	29226	14.95
2	270.55	27	8360	14.5
3	245.55	98	5017	14
4	220.55	164	3651	13.68
5	170.55	284	2442	12.9

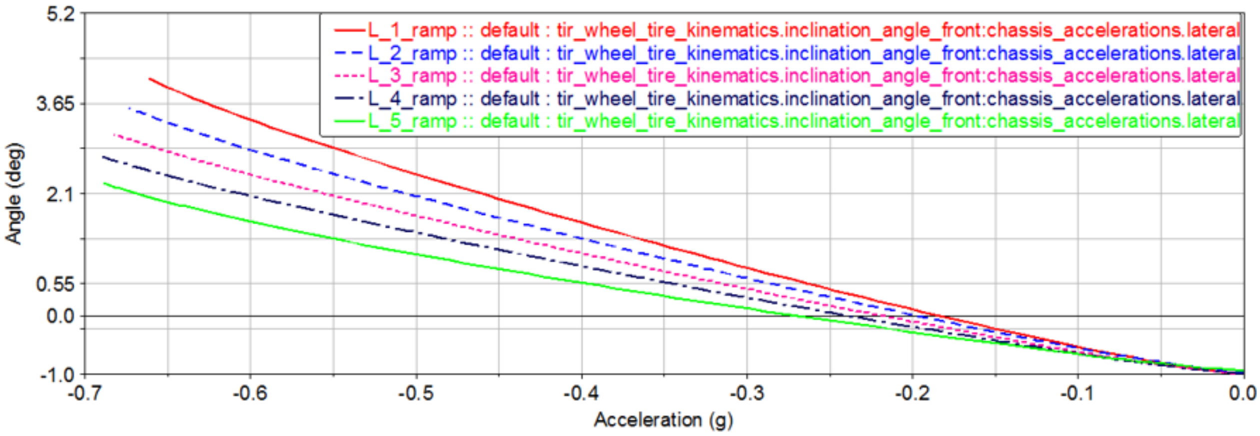

Figure 6.12 Camber angle against lateral acceleration

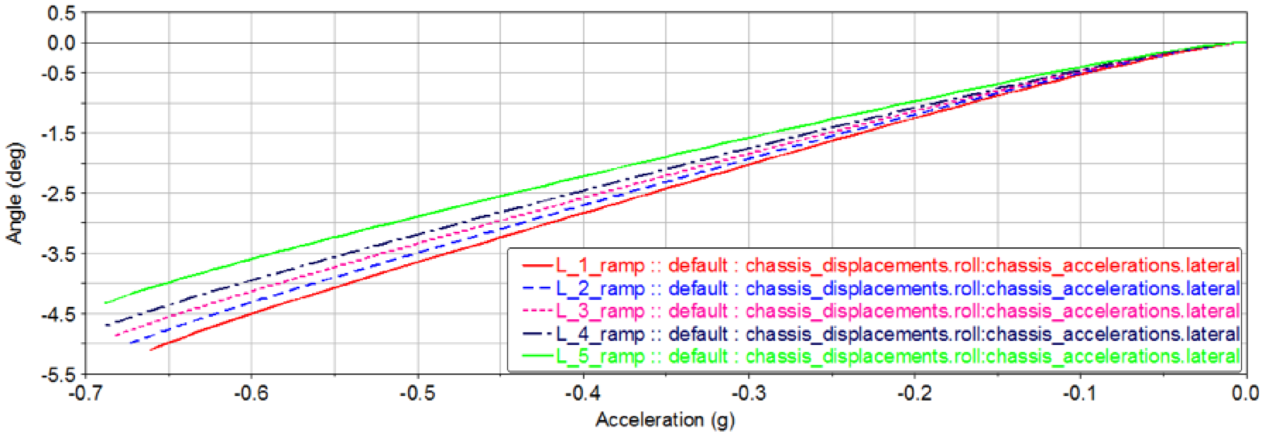

Figure 6.13 Roll angle against lateral acceleration

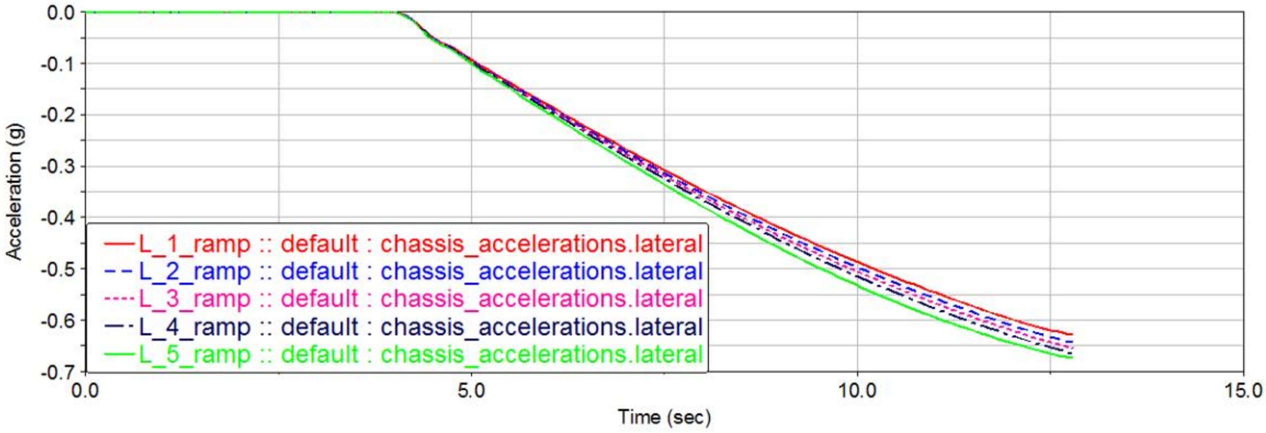

Figure 6.14 Lateral acceleration against time

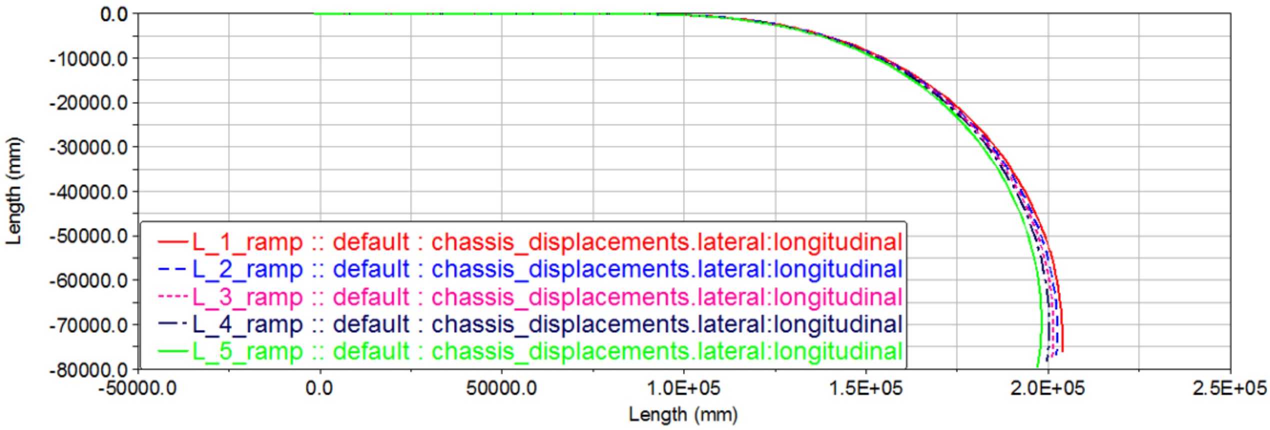

Figure 6.15 Trajectory

7.CONCLUSION

The objective of this master's thesis is the design of a front suspension system for a road vehicle. Starting from general vehicle data, such as mass, wheelbase and track, it was supposed a roll gradient as target. Two different kind suspension layouts have been analysed and designed to highlight the differences of the design and the performance of each layout. The analysis of the suspension is focused on its kinematics that is linked to the position of the main hardpoints. The geometric approach is useful for understanding the kinematics of the suspension. The CAD software,SolidWorks,was used to investigate the effect of each hardpoint on the whole system. The study has demonstrated that each hardpoint can have the same effect on a suspension parameter and an opposite effect on another parameter. This highlights that the design of a suspension is a compromise between several factors and each vehicle needs a specific design depending on the use. The multibody dynamics software Adams\Car was used in order to validate the setting of the hardpoints chosen using the SolidWorks model and to study the real kinematics of the suspension designed during several maniverter analysis highlights that the suspension parameters, like roll center height, camber angle, which affect the behaviour of the vehicle, change during the motion of the suspension.Therefore,during the design process, it is necessary to take into account the variation of the main parameters in order to ensure a good performance in all conditions. The suspension layout designed in thesis are the McPherson strut and the Multi-link. The study emphasises the critical issue of the design and the potential of each layout. After the modelling of both the layouts, it is proposed the comparison between them. It shows the superiority of the Multi-link compared to the McPherson though the effort required from the former makes the Multi-link to be used only in specific case where certain performance need to be achieved. The McPherson strut results to be a good choice for many road cars application. Through a specific optimization methodology is possible to improve the performance of the layout reaching satisfactory performance avoiding the use of costly electronic hardware. At the end of the thesis is proposed a sensitivity analysis of the McPherson strut aimed to study the effect of the hardpoints on the lateral dynamics of the car during cornering. Three different case have been analysed. It turned out that lowering the outer ball joint has the best effects on the vehicle. Increasing the anti-roll bar stiffness is the simplest and effective way to improve the stability of the vehicle, though the increasing of the understeer behaviour.

8. REFERENCES

[1] Morales,E.: Sensitivity study of front suspension parameters in elastokinematics and handling behaviour of a vehicle. Society of Automotive Engineers.2016-36-0182 (2016)
[2] Guiggiani,M.:The Science of Vehicle Dynamics. Springer,(2014)
[3] Milliken,W,Race Car vehicle dynamics. Society of Automotive Engineer,(1995)
[4] Smith,J.:An introduction to Modern Vehicle Design. Butterworth-Heinemann, (2002)
[5] Reimpell,J.,Stoll,H and Betzler J.:The Automotive Chassis: Engineering Principles.Butterworth-Heinemann,(2001)
[6] Taehyun,S. and Pradheep,C.: Influence of Suspension Properties on Vehicle Roll Stability. Society of Automotive Engineers,2006-01-1950 (2006).
[7] Kim,S.,Lee,J.,Oh,Y. and Lee,U.: The development of Multi-link Suspension for Hyundai Genesis.Society of Automotive Engineers,2009-01-0224 (2009).
[8] Frendo,F.: Le sospensioni Automobilistiche (2005)
[9] Dixon,C,J.: Suspension Geometry and Computation (2009)
[10] M S Ramaiah School of Advanced Studies – Bangalore,Slides
[11] Genta,G.,Morello,L.:The Automotive Chassis-Vol 1 Components Design (2008)